Defining the onset of prion infection and neurodegeneration in healthy individuals at risk of prion disease

Tze How Mok

A thesis submitted for the degree of Doctor in Medicine MD(res)

MRC Prion Unit at UCL, Institute of Prion Diseases
University College London (UCL)

2023

DECLARATION

I, Tze How Mok, confirm that the work presented in this thesis is my own. Where information has been derived from other sources, I confirm that this has been indicated in the thesis.

ACKNOWLEDGEMENTS

A considerable amount of nostalgia and reflection surfaces, naturally, as I move ever closer to submitting this body of work for examination. It goes without saying that none of this would have been possible without the help, guidance and support from people within and outside the Unit, and in my personal life. In essence, I came for a job but stayed for the people (as well as the science!).

First, I really ought to thank my primary supervisor, Simon Mead, for hiring me as a clinical research fellow in 2014, and whose irrepressible enthusiasm, wisdom, personal advocacy and generosity over the years have been indispensable. I am indebted to Graham Jackson, my secondary supervisor, for his patience with a novice in a science laboratory, and for being the first to teach me how to perform an RT-QuIC experiment. John Collinge, our Unit director, has been a pillar of encouragement and support, whose comments have always been deeply insightful. I am thankful to Jan Bieschke and Mark Batchelor from the Protein Group, for helping to establish the RML recombinant PrP protocol, and for supplying this project with sufficient stock to completion. I cherish the several insightful conversations I had with Jon Wadsworth and Emmanuel Asante, all of which left indelible marks on my scientific thinking.

At the Clinic, I am fortunate to have enjoyed the camaraderie of several clinical research fellows, many of whom have become close friends. Chief amongst them is Akin Nihat whose banter is unrivalled and whose “comradeship” I prize dearly. I wish to thank Regina Appenteng, our secretary for her generosity especially for keeping me fortified with regular supplies of her unsurpassable Ghanaian hot sauce. I marvel at Sarah Mazdon’s (our Cohort manager) meticulous organisation of our Open Days and Cohort days, without which our sample resource recruitment would have surely been poorer. Last but not least, I am ever so grateful for the company, support and friendship of our clinical nurse specialists past and present – Kirsty McNiven, Selam Tesfamichael, Veronica O’Donnell, Ruby Colley, Philip Parker and Jane Owen.

I owe a tremendous amount of debt to Byron Caughey, Christina Orrù, Andy Hughson and Bradley Groveman for hosting me at the NIH Rocky Mountain Laboratories 2019.

I was deeply touched by their truly altruistic approach to collaboration, helping me refine my RT-QuIC assay technique, supplying recombinant PrP glycerol stocks, and invaluable assistance in troubleshooting recombinant PrP purification and assay kinks.

It would have been impossible to locate, gather, and aliquot the blood and CSF samples from the -80 freezers without the help of Lee Darwent, whose perennial good cheer got me through this ordeal. I will sorely miss the shared enthusiasm and data design wizardry of Nour Majbour! I must thank Henrik Zetterberg for supporting this project from the time of conception, and his team at the UKDRI for performing the Simoa analysis. Without my other collaborators who kindly supplied the necessary control samples, our results would make little sense.

In my personal life, I am indebted to close friends and companions, no less Richard who has put up with my grumpiness during the troughs. I mustn't forget Patsy, who has been a most adorable fungus eating away at the positivity of the household.

The work contained in this thesis would not have been possible without the dedication, foresight and belief of the at-risk and symptomatic participants. I am amazed at their altruism, often attending appointments and giving biofluid samples even in the midst of physical and psychological difficulties, and against their personal needle phobias.

This work was core-funded by the Medical Research Council in the UK award to the MRC Prion Unit. The clinical research activities of the National Prion Clinic are supported by the National Institute of Health Research's (NIHR) UCLH Biomedical Research Centre. I was personally supported by a Fellowship award from Alzheimer's Society, UK [Grant Number 341 (AS-CTF-16b-007)]; I thoroughly enjoyed working with Frank Arrojo and Eric Deeson as project monitors. I am grateful to Richard Newton (Repographics) for supplying and editing the illustrations.

UCL Research Paper Declaration Forms

Chapter 2

UCL Research Paper Declaration Form
referencing the doctoral candidate's own published work(s)

Please use this form to declare if parts of your thesis are already available in another format, e.g. if data, text, or figures:

- *have been uploaded to a preprint server*
- *are in submission to a peer-reviewed publication*
- *have been published in a peer-reviewed publication, e.g. journal, textbook.*

This form should be completed as many times as necessary. For instance, if you have seven thesis chapters, two of which containing material that has already been published, you would complete this form twice.

1. **For a research manuscript that has already been published** (if not yet published, please skip to section 2)

a) **What is the title of the manuscript?**

Seed amplification and neurodegeneration marker trajectories in individuals at risk of prion disease

b) **Please include a link to or doi for the work**

DOI: 10.1093/brain/awad101

c) **Where was the work published?**

Brain

d) **Who published the work?** (e.g. OUP)

OUP

e) **When was the work published?**

June 2023

f) **List the manuscript's authors in the order they appear on the publication**

Tze How Mok, Akin Nihat, Nour Majbour, Danielle Sequeira, Leah Holm-Mercer, Thomas Coysh, Lee Darwent, Mark Batchelor, Bradley R Groveman, Christina D Orru, Andrew G Hughson , Amanda Heslegrave, Rhiannon Laban, Elena Veleva, Ross W Paterson, Ashvini Keshavan, Jonathan M Schott, Imogen J Swift, Carolin Heller, Jonathan D Rohrer, Alexander Gerhard, Christopher Butler, James B Rowe, Mario Masellis, Miles Chapman, Michael P Lunn, Jan Bieschke, Graham S Jackson, Henrik Zetterberg, Byron Caughey, Peter Rudge, John Collinge, Simon Mead

g) **Was the work peer reviewed?**

Yes

h) **Have you retained the copyright?**

Click or tap here to enter text.

i) **Was an earlier form of the manuscript uploaded to a preprint server?** (e.g. medRxiv). If 'Yes', please give a link or doi)

https://doi.org/10.1101/2022.10.30.22281644

If 'No', please seek permission from the relevant publisher and check the box next to the below statement:

☐

*I acknowledge permission of the publisher named under **1d** to include in this thesis portions of the publication named as included in **1c**.*

2. **For a research manuscript prepared for publication but that has not yet been published** (if already published, please skip to section 3)

a) **What is the current title of the manuscript?**

Click or tap here to enter text.

b) **Has the manuscript been uploaded to a preprint server?** (e.g. medRxiv; if 'Yes', please give a link or doi)

Click or tap here to enter text.

c) **Where is the work intended to be published?** (e.g. journal names)

Click or tap here to enter text.

d) **List the manuscript's authors in the intended authorship order**

Click or tap here to enter text.

e) **Stage of publication** (e.g. in submission)

Click or tap here to enter text.

3. **For multi-authored work, please give a statement of contribution covering all authors** (if single-author, please skip to section 4)

Tze How Mok (study conception, sample collection, performed all seed amplification assays, drafted manuscript, performed statistical analyses), Akin Nihat (sample collection, figure illustration, contributed to and edited manuscript), Nour Majbour (figure illustration, contributed to and edited manuscript), Danielle Sequeira (sample collection, editing manuscript) , Leah Holm-Mercer(sample collection, editing manuscript), Thomas Coysh(sample collection, editing manuscript), Lee Darwent (sample processing, sample retrieval, editing manuscript), Mark Batchelor (purified recombinant protein, manuscript contribution and editing), Bradley R Groveman (provided training for RT-QuIC assays, manuscript contribution and editing), Christina D Orru (provided training for RT-QuIC assays, manuscript contribution and editing), Andrew G Hughson (provided training for RT-QuIC assays, manuscript contribution and editing), Amanda Heslegrave (analysed Simoa samples, editing manuscript), Rhiannon Laban (analysed Simoa samples, editing manuscript), Elena Veleva (analysed Simoa samples, editing manuscript), Ross W Paterson (supplied control CSF samples and editing manuscript), Ashvini Keshavan (supplied control CSF samples and editing manuscript), Jonathan M Schott (supplied control plasma samples and editing manuscript), Imogen J Swift (supplied control plasma samples and editing manuscript), Carolin Heller (supplied control plasma samples and editing manuscript), Jonathan D Rohrer (supplied control plasma samples and editing manuscript), Alexander Gerhard (supplied control plasma samples and editing manuscript), Christopher Butler (supplied control plasma samples and editing manuscript), James B Rowe (supplied control plasma samples and editing manuscript), Mario Masellis (supplied control plasma samples and editing manuscript), Miles Chapman (supplied control CSF samples and editing manuscript), Michael P Lunn (supplied control CSF samples and editing manuscript), Jan Bieschke (purified recombinant protein, manuscript contribution and editing), Graham S Jackson (supervision, training, manuscript contribution and editing), Henrik Zetterberg (coordinated Simoa analyses, provided control CSF samples), Byron Caughey (provided RT-QuIC training and expertise, manuscript contribution and editing), Peter Rudge (sample collection, manuscript contribution and editing), John Collinge (study conception, manuscript contribution and editing), Simon Mead (primary supervisor, conception of study, statistical analysis, major contributor to manuscript).

4. **In which chapter(s) of your thesis can this material be found?**

Chapter 2

5. **e-Signatures confirming that the information above is accurate** (this form should be co-signed by the supervisor/ senior author unless this is not appropriate, e.g. if the paper was a single-author work)

Candidate

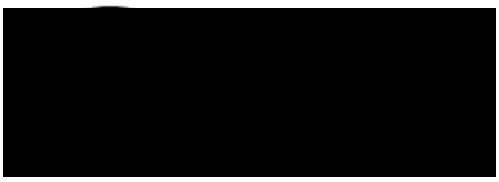

Date:

04/06/2023

Supervisor/ Senior Author (where appropriate)

Date
06/06/2023

UCL Research Paper Declaration Form
referencing the doctoral candidate's own published work(s)

Please use this form to declare if parts of your thesis are already available in another format, e.g. if data, text, or figures:

- *have been uploaded to a preprint server*
- *are in submission to a peer-reviewed publication*
- *have been published in a peer-reviewed publication, e.g. journal, textbook.*

This form should be completed as many times as necessary. For instance, if you have seven thesis chapters, two of which containing material that has already been published, you would complete this form twice.

6. For a research manuscript that has already been published (if not yet published, please skip to section 2)

j) **What is the title of the manuscript?**

Preclinical biomarkers of prion infection and neurodegeneration

k) **Please include a link to or doi for the work**

DOI: 10.1016/j.conb.2020.01.009

l) **Where was the work published?**

Current Opinion in Neurobiology

m) **Who published the work?** (e.g. OUP)

Elsevier ScienceDirect

n) **When was the work published?**

April 2020

o) **List the manuscript's authors in the order they appear on the publication**

Mok TH, Mead S.

p) **Was the work peer reviewed?**

No

q) **Have you retained the copyright?**

No

r) **Was an earlier form of the manuscript uploaded to a preprint server?** (e.g. medRxiv). If 'Yes', please give a link or doi)

No

If 'No', please seek permission from the relevant publisher and check the box next to the below statement:

☒

*I acknowledge permission of the publisher named under **1d** to include in this thesis portions of the publication named as included in **1c**.*

7. For a research manuscript prepared for publication but that has not yet been published (if already published, please skip to section 3)

f) **What is the current title of the manuscript?**

Click or tap here to enter text.

g) **Has the manuscript been uploaded to a preprint server?** (e.g. medRxiv; if 'Yes', please give a link or doi)

Click or tap here to enter text.

h) **Where is the work intended to be published?** (e.g. journal names)

Click or tap here to enter text.

i) **List the manuscript's authors in the intended authorship order**

Click or tap here to enter text.

j) **Stage of publication** (e.g. in submission)

Click or tap here to enter text.

8. **For multi-authored work, please give a statement of contribution covering all authors** (if single-author, please skip to section 4)

Mok TH (drafted manuscript), Mead S (supervised and edited manuscript)

9. **In which chapter(s) of your thesis can this material be found?**

Chapter 2

10. **e-Signatures confirming that the information above is accurate** (this form should be co-signed by the supervisor/ senior author unless this is not appropriate, e.g. if the paper was a single-author work)

Candidate

Date:
04/06/2023

Supervisor/ Senior Author (where appropriate)

Date
06/06/2023

UCL Research Paper Declaration Forms

Chapter 3

UCL Research Paper Declaration Form
referencing the doctoral candidate's own published work(s)

Please use this form to declare if parts of your thesis are already available in another format, e.g. if data, text, or figures:

- *have been uploaded to a preprint server*
- *are in submission to a peer-reviewed publication*
- *have been published in a peer-reviewed publication, e.g. journal, textbook.*

This form should be completed as many times as necessary. For instance, if you have seven thesis chapters, two of which containing material that has already been published, you would complete this form twice.

11. For a research manuscript that has already been published (if not yet published, please skip to section 2)

s) **What is the title of the manuscript?**

Variant Creutzfeldt–Jakob Disease in a Patient with Heterozygosity at *PRNP* Codon 129

t) **Please include a link to or doi for the work**

DOI: 10.1056/NEJMc1610003

u) **Where was the work published?**

New England Journal of Medicine

v) **Who published the work?** (e.g. OUP)

New England Journal of Medicine

w) **When was the work published?**

19/01/2017

x) **List the manuscript's authors in the order they appear on the publication**

Tze How Mok

y) **Was the work peer reviewed?**

Tze How Mok, Zane Jaunmuktane, Susan Joiner, Tracy Campbell, Catherine Morgan, Benjamin Wakerley, Farhad Golestani, Peter Rudge, Simon Mead, H Rolf Jäger, Jonathan D F Wadsworth, Sebastian Brandner, John Collinge

z) **Have you retained the copyright?**

No

aa) **Was an earlier form of the manuscript uploaded to a preprint server?** (e.g. medRxiv). If 'Yes', please give a link or doi)

No

If 'No', please seek permission from the relevant publisher and check the box next to the below statement:

☒

*I acknowledge permission of the publisher named under **1d** to include in this thesis portions of the publication named as included in **1c**.*

12. For a research manuscript prepared for publication but that has not yet been published (if already published, please skip to section 3)

k) **What is the current title of the manuscript?**

Click or tap here to enter text.

l) **Has the manuscript been uploaded to a preprint server?** (e.g. medRxiv; if 'Yes', please give a link or doi)

Click or tap here to enter text.

m) **Where is the work intended to be published?** (e.g. journal names)

Click or tap here to enter text.

n) **List the manuscript's authors in the intended authorship order**

Click or tap here to enter text.

o) **Stage of publication** (e.g. in submission)

Click or tap here to enter text.

13. **For multi-authored work, please give a statement of contribution covering all authors** (if single-author, please skip to section 4)

Tze How Mok (reviewed patient, obtained research and autopsy consent, drafted manuscript), Zane Jaunmuktane (performed autopsy and histological analyses, and contributed to manuscript), Susan Joiner (performed immunoblotting and molecular strain typing from brain homogenate), Tracy Campbell (sequenced prion protein gene), Catherine Morgan (patient's primary physician and contributed to manuscript), Benjamin Wakerley (patient's primary physician and contributed to manuscript), Farhad Golestani (patient's primary physician and contributed to manuscript), Peter Rudge (contributed to manuscript), Simon Mead (contributed to manuscript), H Rolf Jäger (provided MRI illustration, contributed to manuscript), Jonathan D F Wadsworth (performed immunoblotting and molecular strain typing from brain homogenate, contributed to manuscript), Sebastian Brandner (performed autopsy and histological analyses, and contributed to manuscript), John Collinge (head of Unit and contributed to manuscript)

14. **In which chapter(s) of your thesis can this material be found?**

Chapter 3

15. **e-Signatures confirming that the information above is accurate** (this form should be co-signed by the supervisor/ senior author unless this is not appropriate, e.g. if the paper was a single-author work)

Candidate

Date:
04/06/2023

Supervisor/ Senior Author (where appropriate)

Date
06/06/2023

UCL Research Paper Declaration Forms

Chapter 4

UCL Research Paper Declaration Form
referencing the doctoral candidate's own published work(s)

Please use this form to declare if parts of your thesis are already available in another format, e.g. if data, text, or figures:

- *have been uploaded to a preprint server*
- *are in submission to a peer-reviewed publication*
- *have been published in a peer-reviewed publication, e.g. journal, textbook.*

This form should be completed as many times as necessary. For instance, if you have seven thesis chapters, two of which containing material that has already been published, you would complete this form twice.

16. For a research manuscript that has already been published (if not yet published, please skip to section 2)

bb) **What is the title of the manuscript?**

Evaluating the causality of novel sequence variants in the prion protein gene by example

cc) **Please include a link to or doi for the work**

https://doi.org/10.1016/j.neurobiolaging.2018.05.011

dd) **Where was the work published?**

Neurobiology of Aging

ee) **Who published the work?** (e.g. OUP)

Elsevier ScienceDirect

ff) **When was the work published?**

November 2018

gg) **List the manuscript's authors in the order they appear on the publication**

Tze How Mok, Carolin Koriath, Zane Jaunmuktane, Tracy Campbell, Susan Joiner, Jonathan D.F. Wadsworth, Laszlo L.P. Hosszu, Sebastian Brandner, Ambereen Parvez, Thomas Clement Truelsen, Eva Løbner Lund, Romi Saha, John Collinge, Simon Mead

hh) **Was the work peer reviewed?**

Yes

ii) **Have you retained the copyright?**

Yes

jj) **Was an earlier form of the manuscript uploaded to a preprint server?** (e.g. medRxiv). If 'Yes', please give a link or doi)

No

If 'No', please seek permission from the relevant publisher and check the box next to the below statement:

☒

*I acknowledge permission of the publisher named under **1d** to include in this thesis portions of the publication named as included in **1c**.*

17. For a research manuscript prepared for publication but that has not yet been published (if already published, please skip to section 3)

p) **What is the current title of the manuscript?**

Click or tap here to enter text.

q) **Has the manuscript been uploaded to a preprint server?** (e.g. medRxiv; if 'Yes', please give a link or doi)

Click or tap here to enter text.

r) **Where is the work intended to be published?** (e.g. journal names)

Click or tap here to enter text.

s) **List the manuscript's authors in the intended authorship order**

Click or tap here to enter text.

t) **Stage of publication** (e.g. in submission)

Click or tap here to enter text.

18. **For multi-authored work, please give a statement of contribution covering all authors** (if single-author, please skip to section 4)

Tze How Mok (conception, patient recruitment, drafted most of manuscript), Carolin Koriath (performed in silico analyses and contributed to manuscript), Zane Jaunmuktane (histological examination of brain material and drafted significant portion of manuscript and illustration), Tracy Campbell (sequenced prion protein gene), Susan Joiner (performed immunoblotting and molecular strain typing), Jonathan D.F. Wadsworth (performed immunoblotting and molecular strain typing, and draft significant portion of manuscript), Laszlo L.P. Hosszu (protein structural analyses and provided illustration, and drat significant portion of manuscript), Sebastian Brandner (histological examination of brain material and drafted significant portion of manuscript and illustration), Ambereen Parvez (primary physician of patient, and contributed to manuscript), Thomas Clement Truelsen (primary physician of patient, and contributed to manuscript), Eva Løbner Lund (provided brain material), Romi Saha (primary physician of patient, and contributed to manuscript), John Collinge (oversight and contributed to manuscript), Simon Mead (oversight and drafted/edited significant portions of manuscript)

19. **In which chapter(s) of your thesis can this material be found?**

Chapter 4

20. **e-Signatures confirming that the information above is accurate** (this form should be co-signed by the supervisor/ senior author unless this is not appropriate, e.g. if the paper was a single-author work)

Candidate

[redacted]

Date:
04/06/2023

Supervisor/ Senior Author (where appropriate)

[redacted]

Date
06/06/2023

UCL Research Paper Declaration Form
referencing the doctoral candidate's own published work(s)

Please use this form to declare if parts of your thesis are already available in another format, e.g. if data, text, or figures:

- *have been uploaded to a preprint server*
- *are in submission to a peer-reviewed publication*
- *have been published in a peer-reviewed publication, e.g. journal, textbook.*

This form should be completed as many times as necessary. For instance, if you have seven thesis chapters, two of which containing material that has already been published, you would complete this form twice.

21. For a research manuscript that has already been published (if not yet published, please skip to section 2)

kk) **What is the title of the manuscript?**

Characterization of Prion Disease Associated with a Two-Octapeptide Repeat Insertion

ll) **Please include a link to or doi for the work**

doi: 10.3390/v13091794

mm) **Where was the work published?**

Viruses

nn) **Who published the work?** (e.g. OUP)

MDPI

oo) **When was the work published?**

September 2021

pp) **List the manuscript's authors in the order they appear on the publication**

Nicholas Brennecke, Ignazio Cali, Tze How Mok, Helen Speedy, Genomics England Research Consortium, Laszlo L. P. Hosszu, Christiane Stehmann, Laura Cracco, Gianfranco Puoti, Thomas W. Prior, Mark L. Cohen, Steven J. Collins, Simon Mead, and Brian S. Appleby

qq) **Was the work peer reviewed?**

Yes

rr) **Have you retained the copyright?**

Yes

ss) **Was an earlier form of the manuscript uploaded to a preprint server?** (e.g. medRxiv). If 'Yes', please give a link or doi)

No

If 'No', please seek permission from the relevant publisher and check the box next to the below statement:

☒

*I acknowledge permission of the publisher named under **1d** to include in this thesis portions of the publication named as included in **1c**.*

22. For a research manuscript prepared for publication but that has not yet been published (if already published, please skip to section 3)

u) **What is the current title of the manuscript?**

Click or tap here to enter text.

v) **Has the manuscript been uploaded to a preprint server?** (e.g. medRxiv; if 'Yes', please give a link or doi)

Click or tap here to enter text.

w) **Where is the work intended to be published?** (e.g. journal names)

Click or tap here to enter text.

x) **List the manuscript's authors in the intended authorship order**

Click or tap here to enter text.

y) **Stage of publication** (e.g. in submission)

Click or tap here to enter text.

23. **For multi-authored work, please give a statement of contribution covering all authors** (if single-author, please skip to section 4)

Nicholas Brennecke (acquired and analyzed data and drafted a significant portion of the manuscript), Ignazio Cali (acquired and analyzed data and drafted a significant portion of the manuscript), Tze How Mok (acquired some data, analyzed data (penetrance estimation) and drafted a significant portion of the manuscript), Helen Speedy (acquired and analyzed data), Genomics England Research Consortium, Laszlo L. P. Hosszu (drafted a significant portion of the manuscript), Christiane Stehmann (drafted a significant portion of the manuscript), Laura Cracco (drafted a significant portion of the manuscript), Gianfranco Puoti (drafted a significant portion of the manuscript), Thomas W. Prior (drafted a significant portion of the manuscript), Mark L. Cohen (drafted a significant portion of the manuscript), Steven J. Collins (drafted a significant portion of the manuscript), Simon Mead (contribute to conception and design of the study, acquired and analyzed data, and drafted/edited the manuscript), and Brian S. Appleby (contribute to conception and design of the study, acquired and analyzed data, and drafted/edited the manuscript).

24. **In which chapter(s) of your thesis can this material be found?**

Chapter 4

25. **e-Signatures confirming that the information above is accurate** (this form should be co-signed by the supervisor/ senior author unless this is not appropriate, e.g. if the paper was a single-author work)

Candidate

[redacted]

Date:
04/06/2023

Supervisor/ Senior Author (where appropriate)

[redacted]

Date
06/06/2023

TABLE OF CONTENTS

LIST OF FIGURES

LIST OF TABLES

LIST OF ABBREVIATIONS

-AR (suffix)	at-risk e.g. IPD at-risk (IPD-AR)
AD	Alzheimer's disease
ADC	apparent diffusion-coefficient
ANOVA	analysis of variance
BH	brain homogenate
BSE	bovine spongiform encephalopathy
BV	bank vole
c-hGH	cadaver-sourced human growth hormone
C-terminus	carboxy-terminus
c129	codon 129
c129M	codon 129 methionine
c129V	codon 129 valine
CADD	Combined Annotation Dependent Depletion
CJD	Creutzfeldt-Jakob disease
Cryo-EM	cryogenic electron microscopy
CSF	cerebrospinal fluid
CSF-N	CSF for neurodegenerative markers
CSF-R	CSF for RT-QuIC
CV	coefficient of variance
DNA	deoxyribonucleic acid
DWI	diffusion-weighted imaging
EDTA	ethylenediaminetetraacetic acid tetrasodium
EEG	electroencephalogram
EMG	electromyography
fCJD	familial CJD
FDG-PET	fluorodeoxyglucose positron emission tomography
FFI	fatal familial insomnia
FL	full-length
GAL3ST1	human galactose-3-O-sulfotransferase 1 gene
GENFI	Genetic Frontotemporal Dementia Initiative
GFAP	glial fibrillary acidic protein
gnomAD	genome associated database

GPI	glycosylinositolphosphatidyl
GSS	Gerstmann-Straussler-Scheinker
GWAS	genome-wide association study
H&E	haematoxylin and eosin
Ha90	truncated hamster (rPrP)
HC	healthy control
HC90	90th percentile of healthy controls
his-tags	histidine tags
Hu	human (referring to rPrP)
iCJD	iatrogenic CJD
IPD	inherited prion disease
IPD-AR < 2y	IPD at-risk less than 2 years to onset
IPD-AR > 2y	IPD at-risk greater than 2 years to onset
IQ-CSF	second generation (RT-QuIC)
IQR	interquartile range
MM	methionine homozygous
MRC	Medical Research Council
MRI	magnetic resonance imaging
MV	methionine-valine heterozygous
N-terminus	amino-terminus
N4PB	neurology 4-plex panel B (Simoa)
NfL	neurofilament light
NHNN	National Hospital for Neurology & Neurosurgery
NHNN-NiCL	Neuroimmunology Laboratory at NHNN
NHS	National Health Service
NIH	National Institutes of Health
NiNTA	nickel nitrilotriacetic acid
NPC	National Prion Clinic
NPDPSC	National Prion Disease Pathology Surveillance Center
NPMC	National Prion Monitoring Cohort
OPRI	octapeptide insertion
PBS	phosphate buffer solution
PK	proteinase K

PMCA	protein misfolding cyclic amplification
PolyPhen-2	Polymorphism Phenotyping version 2
PQ-CSF	first generation (RT-QuIC)
PRNP	human prion protein gene
PrP	prion protein
PrP^{C}	cellular prion protein
PrP^{D}	detergent-insoluble prion protein
PrP^{Sc}	protease-resistant prion protein
QuIC	quaking-induced conversion
$resPrP^{D}$	detergent-insoluble PK-resistant PrP (see also PrP^{Sc})
RFU	relative fluorescence unit
RML	Rocky Mountain Laboratories
RNA	ribonucleic acid
rPrP	recombinant PrP
RT-QuIC	real-time quaking-induced conversion
sCJD	sporadic CJD
SD	standard deviation
SD_{50}	seeding dose 50
SDS	sodium dodecyl sulphate
SIFT	Sorting Intolerant From Tolerant
Simoa	single molecule array
STX6	human syntaxin 6 gene
ThT	thioflavin T
UCH-L1	ubiquitin carboxy-terminal hydrolase L1
UK	United Kingdom
vCJD	variant CJD
VV	valine homozygous
w/v	weight per volume
YOAD	Young onset Alzheimer’s dementia

ABSTRACT

Healthy individuals at risk of prion disease are expected to exhibit subclinical prion replication followed by emergence of toxicity, heralding proximity to clinical onset, based on mouse inoculation studies. This silent incubation period, if recapitulated in humans, will be amenable to fluid biomarker discovery which may inform study designs for preventative strategies.

The central output of this thesis revolves around testing a longitudinal biofluid archive assembled from individuals with high lifetime risk of prion disease, including 16 whom subsequently developed inherited prion disease (IPD), using real-time quaking-induced conversion (RT-QuIC) assay and single molecule array platforms. Two distinct biomarker trajectories, depending on speed of clinical evolution, were discerned. CSF RT-QuIC seeding activity was detectable with over three years' follow-up in asymptomatic E200K (fast IPD) mutation carriers, but with no definable presymptomatic neurodegenerative phase in one converter. In contrast, P102L (slow IPD) mutation carriers showed sequential rises in plasma glial fibrillary acidic protein followed by neurofilament light up to four years pre-conversion; a bespoke P102L RT-QuIC assay was only partially sensitive. Consequently, we propose a new preclinical staging system featuring clinical, seeding and neurodegeneration components, for validation with larger prion at-risk cohorts, and with potential application to other neurodegenerative proteopathies.

Additionally, we tackled uncertainties that exist over disease penetrance for specific at-risk populations, with implications on epidemiological case definition, and study/trial enrolment eligibility. Firstly, we highlighted the clinical resemblance to sporadic CJD, and necessity of autopsy confirmation, in the first definite case of variant CJD in an individual heterozygous at *PRNP* codon 129, raising concerns over disease surveillance accuracy and ascertainment of population risk. Secondly, we interrogated multiple lines of evidence to resolve ambiguities over the penetrance of rare *PRNP* variants – T201S and 2-OPRI, resulting in their reclassification as either benign or low-risk variants, thus avoiding erroneous inclusion into primary prevention studies/trials.

IMPACT STATEMENT

One of the central enigmas in human prion disease is the remarkably long incubation periods, followed typically by rapid clinical decline. Vital insights from mouse inoculation studies indicate that high infectious prion titres are maintained for a considerable time prior to clinical onset, which if recapitulated in humans, would underpin the observed incubation period and allow for discovering fluid biomarkers capable of predicting proximity to clinical onset in individuals at risk of prion disease.

In our biomarker study, we found distinct biomarker trajectories in fast and slow IPDs. Specifically, we identified several years of presymptomatic seeding activity in E200K, a new proximity marker (plasma GFAP) and sequential neurodegenerative marker evolution (plasma GFAP followed by NfL) in slow IPDs. Elucidation of prodromal fluid biomarker evolution is crucial for healthy at-risk individuals due to its potential influences on therapeutic strategies, which are shifting increasingly towards prevention. Proximity biomarkers can be wielded for risk stratification, enrichment, or as pharmacodynamic endpoints to overcome the infeasibility of adequately powering conventional trials based on simple clinical endpoints, as a result of low annual conversion rates. The long presymptomatic seeding phases have wider relevance to proteopathic neurodegenerative diseases, for which similar seed amplification assays can be developed.

On a personal level, this is highly consequential information which may profoundly affect life choices (e.g. career, family, finances, wills), if an at-risk individual decides to avail of it. For those who suffer from debilitating psychological burden of being at risk, a negative result may be highly reassuring. Indeed, these were the scenarios that were raised and debated by at-risk audience members during our recent Open Day in 2022.

Clearly, larger studies are required to build confidence in observed patterns of biomarker trajectories before allowing these data to be used as above. An oral platform presentation of this work at Prion 2022 in Gottingen sparked significant interest

amongst researchers independently conducting similar studies across Europe, the Middle East and in North America, leading to a preliminary multinational meeting with view to further collaboration.

We reported the first autopsy-confirmed case of vCJD in a patient heterozygous at *PRNP* codon 129, finally putting to bed any doubts as to whether non-129 MM individuals are susceptible to vCJD. This provoked questions about the accuracy of vCJD case ascertainment and the true extent of the population at risk, prompting a call for research proposals from Department of Health & Social Care to address questions posed.

Finally, we drew up a framework drawn from different lines of evidence to evaluate the penetrance of the rare T201S *PRNP* variant, and subsequently applied it to 2-OPRI. This resulted in reclassification of both variants as either benign or low-risk variants, providing reassurance to at-risk relatives, and eschewing the need for predictive testing of at-risk relatives and inclusion into studies of at-risk individuals. We anticipate that this framework can employed to evaluate novel, or other *PRNP* variants of unknown significance provided the necessary information is available.

CHAPTER 1

Introduction to prion disease

General introduction and history of prion discovery

Prion diseases, otherwise known as transmissible spongiform encephalopathies, are a group of lethal and transmissible neurodegenerative diseases affecting both humans and other mammalian species which have provoked intense scientific, media and even political interest particularly in the latter half of the 20th century. In humans it manifests most commonly as sporadic Creutzfeldt-Jakob disease (sCJD) in about 85% of cases, autosomal dominantly inherited prion disease (IPD) in 10-15% of cases, and very rarely as iatrogenic CJD (iCJD) or variant CJD (vCJD) by medical or dietary exposures. Notable prion diseases occurring "naturally" in other mammals include scrapie in sheep, bovine spongiform encephalopathy (BSE) in cattle, transmissible mink encephalopathy in mink, and chronic wasting disease in cervids.

The singularity of prion biology pivots on the fact it is a proteinaceous infectious (prion) agent completely devoid of nucleic acids, which forms the basis of the now accepted "protein-only" hypothesis. Although scrapie, the earliest documented prion disease, entered official records as early as the 1700s in Western Europe, very little was known about its cause, nor its connection to other mammalian prion diseases until well into the 20th century. Nevertheless, its contagious nature, and the efficacy of isolation in stemming the spread amongst a flock were well-recognised over 260 years ago. Subsequent research in the 1800s did uncover spongiosis as a disease hallmark in neuropathological studies, but early efforts to transmit scrapie by inoculation failed merely because the animals were not observed for sufficient time to allow for the long incubation periods (> 18 months)[1]. In the 1920s, the first neuropathological accounts of human prion disease emerged independently from Hans Gerhard Creutzfeldt, and Alfons Maria Jakob, followed by description of familial prion disease by Meggendorfer in the 1930s. However, their significance and links went relatively unappreciated in the next few decades while major discoveries emerged from the study of scrapie, and subsequently a new human prion disease called kuru.

Firstly, with the appropriate duration of observation, scrapie was eventually transmitted to healthy sheep through intraocular inoculation of neural tissue from affected sheep in 1936[2]. Subsequently, all the historical observations supporting its

transmissibility were proven beyond doubt, *incidentally*, through louping ill vaccination using formalin-treated neurovisceral extracts, which of course killed the virus but not the "scrapie agent", causing an outbreak[3]. Secondly, an epidemic of a new neurodegenerative disease linked to ritualistic cannibalism was discovered in the Fore linguistic group of the Eastern Highlands of Papua New Guinea, with intense study culminating in contemporaneous but ultimately unifying observation by Hadlow that its brain pathology resembles that of scrapie[4], and by Klatzo, sporadic CJD (sCJD)[5]. Within a decade, successful experimental transmissions into chimpanzees, first from human kuru brain tissue[6], and then CJD[7], ensued. In the era during which the "central dogma" of molecular biology was ascendant following the discovery of the structure of DNA in 1953[8], these latter discoveries were unsurprisingly attributed to "slow virus" infections, a term first coined by Sigurdsson in the study of scrapie and visna in Icelandic sheep[9]. However, in the 1960s, seemingly radical theories against the grain arose[10,11], with experiments demonstrating the lack of efficacy of ionising radiation, heat and formalin against transmissibility of the scrapie agent, all indicating a mechanism independent of nucleic acids[12-15].

The "protein-only" hypothesis was eventually crystallised in a series of experiments by Stanley Prusiner published in 1982 which demonstrated inactivation of transmissibility of the "scrapie agent" by established protein denaturants, but untouched by nucleases, ultraviolet radiation, psoralen, $Zn(NO_3)_2$, and hydroxylamine chemical modification[16], which attack RNA and DNA. Despite ferocious rebuff from certain quarters of the scientific community, this ignited a surge of research activity and discoveries leading to the elucidation of the prion protein gene (*PRNP*), structure, chemical biochemistry, strain biology, and translation into clinical diagnostics and eventually promising therapeutics.

Prion protein gene (*PRNP*), prion protein (PrP) and prions

In the years following publication of the “protein-only” hypothesis, efforts ensued to unravel the amino acid sequence of PrP and coding sequence of the PrP gene. This began by studying the PrP 27-30 Proteinase K (PK) resistant fragment (PrP^{Sc}) found in scrapie-infected Syrian hamster brains by enrichment, leading to determination of the N-terminus amino acid sequence and mRNA transcript, both shown to be present in both scrapie-infected and uninfected brains[17,18]. Subsequently, cloning experiments employing the cDNA sequence successfully fished out the PrP gene sequence in scrapie-affected hamster brain DNA, and murine and human DNA[19]. The determination of the complete PrP gene sequences in hamster, mouse and human (*PRNP*) soon followed[20,21].

The *PRNP* locus is situated on the short arm of chromosome 20; it contains two exons, with the complete open reading frame being found in the larger exon. Human PrP, comprising 253 amino acids, is entirely encoded within this ORF. Post-translational modifications prior to its attachment to the cell membrane by glycosylinositolphosphatidyl (GPI) anchoring includes cleavage of an N-terminus signal peptide and C-terminus peptide, and N-glycosylation at residues 181 and 197. In its folded state, the N-terminus domain in the mature PrP is unstructured and harbours an octapeptide repeat region, which consists of a nonapeptide followed by four octapeptides. Insertions of four octapeptides or more have been unequivocally proven to be pathogenic. In comparison, the C-terminus domain is highly structured with three α-helices, a single disulphide bond, and a native two-strand anti-parallel β-sheet[22-24].

Polymorphisms within the PrP amino acid sequence are known to have profound influence on various aspects of prion biology including disease susceptibility, clinical phenotype, survival, neuropathology, and molecular strain typing. For example, in humans, *PRNP* codon 129 genotype (c129) heterozygosity (methionine-valine) is associated with slower disease progression, longer survival, and often with ataxic

onset[25,26]; it also confers protection against susceptibility to vCJD[27-30]. One of the most striking examples of c129 genotype effect on clinical phenotypic expression is the differential manifestation of the D178N mutation either as fatal familial insomnia (FFI) or familial CJD (fCJD) depending on whether it is co-allelic with 129M or 129V, though some overlap has been observed[31-33]. Examples of protective *PRNP* polymorphisms aside from c129 include the G127V against kuru and the E219K in Far Eastern populations against sCJD but not vCJD[34-37]. In addition to *PRNP* polymorphisms, the largest GWAS study for sCJD to date also found novel loci – *STX6* and *GAL3ST1*, elsewhere that implicate alterations in sphingolipid metabolism and endosomal transport respectively in risk of developing the disease[38].

It is now fully accepted that prion diseases are characterised by the accumulation of multimeric assemblies composed of abnormal PrP isoforms. These result from conformational shift of the predominantly α-helical, soluble, monomeric host-encoded cellular PrP (PrP^{C}) to the β-sheet rich fibrillar isoforms which are prone to aggregation. A proportion of these disease-related PrP isoforms (prions), are detergent-insoluble and resistant to partial PK-digestion, known as PrP^{Sc}[39,40]. Different disease isoforms, each with their own distinct chemical and biophysical properties despite identical PrP primary structure, can co-propagate within a single host, giving rise to the concept of prion strain conformational selection model[41]. Prion strain properties can be faithfully maintained through serial passages in animal transmissions, and its protean conformational diversity has historically been most commonly inferred from distinct PrP^{Sc} fragments on Western Blotting or by glycoform ratio analyses[42,43]. Recent noteworthy advances in cryogenic electron microscopy (cryo-EM) visualisation of purified *ex vivo* hamster and mouse-adapted prions have not only cemented the parallel in-register intermolecular β-sheet (PIRIBS) as the shared core structural configuration, but also shed light into how ultrastructural variations encipher strain diversity[44-46].

There is no doubt that prion propagation through autocatalytic conversion of PrP^{C} to disease-related PrP isoforms by templated recruitment is a fundamental requirement for pathogenesis. However, evidence abounds for subclinical prion infection where animals have been observed to harbour high levels of infectious prions despite normal lifespans and without exhibiting any signs of disease, suggesting that neurotoxicity is

not necessarily an inevitable consequence[47]. Correspondingly, one of the most remarkable aspects of human prion disease is the apparent long incubation phase between prion infection/exposure and disease onset, lasting up to five decades in kuru and cadaver-sourced human growth hormone-related iCJD, followed typically by rapid clinical decline and death within months[48,49]. Fortunately for the field, prions are reliably transmissible by inoculation to laboratory inbred mouse lines which similarly exhibit a prolonged incubation phase, but most crucially have minimal variation in disease onsets. This has allowed for the elucidation of the sequence of prion infection, propagation and toxicity, shown to involve two mechanistically distinct phases. Specifically, following inoculation, infectious prion titres rise exponentially to reach a plateau, which continues for a considerable time until disease onset. Infectivity and toxicity are therefore uncoupled, with the length of the plateau being inversely proportional to PrP expression level (Figure 1)[50,51]. If this two-phase kinetics model is applicable to human disease, the clinically silent incubation phase marked by high prion titres hypothetically offers a window of opportunity for discovery of fluid biomarkers that predict proximity to onset e.g. potential dynamic changes in measures of seeding activity and/or neurodegenerative markers. Moreover, if borne out in humans, the two-phase kinetics model would provide a foundation for targeted primary prevention strategies in prion disease[52,53].

.

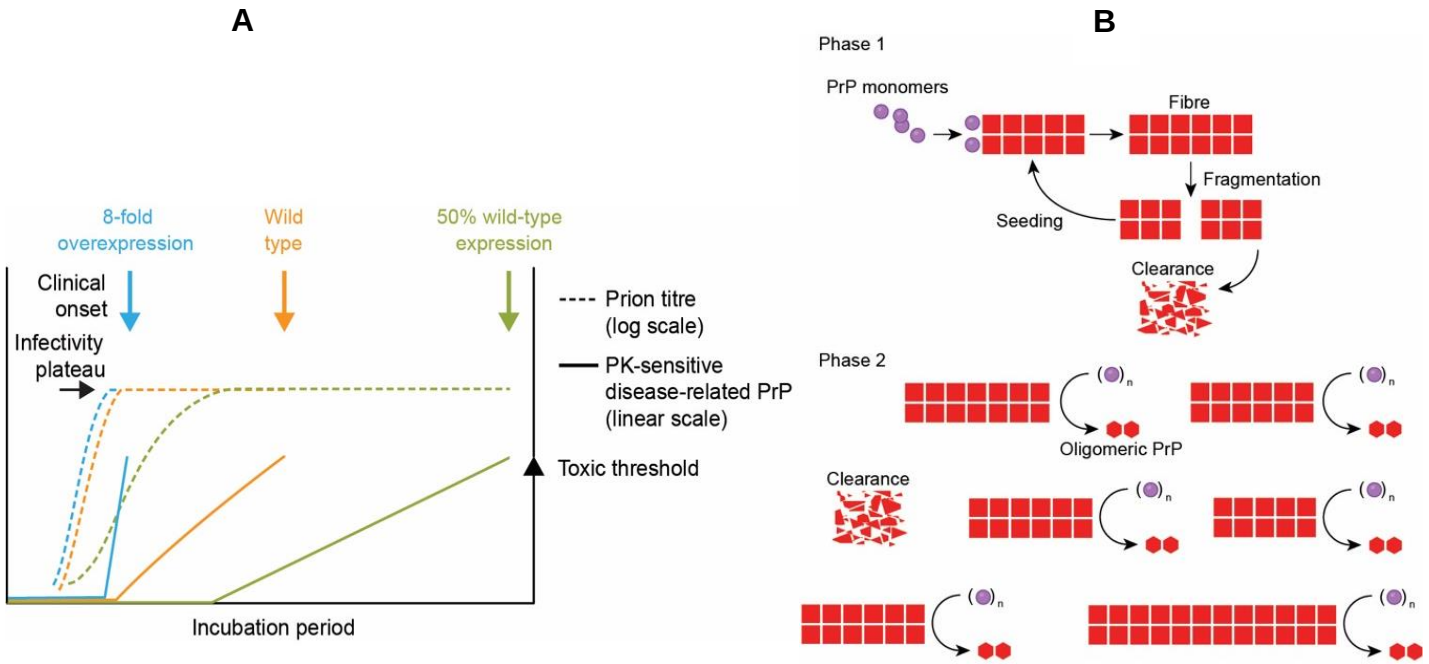

Figure 1The two-phase kinetics model derived from Rocky Mountain Laboratory (RML) prion propagation.

(**A**) This graph shows the propagation of RML prions in brains in 3 lines of congenic mice expressing different levels of PrP^C – wild-type level (orange), 8-fold overexpression (blue), and 50% wild type level (green). Levels of infectious prions (dotted lines), measured in log(infectious units) by the Scrapie Cell Assay, show exponential rises to a maximal plateau (infectivity plateau) within days, regardless of PrP^C expression levels [(**B**) Phase 1)]. This clinically silent incubation phase of saturated infectivity [(B) Phase 2)] continues until clinical onset marked by downward vertical arrows, with the length of the incubation phase being inversely proportional to PrP^C expression level. At the transition between the exponential and plateau phases, levels of PK-sensitive disease-associated PrP isoforms increase in a linear fashion at the rate proportional to the PrP^C expression level. Clinical onset occurs once a common toxic threshold of PK-sensitive disease-associated PrP isoforms is exceeded regardless of PrP^C expression level. (**B**) Once prion propagation is saturated by autocatalytic conversion (Phase 1), there is a pathway ”switch” to production of toxic PrP species (Phase 2) in a process now dependent on PrP^C concentration. Reproduced from Collinge 2016; DOI: 10.1038/nature20415.

Human prion disease

Sporadic CJD (sCJD)

sCJD is the most commonly encountered human prion disease worldwide, with an annual incidence of 1-2 per million population[54]. Consistent with its nomenclature, sCJD most likely arises from rare stochastic event involving conformational shift of PrP^{C} into disease-associated isoforms capable of initiating the cascade of infectivity, saturation and toxicity reflected in the two-phase kinetics model of prion propagation. Extensive discourse about alternative explanations including yet identified environmental causes or unrecognised iatrogenic exposures, mainly through case-control studies over 20 years, have been inconclusive at best[55,56].

Clinically, it typically presents as with the triad of rapid cognitive decline, ataxia and/or myoclonus, with a median survival of 5 months from diagnosis; peak incidence is in the UK is between 70-75 years of age[57]. Other distinct CJD clinical phenotypes such include the Heidenhain variant with predominant higher visual dysfunction at onset, the slowly progressive ataxic variant, thalamic (sporadic fatal insomnia), pure cognitive and neuropsychiatric onset; it can also mimic other neurological/neurodegenerative diseases with presentations almost identical to stroke, Alzheimer's disease (AD), and corticobasal syndrome[58]. Factors associated with longer survival include younger age at onset, female sex and *PRNP* c129 heterozygosity[25,26].

Neuropathology, either through autopsy or brain biopsy, endures as the sole means of achieving a definitive diagnosis, by demonstrating the presence of spongiosis, astrogliosis and neuronal loss, associated with abnormal PrP immunohistochemical staining patterns. Western blotting of brain material after partial PK-digestion characteristically yields three PrP^{Sc} fragments of different motility patterns, allowing for molecular typing, classifiable according to either the Parchi or the London systems; for this thesis, the London classification is the default reference system[42,59].

Recent advances in MRI brain imaging [diffusion-weighted imaging (DWI)] and seed amplification assays [real-time quaking-induced conversion (RT-QuIC)] have boosted

in-life diagnostic sensitivity to over 90% and with a specificity close to 100%[60-63]. These have largely superseded fluid biomarkers such as CSF protein 14-3-3, and the finding of generalised periodic sharp wave complexes on electroencephalogram (EEG), though they still possess some supportive diagnostic utility in certain circumstances.

Inherited prion disease (IPD)

Over 60 *PRNP* mutations covering missense, structural and truncation mutations, of varying penetrance are known to date (Figure 2). The pattern of inheritance for the archetypal IPDs e.g. E200K, D178N, P102L and large OPRIs, is autosomal dominant with almost complete penetrance, but pathogenic mutations with partial penetrance are also known e.g. Q212P and V210I[64-66]. Mutation carriers undergo seemingly normal neurodevelopment and are completely asymptomatic until conversion typically in later life with 6-OPRI being the exception where a premorbid personality disorder has been suspected but never conclusively proven[67]. Unlike familial AD or frontotemporal dementia, IPDs are notorious for their highly variable ages at onset with standard deviations of ~10 years around their respective means, an issue which will be further addressed later on in Chapter 2 (Estimating proximity to conversion in IPD-AR individuals) As such, even in *PRNP* mutations associated with high penetrance, the annual risk of conversion remains low[65].

In the early days following the discovery of *PRNP* pathogenic mutations, at which point they were only a handful, IPDs were classified on the basis of their clinical phenotypic expressions into three canonical or eponymous syndromes i.e. fCJD (E200K), FFI (D178N) and Gerstmann-Straussler-Scheinker syndrome (GSS, typically P102L)[68]. This endured even as more pathogenic mutations (and phenotypic diversity) came to light, and these categories increasingly seemed unnecessarily restrictive. For example, other long-duration IPDs (e.g. large OPRIs, P105L, P105S, A117V, F198S, and H187R) tended to be condensed into the GSS category despite significant divergence from the original description for P102L-GSS; furthermore, this appeared to ignore the distinct clinical phenotypes can result from the same mutation e.g. fCJD and pure cognitive-behavioural phenotypes in P102L, and classical and fCJD phenotypes in 4-, 5- and 6-OPRIs. This archaic system also failed to incorporate a

completely novel category of IPD caused by truncation mutations such as Y163X resulting in PrP systemic amyloidosis. Given the genotype-phenotype variation, reference to the precise *PRNP* mutation is preferred over syndromic/eponymous reference. In this thesis, GSS will only be used in the context of the original P102L clinical description.

IPDs in general share some core neuropathological features with sCJD with regards to spongiosis (but with regional variability depending on mutation), astrogliosis and neuronal loss. There are, however, fairly specific abnormal PrP immunohistochemical staining patterns observed in IPDs such as large multicentric plaques in P102L-GSS, “striped” or “tigroid” cerebellar staining perpendicular to pial surface, filamentous white matter deposits in predominantly N-terminus mutations, and PrP amyloid angiopathy in C-terminus truncation mutations; synaptic labelling in E200K is indistinguishable from that seen in sCJD[69-71]. Western blotting of IPD brain homogenates usually show the typical three PrP^{Sc} bands with different migration patterns, but a single low molecular weight band at ~8 kDa isolation is also seen, sometimes in isolation. Molecular typing by PrP^{Sc} glycoform ratios demonstrate that *PRNP* point mutations have a different ratio to sCJD and large OPRIs, the latter two being identical[43].

In a comprehensive review of IPD worldwide literature, four highly-penetrant mutations – E200K, P102L, D178N and OPRIs, were found to account for over 70% of all cases compiled[72]. As such, there is worth in reviewing key clinicopathological aspects of these well-represented mutations. In IPD, as in sCJD, *PRNP* c129 (and c219) genotype has a significant disease modifying effects, with heterozygosity overall being associated with delayed ages at onset.

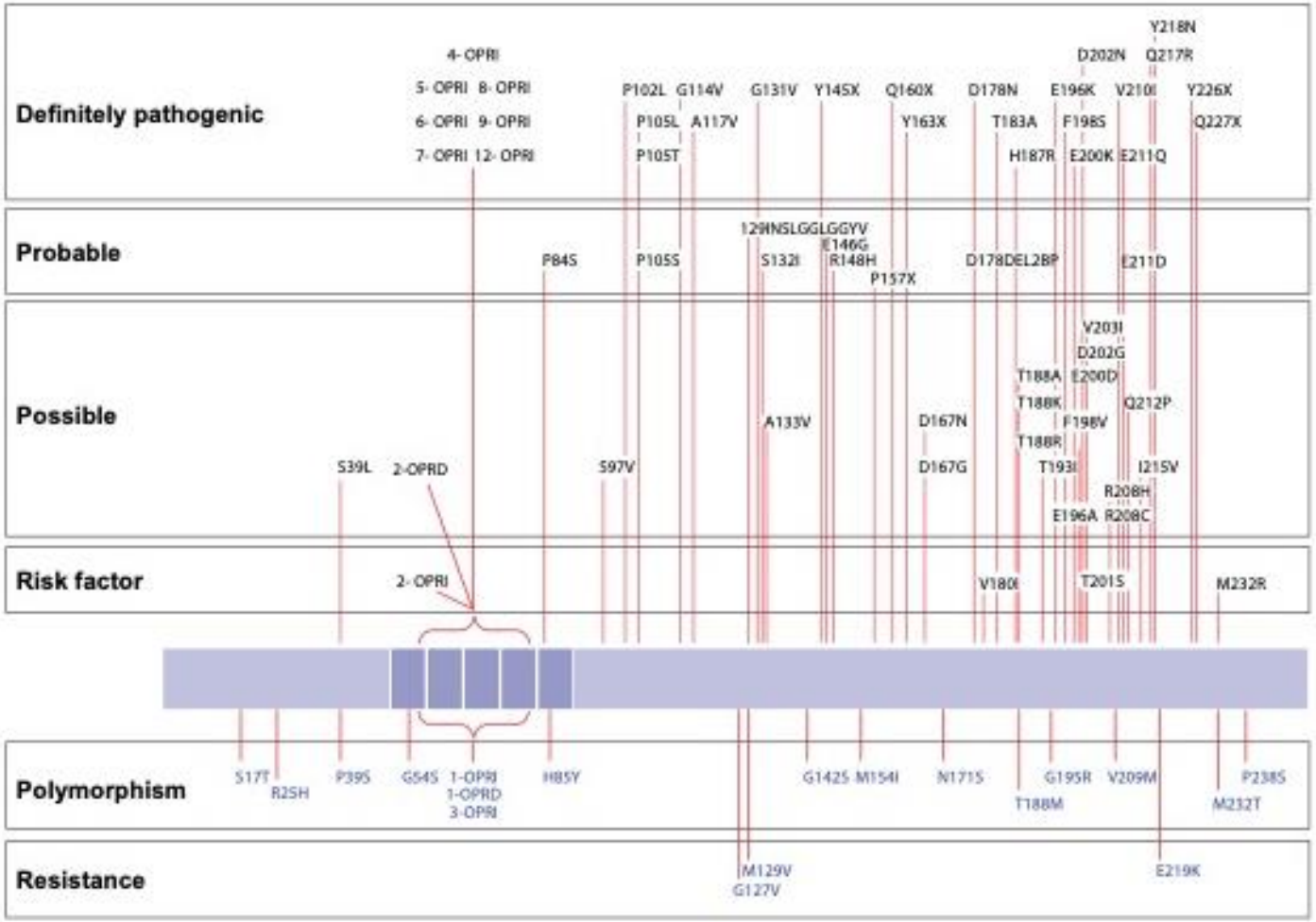

Figure 2 Mutations in the prion protein gene (*PRNP*) known to date, classified by pathogenicity.

PRNP mutations, graded by pathogenicity are shown above the bar representing the PrP amino acid sequence (N-terminus *left*; C-terminus *right*), while benign polymorphisms and protective mutations are shown below.

E200K

E200K IPD is perhaps the *PRNP* mutation associated with the least marked clinical phenotypic diversity here; the entire gamut of its clinical manifestation can be encapsulated by phenotypic variations seen within sCJD[73,74]. Unsurprisingly it is the most common IPD found in surveillance datasets which are naturally biased towards CJD-like phenotypes. E200K has been found to cluster in Libyan Jews, and in Slovakia where its incidence outstrips that of sCJD[75,76]. The updated mean (± SD) age of onset is 61.3 ± 10 years, which is lower than that of sCJD[77]. Other *PRNP* mutations exclusively associated with the fCJD phenotype include V210I, E196K and D178N-129V.

The MRI Brain in affected individuals show restricted diffusion in the deep nuclei and/or cortical ribbon identical to sCJD[78]. Neuropathological findings are again similar to sCJD with the exception of the “striped” or “tigroid” PrP deposition pattern that has been observed in association with at least one c129M allele, and very occasional filamentous subcortical white matter PrP deposition[70,79]. CSF RT-QuIC results for E200K fCJD aggregated from testing large CJD surveillance datasets suggest a high sensitivity comparable to that of sCJD[80-83].

P102L

P102L is the second pathogenic *PRNP* mutation discovered to be linked to inherited prion disease in 1989[84]. However, recorded description of its clinical manifestation predates this by over 50 years in members of the Austrian ‘H’ family. In the earlier half of the 20th century, affected family members were frequently misdiagnosed to have syphilitic tabes dorsalis by their local doctors[68].

The quintessential GSS clinical syndrome features slowly progressive cerebellar ataxia, distal lower limb sensory loss and pain, subtle pyramidal signs (extensor plantars) and a mild frontal dysexecutive syndrome at onset, with clear-cut cognitive impairment only arising much later in the course of the disease. The mean age at onset (± SD) is 53.7 ± 10.6 years, and the mean duration of illness (± SD) is 49 (4

years) ± 26.1 months, range from 7 – 132 months[85]. Due to the subtlety of symptoms and signs in the early course of the disease and the insidious progression, precise determination of the point of clinical conversion has been notoriously difficult. Clinical neurophysiological studies reveal abnormal thermal thresholds (warm first) and loss of the H-reflex around the time of diagnosis, or earlier in the presymptomatic stage demonstrating worsening indices with time, all attributable to abnormal PrP deposition in the spinal cord at autopsy[86]. The DWI on MRI Brain is unremarkable (unless there are superimposed CJD-like features or "switch" to CJD phenotype), but brainstem and/or cerebellar atrophy may be appreciated; the CSF RT-QuIC is usually negative.

In my clinical experience at the UK NHS National Prion Clinic, one of the most remarkable aspects of P102L IPD is the manifestation of clinical phenotypic expressions that are completely distinct from classical GSS. These include the pure cognitive-behavioural syndrome (P102L-Cognitive), devoid of any classic GSS-related lower limb sensory symptoms and cerebellar ataxia at onset, with no associated DWI MRI abnormalities and negative PQ- or IQ-CSF RT-QuIC. It is not difficult to see how such presentations can be mistaken for early onset AD or frontotemporal dementia, and anecdotal remarks from some quarters of P102L kindred indicate that this may not have been recognised as the "family illness", potentially introducing some bias or errors in the construction of pedigrees. Loss of ankle reflexes was found in one of these individuals only towards the end stage, suggesting the possibility "strain overlap". The rarest non-GSS manifestation is the fCJD or CJD-like presentation (P102L-CJD) which can be indistinguishable from sCJD clinically, associated with DWI MRI abnormalities and sometimes a positive CSF RT-QuIC. Even more interesting is how on rare occasions we encounter a "switch" from one phenotype to another, usually at least midway through the disease course, e.g. from P102L-GSS to P102L-CJD.

The precise underlying molecular mechanisms for the phenotypic diversity and phenotypic "switch"/overlap remain obscure but they are likely underscored by the concept of conformation selection model of prion strain biology. By default, it had been assumed that P102L PrP was responsible for generating all disease-associated PrP isoforms. However, Wadsworth et al. 2006 showed, through the differential binding properties of monoclonal antibodies ICSM-35 (fails to bind P102L mutant PrP) and ICSM-18 (binds both wild type human and P102L mutant PrP), that wild type human

PrP accounts for up to 30-40% undigested fragments, and up to 10% f protease-resistant fragments on Western Blot[87]. Additionally, the low molecular weight PrP^{Sc} fragment ~8 kDa was comprised entirely of P102L mutant PrP. This suggests that the contribution of wild type human PrP to disease-related PrP isoforms in P102L disease may influence clinical phenotype with tendency towards PrP synaptic labelling, and hence towards the CJD-like end of the spectrum. Indeed similar involvement of wild type human PrP in E200K, V210I and 5-/6-OPRIs, but not D178N, have been reported, suggesting that disease-associated mutant PrP isoforms may "cross-trigger" misfolding of the wild type human PrP[88-90].

D178N

Although the D178N mutation was first described in a Finnish family with the fCJD phenotype in 1991, the original "Backer" family with fCJD described by Kirschbaum in 1924 and Meggendorfer in 1930 was later attributed to D178N by sequencing DNA from archived brain tissue[91,92]. A completely different clinical phenotype presenting with progressive insomnia and dysautonomia, and later motor features and myoclonus in an Italian family was reported shortly after; the neuropathology is marked by selective atrophy of the ventral anterior and dorsomedial thalamus, but variable cortical spongiosis and faint PrP staining. This combination was termed FFI, and the coupling of insomnia and autonomic hyperactivation earned the rather fanciful term of "agrypnia excitata"[93,94]. Collectively, the mean age at onset (± SD) is 51.3 ± 11.8 years. The MRI in D178N-CJD is indistinguishable from sCJD, while the appearances in FFI are fairly unremarkable. Conventional 1st generation (PQ-CSF) and 2nd generation (IQ-CSF) RT-QuICs are negative.

As previously stated, it was initially established the FFI phenotype co-segregated with c129M while the CJD phenotype co-segregated with c129V but this haplotype-phenotype association is now no longer considered to be as clearly delineated. Co-propagation of wild type and D178N mutant PrP cannot be invoked to explain the overlap as it was shown that all disease-associated detergent-insoluble and protease-resistant PrP isoform are derived sole from D178N mutant PrP[88]. However, the

number of cases in that study was small and it was not clear if brain material included were from families where both FFI and CJD phenotypes were present.

OPRIs (≥ 4 repeats)

6-OPRI was the very first pathogenic *PRNP* mutation to be described, in a small family in South East England in 1989[95], pipping P102L to the post by a mere 2 months. Since then, OPRIs ranging from four to twelve repeats have been reported in association with prion disease. Of these, insertions of four to six octapeptide repeat insertions remain the best characterised so far, merely because of the greater number of cases examined. OPRIs fewer than four repeats are likely to be either benign or at most a low risk factor; the penetrance of 2-OPRI will be further elucidated in Chapter 4 (Determining the penetrance of novel *PRNP* variants of uncertain significance by examples).

In many ways, 6-OPRI disease encapsulates many of the shared clinicopathological features in OPRIs of greater than three repeats, but to varying degrees[96,97]. The predominant clinical picture in affected 6-OPRI individuals is a long duration (mean 9 years, but up to nearly 20 years) cognitive-behavioural syndrome with profound apraxia, but with remarkably preserved mobility for many years. Rarely, some affected members of the pedigree have a clinical course resembling fCJD from the outset with a short duration of illness lasting months. Intriguingly, a compelling account of phenotypic “switch” from classical 6-OPRI to fCJD in a patient is discussed further in Chapter 2 (Seed amplification and neurodegenerative marker trajectories in individuals at risk of prion disease)[98].

A couple of interesting trends with regards to phenotypic expressions relative to OPRI size have been observed. Firstly, the mean age of onset has been found to be inversely proportional to the OPRI size, i.e. the larger the OPRI, the lower the age of onset[97,99]. Secondly, the balance between dichotomous phenotypes (fCJD vs long duration cognitive-behavioural-apraxic syndrome) appear to shift according to OPRI size i.e. fCJD dominates in 4-OPRI, while the other phenotype becomes increasingly

dominant from 5-OPRI onwards as the former dwindles. It ought to be pointed out that this remains anecdotal, as formal statistical analyses have yet to be performed.

MRI brain findings are similarly dichotomous reflecting the clinical phenotype. DWI abnormalities are seen in those with the fCJD phenotype, while cerebral and cerebellar cortical atrophy is seen in the long duration phenotype. As a whole, neuropathology with regards to spongiosis and astrocytosis is varied which is not entirely surprising given the dichotomous phenotypic expression. PrP amyloid plaques are only found in some larger OPRIs, while the “striped” or “tigroid” cerebellar PrP immunostaining pattern is seen most often in 4-, 5-, and 6-OPRIs. The synaptic PrP staining pattern associated with CJD is seen in those presenting with the fCJD phenotype, especially in 4-OPRI.

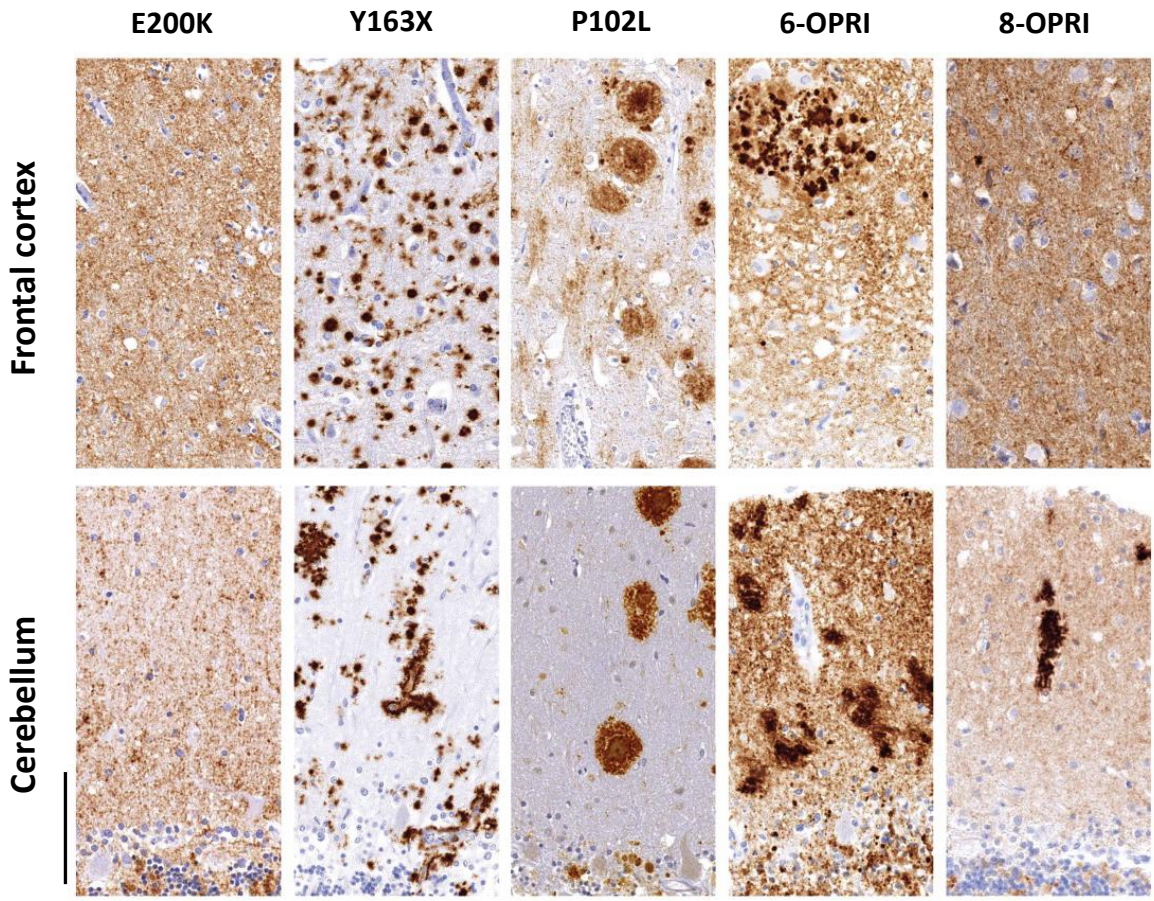

Figure 3 Characteristic histopathological appearances of PrP deposits in a selection of IPDs.

This graph shows ICSM35 PrP immunohistochemical staining pattern in the frontal cortex and cerebellum in different IPDs. The predominantly synaptic pattern seen in E200K is indistinguishable from certain forms of sCJD. Y163X causes truncation of the C-terminus of PrP including the GPI anchor, resulting is PrP amyloidosis, seen as as plaques in the frontal cortex and cerebellum, and cerebral amyloid angiopathy in the cerebellum. Large multicentric plaques predominate in classical P102L-GSS. The large OPRIs show synaptic PrP deposts in the neocortex together with granular or mini plaques, and the ”striped” or “tigroid” pattern perpendicular to the pial surface in the cerebellum. Scale bar (100 µm). Reproduced from DOI: 10.1146/annurev-genet-120213-092352.

Variant CJD (vCJD)

vCJD is introduced in further detail in Chapter 3 (Implications of vCJD in a *PRNP* c129 MV patient).

Iatrogenic CJD (iCJD)

A variety of medical/surgical exposures (discussed in Chapter 2; Individuals at risk of prion disease) have been identified for iCJD, but are largely of historical interest given fairly effective prevention measures in place, with the exception of cadaver-sourced human growth hormone exposure prior to the advent of recombinant human growth hormone in 1985 in the UK. In Japan, roughly 20,000 individuals were thought to have received Lyodura dural grafts (manufactured between 1983 and 1987) implicated in iCJD, with 154 deaths by the end of 2017[100]. This remains relevant because considerable numbers of recipients are still alive, and a handful of new cases continue to be recorded infrequently with incubation periods of up to 40 years, mirroring that of kuru. More interestingly, recipients are now known to be at risk of amyloid beta transmission mainly as cerebral amyloid angiopathy[101-104].

Gait ataxia and lower limb pain are frequently the leading symptoms but the profound lower limb pyramidal weakness that surfaces soon after distinguishes it from sCJD; cognition is relatively preserved until late in the symptom evolution. The MRI Brain in iCJD shares many features with sCJD but additional cortical DWI restriction in the paracentral lobule representing the “leg area” and along the motor strip, which is hardly ever observed seen in sCJD, is commonly seen. Neuropathological findings in most examined cases revealed the synaptic pattern of PrP immunohistochemical staining and numerous kuru plaques. A peculiar observation is that the c129 genotypes in the earliest cases were mostly VV and the more recent cases were MM; MV cases arose after the peak of VV cases and their incidence has remained fairly constant. A speculation is that the original source of disease associated PrP isoform contained the polymorphic valine residue at c129, facilitating prion propagation through homotypic interactions in decreasing order of VV, MV, and MM. Despite the longer incubation, MM cases have the shortest duration of illness[49].

CHAPTER 2

Seed amplification and neurodegenerative markers in individuals at risk of prion disease

Publications:

Mok TH, Mead S. ***Preclinical biomarkers of prion infection and neurodegeneration.*** *Curr Opin Neurobiol. Apr 2020;61:82-88. doi:10.1016/j.conb.2020.01.009*

Mok TH, Nihat A, Majbour N, et al. ***Seed amplification and neurodegeneration marker trajectories in individuals at risk of prion disease.*** *Brain. Mar 28 2023; doi:10.1093/brain/awad101*

Introduction

Individuals at-risk of prion disease

Defined populations with higher lifetime risk of prion disease relative to the general population, can be condensed into those who are at risk of inherited prion disease (IPD-AR), and those exposed through either medical (iCJD ± vCJD) or dietary means (vCJD and kuru). Undoubtedly, prospective cohort studies of these populations with longitudinal biofluid sampling through to disease onset afford the best opportunity to elucidate the sequence of biomarker evolution in the presymptomatic phase. Yet, not all of these are amenable to study at the present time chiefly due to variation in disease penetrance and in some sub-populations, due to the waning incidence of disease.

The IPD-AR population remains the principal and least problematic cohort to interrogate. One of the key reasons is that all well-characterised canonical IPD phenotypes are caused by autosomal dominantly inherited, and highly penetrant *PRNP* mutations. Aside from these, there exist a number of *PRNP* mutations of low (e.g. V210I and Q212P) or uncertain penetrance (e.g. V180I), while some, e.g. T201S and 2-OPRI, have recently been reclassified as either benign or extremely low-risk gene variants (see Chapter 4). The UK NHS National Prion Clinic, having sequenced *PRNP,* and provided specialist clinical services in prion disease almost exclusively in the UK for the past 30 years, is in a unique position to recruit and study these individuals within the National Prion Monitoring Cohort (NPMC) through its liaison with the various IPD families[105,106]. Indeed, a recent study using the capture-recapture method, estimated that over 1,000 individuals in the UK are at risk of IPD[107]. Internationally, similar but more recently established prospective IPD-AR cohort studies under way in the United Stated of America (USA) and Israel have both reported interim fluid biomarker analyses[108,109].

Sources of medical exposure have been highly varied, including recipients of cadaver-sourced human growth hormone (c-hGH), implicated blood products, lyophilised dural (Lyodura before 1987) and corneal grafts, or those exposed to contaminated neurosurgical instruments and intraoperative EEG depth electrodes[110-112]. Amongst

these, only individuals at risk of iCJD (iCJD-AR) from c-hGH continue to be viable to study in the UK despite its declining incidence (roughly 1/year in last 10 years)[57], largely because an accessible registry of at-risk individuals coupled to whether they received the implicated batches, continues to be maintained for surveillance. Between 1958 and 1985, c-hGH was administered to 1,849 UK individuals, of whom 81 have succumbed to iCJD to date. Relative to highly penetrant *PRNP* mutations causing IPD, the estimated penetrance of iCJD in this population is vastly lower at 4.5%[49,113]. However, in the recent years, renewed interest in the c-hGH iCJD-AR individuals has arisen following the discovery of co-transmission of amyloid-beta seeds, as well as prion seeds[102]; more recently this was further corroborated by mouse transmission studies[101]. Subsequently, it ignited a cascade of reports, implicating dural grafts and previous neurosurgery in transmission of cerebral amyloid angiopathy[103,114]. The remainder of the medical routes of iatrogenic exposure are no longer of great concern given the advances in medical technology leading to better ante mortem recognition of CJD and institution of infection control measures. Despite sporadic exposures through neurosurgical instruments, no new cases of iatrogenic CJD (other than from c-hGH) have been recorded in the UK for more than 15 years[57].

Dietary exposures have caused epidemics previously, attracting considerable disproportionate media, public health, and political attention. The first well-documented outbreak was kuru through ritualistic cannibalism in the Fore linguistic group of the Papua New Guinean Eastern Highlands. This is now of historical interest but one of the key lessons gleaned from studying this outbreak was the demonstration of long incubation periods of up to 50 years after cessation of cannibalistic practices, determined by *PRNP* codon 129 polymorphism[48]. This will prove to be of particular interest in the latent risk of vCJD in individuals heterozygous at codon 129, but this will be discussed in greater detail in Chapter 3[30].

Ultimately, accrual of longitudinal biofluid sample resources from prospective cohort studies targeting IPD-AR and iCJD-AR populations will not only allow for repeated interrogations for biomarker discovery, but also for ascertainment of rates of change as even more sensitive predictors of disease onset[115]. This is highly relevant to individuals at risk of prion disease as therapeutic strategies and study designs increasingly shift towards prevention. It may not be feasible to adequately power

clinical trials for prevention in prion disease for a simple clinical endpoint[77] but characterisation of presymptomatic biomarkers could inform different strategies, enrichment in and learning from trials.

Fluid biomarkers of prion infection and neurodegeneration

At the conception of this MD(res) project in 2015, we faced a number of “unknowns”, any of which could have thwarted our chances of uncovering fluid biomarkers indicating proximity to clinical conversion. First, hardly anything was known about preclinical disease-associated processes in at-risk humans, and whether any, if present, would predate clinical conversion by a sufficient length of time to be discoverable. Should it have turned out to be short months or weeks before disease onset, the default annual sampling intervals would have had very low chances of capturing any changes. Secondly, it was unknown if optimisation and adaptation of exciting new biomarker detection technologies would be capable of detecting the subclinical disease-associated changes.

The feasibility of our study was founded upon the presence of a clinically silent prolonged incubation phase in associated with high infectious prion titres observed in the two-phase kinetics model (see Figure 1)[50]. We were further encouraged by a subsequent publication detailing the sequence of neuropathological changes that preceded clinical disease (day 168 ± 2.5), showing established synaptic PrP deposits by day 50, microglial activation by day 65, and synaptic loss in brains by day 125 of prion-inoculated transgenic mice expressing human PrP[51]. At the time, scattered reports of non-fluid biomarker changes in a handful of IPD-AR individuals, including serial volumetric MRI brain changes by registration in a P102L carrier, and fluorodeoxyglucose positron emission tomography (FDG-PET) brain and sleep studies in FFI, both indicated that at least some pathological processes were afoot before clinically evident disease[116,117].

The emphasis on fluid biomarkers in prion disease has been focussed on their role in supporting the clinical diagnosis of sCJD. Their utility (and limitations) in the clinical phase of the disease is established beyond doubt but little was known about whether

they are sufficiently sensitive to detect changes predictive of disease onset in the preclinical phase. Historically, these comprised of neurodegenerative biomarkers reflecting either catastrophic neuronal loss (CSF protein 14-3-3 and total tau) or astrogliosis (s100b), with CSF protein 14-3-3 being the sole fluid biomarker officially incorporated by the UK National CJD Research & Surveillance Unit[118] into the diagnostic criteria for epidemiological case definition up to 2017[118-120]. The relatively recent introduction of cell-free conversion assays, namely the CSF RT-QuIC which works through proteopathic seed-specific amplification, and high-throughput ultrasensitive digital immunoassay platforms, allowed us to probe distinct and possibly sequential aspects of presymptomatic prion propagation – PrP-amyloid seeding activity (seeding-competent aggregates in infectivity phase) and neurodegeneration (toxicity).

Cell-free conversion assays (PrP seed amplification)

Cell-free conversion assays possess great appeal because they seek to replicate a key component of prion disease mechanism *in vitro*, i.e. seed amplification, which is mostly likely reflective of disease processes happening during infection stage. The two types of assays in clinical and research use at present are the RT-QuIC and Protein Misfolding Cyclic Amplification (PMCA) assays.

The genesis and proof of concept for cell-free conversion of PrP^{C} to PrP^{Sc} date back to the 1990s, but subsequent innovative modifications led to the development of PMCA using sonication as the kinetic accelerant, and later QuIC using shaking, both of which relied on western blot of amplification products as readouts[121-123]. A further modification to QuIC by replacing western blot with thioflavin T (ThT) fluorescence readout adopted from prion amyloid seeding assay, gave rise to the current version of the RT-QuIC assay[123-125]. Both RT-QuIC and PMCA revolve around the presumed presence of seeding-competent disease-related PrP isoforms in prion-infected biological samples capable of converting recombinant PrP (rPrP) or brain-derived PrP (for PMCA) to aggregates of PrP-amyloid when incubated together in a reaction mix.

The cycles of seeded polymerisation and fission are then accelerated by intermittent exposure to kinetic energy, with some differences between them (Table 1).

Table 1 Comparison of key aspects between RT-QuIC and PMCA assays

	RT-QuIC	PMCA
Conversion substrate	rPrP	PrP^C in brain homogenate
Kinetic energy	Shaking	Sonication
Readout	ThT fluorescence	Western Blot
Products	Non-infectious PrP amyloid	Infectious prions with strain fidelity
Applications in human prion disease	sCJD, iCJD, certain IPDs	vCJD
Applicable human biofluid types	CSF, olfactory mucosa, skin, tears	CSF, blood, urine

Adapted from Mok TH, Mead S. Preclinical biomarkers of prion infection and neurodegeneration. *Curr Opin Neurobiol*. Apr 2020;61:82-88. doi:10.1016/j.conb.2020.01.009

The chief distinction in the resulting assay products is that PMCA generates true infectious prions with strain fidelity[126], while RT-QuIC products are merely PrP-amyloid structures which have completely distinct physicochemical properties to the original prion seed in the tested sample. However, the application of classical PMCA to date is largely confined to vCJD, and is laborious to undertake, though recent more rapid iterations are said to show some potential for use in other prion diseases. Naturally, the decision was made to develop and optimise RT-QuIC, instead of PMCA as the cell-free conversion assay of choice in this project.

RT-QuIC, regardless of its limitations above, has proven to be an ultrasensitive *reporting* assay capable of detecting PrP-amyloid seeding down to the attogram (10^{-18} g) range. Such is its versatility that RT-QuIC has been successfully applied to various biological tissues beyond brain homogenates, including CSF, olfactory mucosa, skin and in a very recent development, remarkably, even tears[127-130]! Reassuringly, Orru *et al.* 2012 used RT-QuIC to demonstrate high levels of seeding

activity in brain and CSF of hamsters experimentally inoculated with 263K prions in the clinically silent incubation period before disease onset, paralleling prion bioassay findings in the two-phase kinetics model[131]. In an even more encouraging development, Vallabh *et al.* 2020 identified presymptomatic RT-QuIC seeding activity for at least a year's duration in a single elderly E200K mutation carrier[108].

Based on the emerging biochemical work at the time, I expected that the viability of RT-QuIC in detecting seeding-competent PrP during the preclinical stage would be dependent on two key factors – the concentration of seeding-competent PrP isoforms in biofluid samples (sensitivity) and seed-substrate (seed-rPrP) compatibility. The assay sensitivity can be enhanced by adjusting microplate reader settings (e.g. incubation temperature and shaking parameters) or components of the reaction mix (buffer type, pH, salt concentration, sodium dodecyl sulphate, and Hofmeister salt effects), all of which must be balanced against erosion of assay specificity[132,133]. On the matter of seed-substrate compatibility, rPrPs used in conventional RT-QuIC protocols designed for sCJD diagnosis (full-length or truncated hamster, sheep-hamster chimera) can be readily seeded by clinical samples from symptomatic individuals with IPD mutations manifesting with the fCJD phenotype (E200K, V210I and E196K)[80-83]. However, this remains unresolved for non-fCJD IPDs e.g. P102L-GSS, P102L-Cognitive, A117N, D178N, OPRIs and Y163X, by virtue of presumed conversion barriers, or simply lack of exploration. Comparisons of 1st (PQ-CSF) and 2nd (IQ-CSF) generation RT-QuIC assays highlighting their differences is summarised in Table 2. in To complicate matters, differential co-propagation of distinct disease-associated PrP isoforms is established even within a single affected individual harbouring the same mutation, such as that proven in P102L and 5/6-OPRIs (wild type vs. mutant prions), each potentially with its own unique seed-substrate compatibility[87,89]. In this regard, RT-QuIC using bank vole (BV) rPrP seemed to offer a glimmer of hope in the search for a "universal" substrate when it showed an impressively wide range of seed compatibility[134,135]. Equally full-length human rPrP, when used in completely different RT-QuIC setup, was successful for CSF from E200K, D178N-129M and P102L patients[136]. It is also possible that rPrP sequence homology may be required for certain mutations such as P102L and A117V i.e. using human P102L or A117V rPrPs, drawing on experience from mouse transmission studies[137,138]. Ideally, it would require an exhaustive, methodical, and iterative

interrogation approach to unravel the optimum seed-substrate pairing for non-fCJD IPD mutations before RT-QuIC can realise its full potential in defining the onset of

Table 2 Summary of comparisons between PQ-CSF and IQ-CSF RT-QuIC assays

Assay conditions	PQ-CSF RT-QuIC (1st generation)	IQ-CSF RT-QuIC (2nd generation)
Buffer	10 mM phosphate buffer pH 7.4 (per well)	10 mM phosphate buffer pH 7.4 (per well)
Salt	NaCl 300 mM (per well)	NaCl 300 mM (per well)
EDTA	1 mM (per well)	1 mM (per well)
SDS	0.002% (per well)	None
ThT	10 mM (per well)	10 mM (per well)
rPrP species	Full length hamster (Ha23-231)	Truncated hamster (Ha90)
rPrP concentration	0.1 mg/ml (per well)	0.1 mg/ml (per well)
CSF seeding volume	20 or 15 µl (per well)	20 or 15 µl (per well)
Total volume	100 µl (per well)	100 µl (per well)
Microplate reader	BMG FLUOstar or POLARstar or OPTIMA	BMG FLUOstar or POLARstar or OPTIMA
Shaking speed	700 rpm	700 rpm
Shaking motion	Double orbital	Double orbital
Shake/rest intervals (on/off)	60s/60s	60s/60s
Incubation temperature	42 °C	55°C
Time cut-off	50 or 90 hrs	24 hrs

Shaded rows denote conditions that are different between PQ-CSF and IQ-CSF RT-QuIC assays

prion infection in the at-risk population.

Fluid biomarkers of neurodegeneration

Neurodegenerative biomarkers in prion disease are essentially downstream products of either neuronal injury (synaptic and/or axonal), astrogliosis and inflammation, or other secondary disease pathologies. None are strongly discriminatory between neurodegenerative diseases, particularly with cross-sectional values, but tracking biomarker dynamics over time may segregate mutation carriers approaching disease onset from aging effects in normal controls, eschewing the need to rely individual cross-sectional values based on arbitrary definitions of “normal” ranges[115]. A further advantage in prion disease includes the low mean ages of clinical onset across IPD making it unlikely to be confounded by elevation of markers attributable to significant co-pathologies such as AD and dementia with Lewy bodies usually present in later life. One would also expect lower chances of overlapping values considering the

catastrophic degeneration in prion disease relative to other neurodegenerative diseases.

The introduction of digital immunoassay platforms has transformed biomarker detection sensitivity, now down to single molecule resolution (e.g., Singe molecule array, Simoa), instead of relying solely on overall chemiluminescence intensity[139]. Midway through the project, our Unit demonstrated segregation of plasma tau and neurofilament-light (NfL) levels between IPD mutation carriers from symptomatic IPD individuals, and more importantly showed rising levels in the two years prior to symptom onset in small numbers of converting individuals, through use of simplex Simoa assays[140]. Further advances in Simoa technology since then now allows for multiplex arrays measuring up to four candidate biomarkers, limiting depletion of precious biofluid resources.

A select number of neurodegenerative markers were being considered for inclusion based on either promising pilot data or mechanistic relevance. Needless to say, **NfL** and **tau**, being markers of axonal injury, were amongst the frontrunners due to their promising preclinical trajectories in the pilot data mentioned above. **CSF neurogranin**, a protein concentrated on the dendritic spine of the post-synaptic membrane (marker of synaptic function) was of interest because of neuropathological evidence from the two-phase kinetic model[51,141]. **CSF α-synuclein**, another surrogate of neuronal destruction, was felt perhaps to hold promise in for tracking fCJD because of its utility in distinguishing between sCJD and controls, but not between D178N and P102L, and controls[142]. **Glial fibrillary acidic protein (GFAP)** and **YKL-40** are markers of astrogliosis, central to prion disease pathology, were considered as good candidates on the basis of mechanistic relevance[143,144]. **CSF total PrP**, while not strictly a marker of neurodegeneration, is discussed here as it has been shown to be significantly reduced in sCJD and a handful of IPD patients. More importantly, it has attracted attention as a promising pharmacodynamic marker of PrP-depleting therapies currently in development. However, processing of CSF samples for total PrP quantification requires special care to avoid spurious results due to PrP loss, the protocol of which was not instituted at our Unit at the time[145-147].

In theory, a great choice (and possibly an inexhaustible number) of neurodegenerative marker tests, can be used to interrogate a biofluid archive of interest. In practice, however, ambitions are frequently curbed by limitations on sample resource volumes and cost. This MD(res) project was not immune to these, and alongside the unexpected curtailment human resources and laboratory access during the COVID-19 pandemic, the Simoa Neurology 4-plex panel B platform was felt to be the best choice. The biomarkers tested in this panel include GFAP, NfL, tau and ubiquitin carboxy terminal hydrolase L1 (UCH-L1).

Methods

National Prion Monitoring Cohort Recruitment

The NPMC began enrolling eligible individuals from October 2008 onwards, and it encompassed those symptomatic of all forms of prion disease (sCJD, iCJD, vCJD and IPD), those asymptomatic but at risk of developing prion disease (IPD-AR, iCJD-AR, and vCJD-AR), and healthy controls (HC). Asymptomatic at-risk individuals classified as IPD-AR are either confirmed carriers of pathogenic *PRNP* mutations, or untested individuals who are blood relatives of mutation carriers. The iCJD-AR population is principally composed of c-hGH recipients up to 1985[49], while the vCJD-AR population are individuals exposed to implicated blood products derived from individuals whom eventually developed vCJD[55]. Ethical approval was obtained from the Scotland A Research Ethics Committee (05/MRE/65) and from the local research ethics committees of UCL Institute of Neurology and the National Hospital for Neurology & Neurosurgery.

Assessment intervals, and hence biofluid sampling intervals were determined by the stratum in which participants fall, based on expected rate of clinical progression, and by clinical need[106]. In brief, *fast progressors,* e.g. sCJD, iCJD, and E200K, fell into Stratum 1, and are assessed every 6-8 weeks; *slow progressors* e.g. P102L, 6-OPRI, 5-OPRI, and A117V, fell into Stratum 2, and were assessed every 6-12 months; normal controls and asymptomatic at-risk individuals fell into Stratum 3 and were

assessed every 6-12 months. Enrolled individuals were all assessed face-to-face from October 2008 up until March 2020, at which point all F2F assessments ceased completely for 4 months; thereafter a hybrid virtual/F2F resumed based on clinical need, interrupted by a 4-month lockdown restriction in early 2021.

Research blood samples were obtained by NPC staff with written informed consent from both the enrolled individual, and from friends/non-blood relatives in attendance as controls, at each assessment. From 2015 onwards, up to 10 mls of CSF were collected through bedside lumbar puncture from individuals at risk of, or symptomatic of prion disease at the National Hospital for Neurology and Neurosurgery on Queen Square, following an amendment to 05/MRE/63. Typically, up to about 10 mls of additional CSF was retained for research purposes when an LP was done for clinical diagnostic work-up of each symptomatic individual at or near 1st assessment. Thereafter, for this category of patients, no further CSF sampling has occurred to date due to logistical difficulties from disease progression and long travel distances. In a separate schedule in accordance with Stratum 3, asymptomatic at-risk individuals (IPD-AR and iCJD-AR) underwent LPs to collect research CSF and venepuncture for research bloods every 6-12 months during a dedicated day of research investigations which included clinical neurophysiology (EEG and/or EMG), neuropsychology and MRI Brain, and research and an NHS clinical assessment.

For neurodegenerative marker measurements, healthy control CSF samples were sourced from the young-onset Alzheimer's disease (AD) spouses or non-blood relatives, British 1946 Birth Cohort (Insight-46), CONFLUID cohorts, and internally from the NPMC (initially untested at-risk participant subsequently mutation-negative on predictive testing). Healthy control plasma samples were sourced from NPMC internally and from non-mutation carriers the Genetic Frontotemporal Dementia Initiative (GENFI) cohort. For CSF RT-QuIC analyses, non-prion control samples were sourced from Institute of Neuroscience & Physiology at University of Gothenburg, NHNN Neuroimmunology Laboratory (NHNN-NiCL) and internally from the NPMC. The Swedish CSF samples (n = 39) are high quality clinical samples from individuals symptomatic of neurodegenerative diseases subsequently classified as AD or non-AD based of biomarker profile. The NHNN CSF samples (n = 19) came from non-neurodegenerative clinical referrals.

Estimating proximity to conversion in IPD-AR individuals

Studies of similar cohorts of familial neurodegenerative conditions containing both at-risk, converter and symptomatic individuals have shown correlations between an individual's age of onset and mean age of onset with the family, and/or parental age of onset. As such, the proximity of clinical onset/conversion for at-risk individuals in these cohorts can be reliably calculated, simply by subtraction from the mean age of onset within the family, or parental age of onset[148,149]. However, this is unlikely to be a reliable strategy for clinical conversion proximity estimation in the IPD-AR cohort due to the highly variable ages of onset even within the same pedigree, exemplified by the large standard deviations from mean ages of onset between 8-14 years, resulting in considerable number of IPD-AR individuals living beyond the mean age of onset of a given *PRNP* mutation [77,150].

Here, we propose a novel method of estimating the age of onset of an IPD-AR individual at a given age (x_c) based on the mean age of onset (μ) and standard deviation (σ) of a given *PRNP* mutation. On the assumption of a normal distribution of age-related *z* scores against the probability density of clinical conversion, the *z* score associated with the current age (z_c) of the individual is first determined, from which the cumulative distribution function at z_c (*P* ($z \leq z_c$)) is derived. We then assume that the individual's residual cumulative risk (area under the curve) lies to the right of z_c which is the inverse i.e. (1 – *P* ($z \leq z_c$)) and that the cumulative risk at z_p (*P* ($z \leq z_p$)) is the sum of *P* ($z \leq z_c$) and half of its inverse (1 – *P* ($z \leq z_c$))/2 i.e., *P* ($z \leq z_p$) = *P* ($z \leq z_c$) + (1 – (*P* ($z \leq z_c$)/2)) (Figure 4). This can be expressed as a Microsoft Excel formula x_p =NORM.INV(1-(1-NORM.DIST(A2,A3,A4,TRUE))/2,A3,A4)-A2 where A2 is the individuals current age (x_c), A3 is the mutation mean age of onset, and A4 is the mutation standard deviation.

For example, the *z* score (z_c) of an E200K IPD-AR individual aged 60 (x_c) with a mutation mean (μ) of 58.5 and standard deviation (σ) of 8.0 years is calculated as follows:

$$z_c = \frac{x_c - \mu}{\sigma}$$

$$z_c = \frac{60 - 58.5}{8.0}$$

$$z_c = 0.1875$$

P ($z \leq z_c$) of z_c (0.1875) is 0.5753, and therefore the inverse is 1 – 0.5753 = 0.4247. Half of 0.4247 is 0.4247/2 = 0.2123; and as such the z_p corresponds to *P* ($z \leq z_p$) = 0.5753 + 0.2123 = 0.7876 is 0.8. Hence,

$$z_p = \frac{x_p - \mu}{\sigma}$$

$$x_p = (z_p \times \sigma) + \mu$$

$$x_p = (0.8 \times 8.0) + 58.5$$

$$x_p = 64.9$$

Finally, years to predicted onset is $x_c - x_p$= 60 – 64.9

= – 4.9

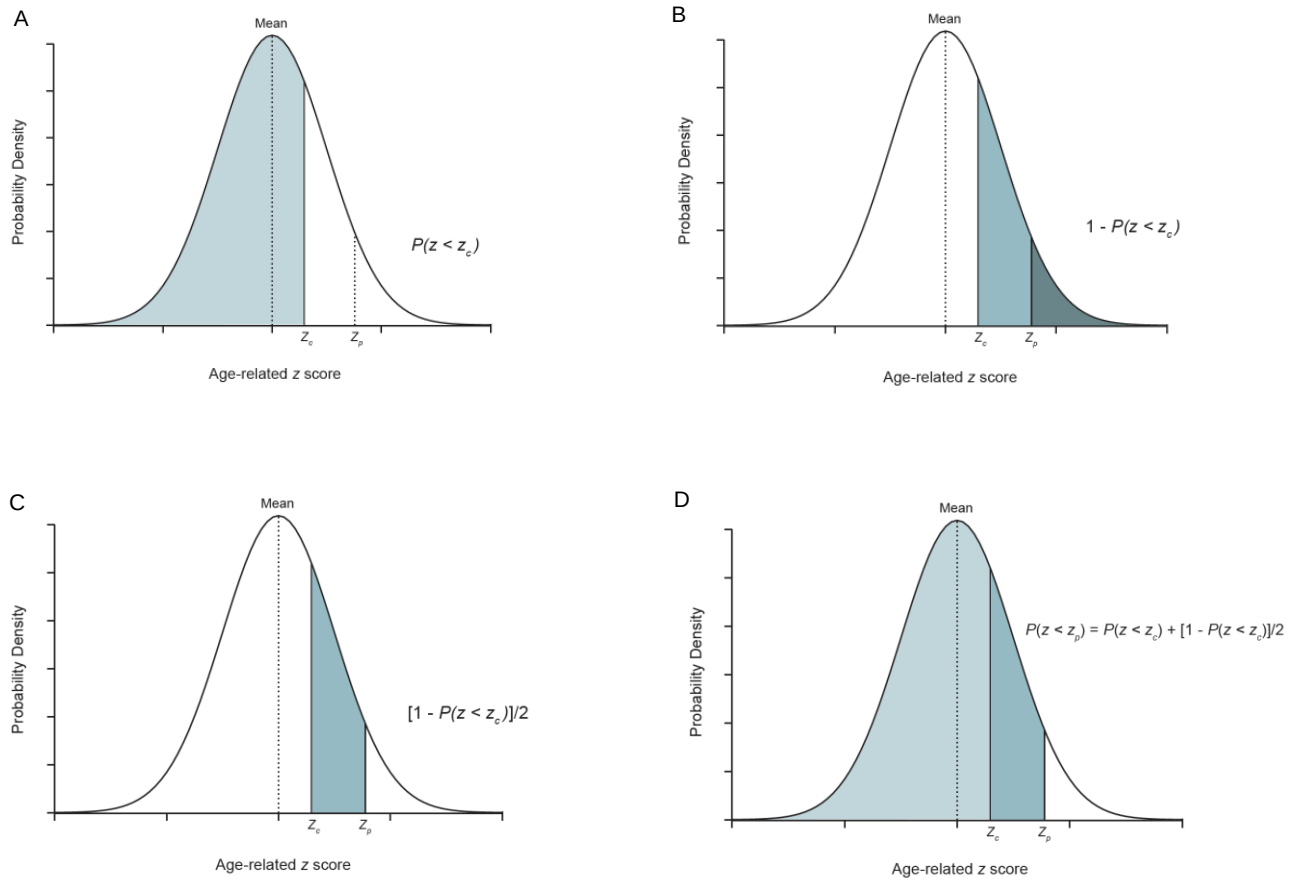

Figure 4 Determination of predicted age of onset for IPD-AR and iCJD-AR individuals.

(**A**) This shows the cumulative distribution function associated with the *z* score at the age of sampling ($P(z < z_c)$). (**B**) The total shaded area is the cumulative distribution function of the residual risk ($1 - P(z < z_c)$) and half of it is the estimated residual risk. (**C**) for the individual at age of sampling ($1 - (P(z < z_c)/2)$). So (**D**) represents the cumulative distribution function of the age-related *z* score at estimated onset z_p i.e. $P(z < z_c) + (1 - (P(z < z_c)/2))$. Reproduced from Mok *et al.* 2023 (https://doi.org/10.1093/brain/awad101).

Biofluid sample processing and brain homogenate preparation

Blood

Whole blood samples collected in EDTA tubes (or Citrate tubes if EDTA not available) were centrifuged at 2000*g* for 10 minutes at room temperature (22°C), on arrival to laboratory. The supernatant (upper plasma phase) is then divided into aliquots of 0.5 – 2.0 mls in Nunc Cryovials, and then frozen at -80°C.

CSF

Immediately following lumbar puncture, 10 mls (where possible) of neat CSF was equally divided into 2 separate polypropylene tubes (Sarstedt 62.610.018), and delivered to the laboratory. One of two CSF samples is designated CSF-R (R for RT-QuIC), and is first gently mixed by hand before being separated into aliquots of 0.5-2.0 mls in Nunc Cryovials; the other half is designated CSF-N (N for neurodegenerative markers), and is centrifuged at 2200*g* for 10 mins at room temperature, before having the supernatant separated into aliquots of 0.5-2.0 mls in Nunc Cryovials. Aliquots from both CSF-R and CSF-N are then frozen at -80°C within 1 hour from sample collection.

On occasions where it was not possible to process and store the CSF samples within 1 hour of collection, the samples were immediately frozen *en bloc* at -80°C, and processed per protocol at a later time.

A separate sample from those processed above was sent contemporaneously for cell count and routine biochemistry analyses (glucose and protein) at NHNN-NiCl.

Brain homogenate preparation

Archived 10% w/v human and mouse brain homogenates (BH) were used as seed in RT-QuIC reactions. BH samples were prepared as previously described[151]. Briefly, homogenisation was achieved by serial passage of thawed frozen cortex through

needles of decreasing diameter, and suspended in Dulbecco's saline phosphate buffer lacking Ca^{2+} and Mg^{2+} ions.

Recombinant PrP (rPrP) expression and purification

Full length human (FL Hu rPrP; aa residues 23-231; accession M13899) and bank vole rPrP (FL BV rPrP; aa residues 23-231; accession AF367624), and truncated hamster (Ha90 rPrP; aa residues 90-231; accession K02234) and bank vole rPrP (BV90 rPrP; aa residues 90-231; accession AF367624) were purified according to previously established methods[152,153]. In brief, glycerol stocks of *Escherichia Coli* with vectors containing the respective *PRNP* sequences above (sourced from the NIH Rocky Mountain Laboratory (RML)) were used to inoculate cultures which were subsequently grown in Luria Broth medium together with kanamycin and chloramphenicol. The isopropyl β-D-1-thiogalactopyranoside (IPTG; at MRC Prion Unit) or autoinduction (at NIH RML) system was then used to stimulate protein expression. Purification of rPrP from inclusion bodies in denaturing conditions was done through a Ni-nitrilotriacetic acid (NiNTA) superflow resin (Qiagen) with an ÄKTA Pure, before refolding through a guanidine HCl gradient and elution through an imidazole gradient. The eluted rPrP was sequentially dialysed extensively in 10 mM of sodium phosphate buffer pH 5.8, filtered through 0.22 µm syringe filter, its concentration determination by absorbance measurement at 280 nm, separated into aliquots, and frozen at -80°C. Prior to use, rPrP was thawed, filtered 100 kDa spin filter (Pall Nanosep), and concentration again similarly measured. The rPrP constructs purified with this method are free of histidine tags (his-tags).

The full length human P102L rPrP (FL Hu P102L rPrP; aa residues 23-231; accession M13899) construct, which contains his-tags, was developed at the MRC Prion Unit at UCL, and purified through a different protocol[154] with some minor modifications. *Escherichia Coli* cultures containing the vector with this FL Hu P102L PrP sequence were grown Luria Broth medium, and in the presence of ampicillin. PrP expression was induced using IPTG, and purified from inclusion bodies, similarly under denaturing conditions through NiNTA superflow resin (Qiagen) with an ÄKTA Pure, before refolding through a guanidine HCl gradient and elution through an imidazole gradient.

The eluted rPrP was dialysed extensively against 20 mM Bis Tris pH 6.5, and then had its his-tags cleaved by addition of 2.5 mM $CaCl_2$ and 50U Thrombin (VWR). The cleaved his-tags were subsequently removed from the preparation by a second run through NiNTA superflow resin (Qiagen) with an ÄKTA Pure. The preparation then undergoes dialysis against 10 mM of sodium phosphate buffer pH 5.8, and treated exactly as above at its corresponding stage of handling (Figure 5).

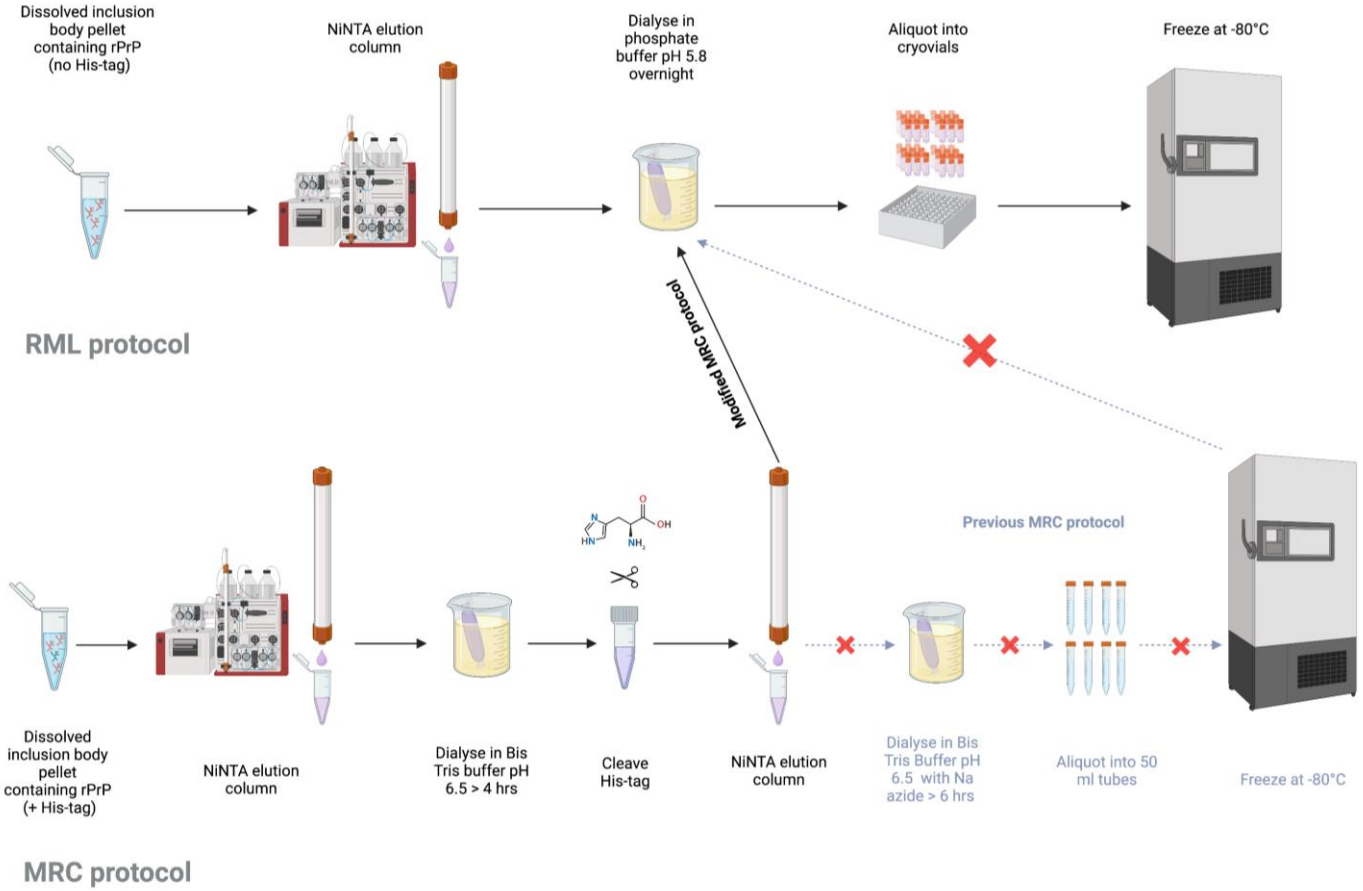

Figure 5 Comparison of the key steps in the RML and MRC methods of rPrP purification.

The upper panel represents the RML protocol while the lower panel represents the MRC protocol for rPrP purification. The MRC protocol contains additional steps due to the introduction of his-tags in the construct, which need to be cleaved by thrombin, and interim freezer storage in pH 6.5 requiring further dialysis before use. The modified MRC protocol used for Hu P102L rPrP bypasses the extra dialysis and interim storage.

RT-QuIC assay

For the RT-QuIC reactions seeded by BH, thawed 10% BH is serially diluted in 0.1% SDS/PBS/N2 (Gibco) when used in reactions with Ha90 rPrP, or in 0.05% in the final required dilutions when used in reactions with FL Hu rPrP, FL Hu P102L rPrP, FL BV rPrP and BV90 rPrP.

The standard RT-QuIC reaction mix per well is composed of 10 mM buffer (sodium phosphate (PBS) pH 7.4, HEPES pH 7.4/8.0, or PIPES pH 7.0), 130-500 mM NaCl or NaI, 0.1 or 0.05 mg/mL rPrP, 10 µM Thioflavin T (ThT), 1 mM ethylenediaminetetraacetic acid tetrasodium salt (EDTA), and 0.001 or 0.002% SDS. Reactions were prepared in 96-well optical clear-bottomed plates (Nalgene Nunc International 265301). For BH-seeded reactions, 98 µL of reaction mix in each well was seeded by 2 µL of BH, bringing the final volume up to 100 µL per well; for CSF-seeded reactions, 80 or 85 or 95 µL of reaction mix was seeded with 20 or 15 or 5 µL of CSF respectively, again bringing the final volume up to 100 µL per well.

Thereafter, the loaded plates were sealed (Thermo Scientific Nunc 232702) and incubated in BMG FLUOstar Omega/Omega Lite or POLARstar Omega microplate readers between 42°C and 55°C, at double orbital shake/rest cycles of 60s/60s at 700 rpm. ThT fluorescence readings (excitation 450 ± 10 nm, emission 480 ± 10 nm; bottom read) were recorded at intervals of 45 mins. Each sample was test in quadruplicate and is classed as *positive* if the relative fluorescence units (RFU) in more than 2/4 wells exceed the 10% baseline-corrected threshold within the cut-off time points[62]. Samples with 1/4 positive wells were tested again, and if the outcome remained the same, these are classified as “equivocal”. Time cut-off points were determined by incubation temperature i.e. 50 hrs for 42°C, 30 hrs for 50°C, and 24 hrs for 55°C[132].

Endpoint quantitation of seeding activity

CSF and BH seeding doses were calculated by endpoint quantitation of RT-QuIC prion seeding activity using the Spearman-Kärber method[153,155]. For CSF, each sample was diluted serially by one third using the same non-prion control CSF sample to reconstitute the seeding volume to 20 µl per well; for BH, each sample was serially diluted by 10-fold in 0.1%SDS/1X PBS/N2, to reconstitute the seeding volume of 2µl. The seeding dose 50 (SD_{50}) is defined as the log_{10} dilution of a particular biosample tested which results in 50% of the replicate wells (2/4 wells; seeding dose 50 (SD_{50})) registering positive responses according to the criteria above. $Log SD_{50} = x_{p=1} + 1/2d - d\sum p$ where $x_{p=1}$ being the highest log_{10} dilution with 4/4 positive wells; d = log dilution factor; p = proportion positive at a given dose; $\sum p$ = the sum of values of p for $x_{p=1}$ and all higher dilutions.

The SD_{50} can be further adjusted to report seeding units per mg of BH, or per unit volume of CSF (e.g. per µl). When a neat positive CSF sample at 20 µl per well yields fewer than 4/4 positive wells, this sample was calculated to contain either 1.5 SD_{50} (per 20 µl) if 3/4 wells positive or 1.0 SD_{50} (per 20 µl) if 2/4 wells positive.

Measurement of biomarkers of neurodegeneration

Plasma and CSF GFAP, NfL, Tau and UCH-L1 were measured by Simoa Neurology 4-plex B (N4PB) kit on a HD-X Analyser (Quanterix), according to the manufacturer's protocol[156]. In brief, samples were thawed and centrifuged at 10,000*g* for 5 minutes at room temperature (21°C) to precipitate any debris. Then, they were transferred to designated wells on the plates, diluted at 1:4 for plasma and 1:40 (or 1:100) for CSF with sample diluent, and bound to paramagnetic beads coated with capture antibodies specific for human GFAP, NfL, Tau and UCH-L1. Longitudinal samples from a single patient , where available, were analysed on the same plate. The biomarker-bound beads were then incubated with the respective biotinylated detection antibodies which in turn are conjugated to streptavidin-β-galactosidase complex which serves as a fluorescent tag. Hydrolysis of the complex by a resorufin β-D-galactopyranoside substrate results in a fluorescent signal proportional to the concentration of the

respective biomarkers present. Biomarker measurements for each sample were extrapolated from a standard curve, fitted to a 4-parameter logistic algorithm. Coefficients of variation (CVs) were determined using four internal quality control samples, and were < 20% and < 10% for intra-assay and inter-assay comparisons.

Data and statistical analyses

Plasma and CSF samples from the analysed cohort were subdivided into healthy controls (HC), IPD at-risk individuals greater or less than 2 years to predicted/actual onset (IPD-AR > 2y and IPD < 2y respectively), symptomatic IPD individuals (IPD), grouped sCJD/iCJD/vCJD, and iCJD at-risk individuals (iCJD-AR). All the N4PB values from our sample cohorts including healthy controls (HC) had positively skewed distributions, similar to our previous Simoa assay results for NfL and Tau[140]. Log_{10} transformation of reduced skewness to largely between -1 and 1 across our sample cohorts, rendering them roughly normally distributed, allowing group-wise comparisons of means using Single Factor ANOVA followed by pairwise t-tests.

The normal aging effects of GFAP, NfL and Tau[157-160] were addressed by first determining that the coefficients of linear regression of HC and IPD-AR>2y cohorts (found to be similar, and hence merged), and applied to the remaining cohorts to calculate age-normalised values, except for UCH-L1 which did not demonstrate any age effect. Single-factor ANOVA followed by pairwise Student's t-test (assuming α = 0.05) was then applied to compare means of age-normalised values grouped by the respective cohorts. Mixed effects models with random effects of slopes and intercepts were used to model individual biomarker slopes.

Statistical analyses were carried out using STATA v15.1, Microsoft Excel, and GraphPad Prism (version 9.2.0).

Results

Introduction of RML rPrP purification protocol

The Molecular Diagnostics Group at the MRC Prion Unit at UCL had independently adapted the RT-QuIC assay from previously published protocols, with the use of bank vole (BV) rPrP in high throughput 384-well format to explore seeding activity in BH and post-mortem CSF from a variety of prion diseases with reasonable success (discussed in separate chapter)[135]. However, prior to 2020, the Unit possessed no experience in testing ante-mortem CSF samples despite the at-risk cohort being entirely composed of this biofluid medium, which also represents a completely different sample matrix compared to BH and post-mortem CSF. Moreover, of the differences identified in comparison with the firmly established and widely used core RT-QuIC protocol from the NIH RML, rPrP purification and hence the rPrP species is felt to be one of the key determinants for amplification efficiency and assay specificity. In essence the Unit expressed and purified rPrP using constructs with histidine tags, which required thrombin cleavage and elution through a second NiNTA column. Additionally, the rPrP was stored frozen at -80°C at a higher (more destabilising) pH, and required further processing involving multiple freeze-thaw cycles prior to use in experiments.

A 6-week research sabbatical and technical training residency in the RT-QuIC assay was arranged at NIH RML in Hamilton, Montana in Sept – Oct of 2019, under the supervision of Prof Byron Caughey, Dr Christina Orrù and Mr Andrew Hughson, to achieve proficiency in setting up and performing RT-QuIC assays. On return to MRC Prion Unit at UCL, a direct comparison between MRC and RML purified Ha90 rPrP species' performance in sCJD BH seeded RT-QuIC was conducted under similar conditions (shared 96-well plate, reaction mix, sCJD BH dilutions and microplate reader); the RML Ha90 rPrP preparation was made at RML and imported to the Unit. This head-to-head comparison established that the dilution series using RML Ha90 rPrP not only had a higher SD_{50} (7.95 (RML) vs 7.45 (MRC)), but also that spontaneous fibrillisation is less likely to occur with RML purification (Figure 6.). Subsequently, our Unit fully adopted the RML protocol for RT-QuIC including its rPrP

purification for full length human (Hu), Ha90, BV and truncated BV (BV90) using the respective glycerol stocks supplied directly by RML[161].

The exception to this is purification of Hu P102L rPrP as RML does not possess glycerol stocks for this construct, having never experimented with this before. As such, the Hu P102L rPrP was purified according to the original MRC protocol but with modifications made to shorten and streamline the process (Figure 5). Following the second elution through the NiNTA columns, the preparation was immediately dialysed in PBS pH 5.8, filtered, aliquoted and frozen at -80°C. This shortens the entire purification process, bypassing the additional steps in the original MRC protocol (Figure 5).

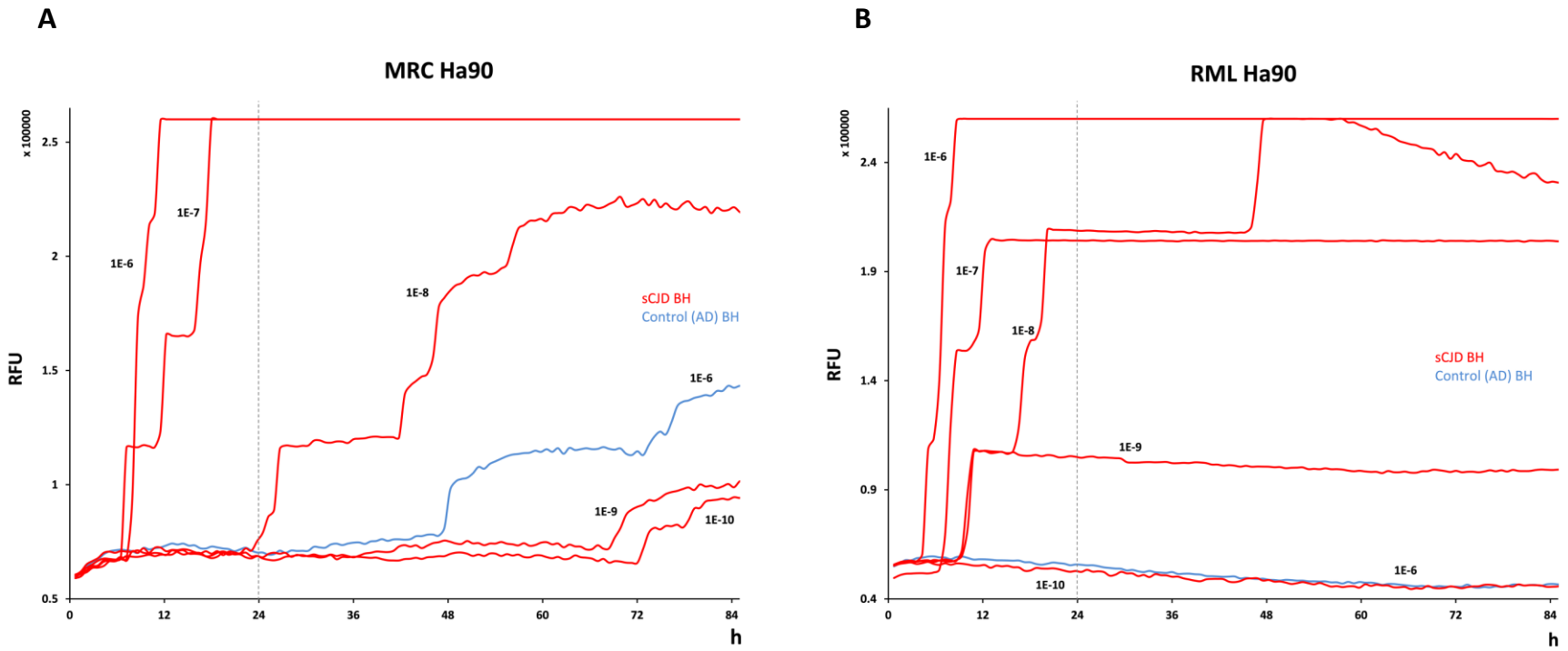

Figure 6 Head-to-head comparison of RT-QuIC assay performance between Ha90 rPrP species purified from MRC and RML protocols.

(**A**) This graph shows the averaged RT-QuIC traces of the dilution series of sCJD BH (red traces) seeded reactions using Ha90 rPrP purified through the MRC protocol. The SD_{50} is calculated to be *7.45*, and the control wells (blue trace) showed spontaneous fibrillisation in after 45h. (**B**) This graph shows the averaged RT-QuIC traces of the dilution series of sCJD BH (red traces) seeded RT-QuIC reactions using Ha90 rPrP purified through the RML protocol. The calculated SD_{50} is *7.95*, and the control wells (blue trace) remained negative for the duration of the reaction. The vertical dotted line indicates the time time cut-off for this assay.

NPMC biofluid sample cohort

The CSF and plasma biofluid sample archive from both IPD and IPD-AR individuals covers *PRNP* mutations including 5-OPRI, 6-OPRI, P102L, P105S, A117V, P157X, D178N-129V, D178N-129M, Y163X and E200K. In the CJD cohort, we collected samples from individuals symptomatic sCJD, iCJD and vCJD (plasma only); the iCJD-AR cohort comprised only of those exposed to implicated batches of cadaver-sourced human growth hormone.

We defined *converters* as at-risk individuals in whom we obtained at least one biofluid sample (CSF or plasma) in their presymptomatic stages before becoming symptomatic (clinical conversion). Clinical conversion is said to have taken place with the emergence of characteristic neurological symptoms and signs, and/or functional decline measurable by validated prion disease-specific rating scale scores (MRC Prion Disease Rating Scale[106], MRC Prion Disease Cognitive Scale or MRC Prion Disease Motor Scale scores[162]), supported by disease-specific investigation findings (e.g. DWI in fCJD[78], thermal thresholds in P102L-GSS[86], and polysomnography in FFI[163]). The entire IPD-AR, iCJD-AR and converter cohorts are illustrated in Figure 7.

Fast IPD is arbitrarily considered as disease durations that typically last 12 months or less, while *slow* IPD refers to disease typically greater than 12 months.

Summaries of the sample demographics, and individual baseline demographics are shown in Table 3 and Table 4 respectively; individual-level demographic details are listed in Table 11 in Appendices.

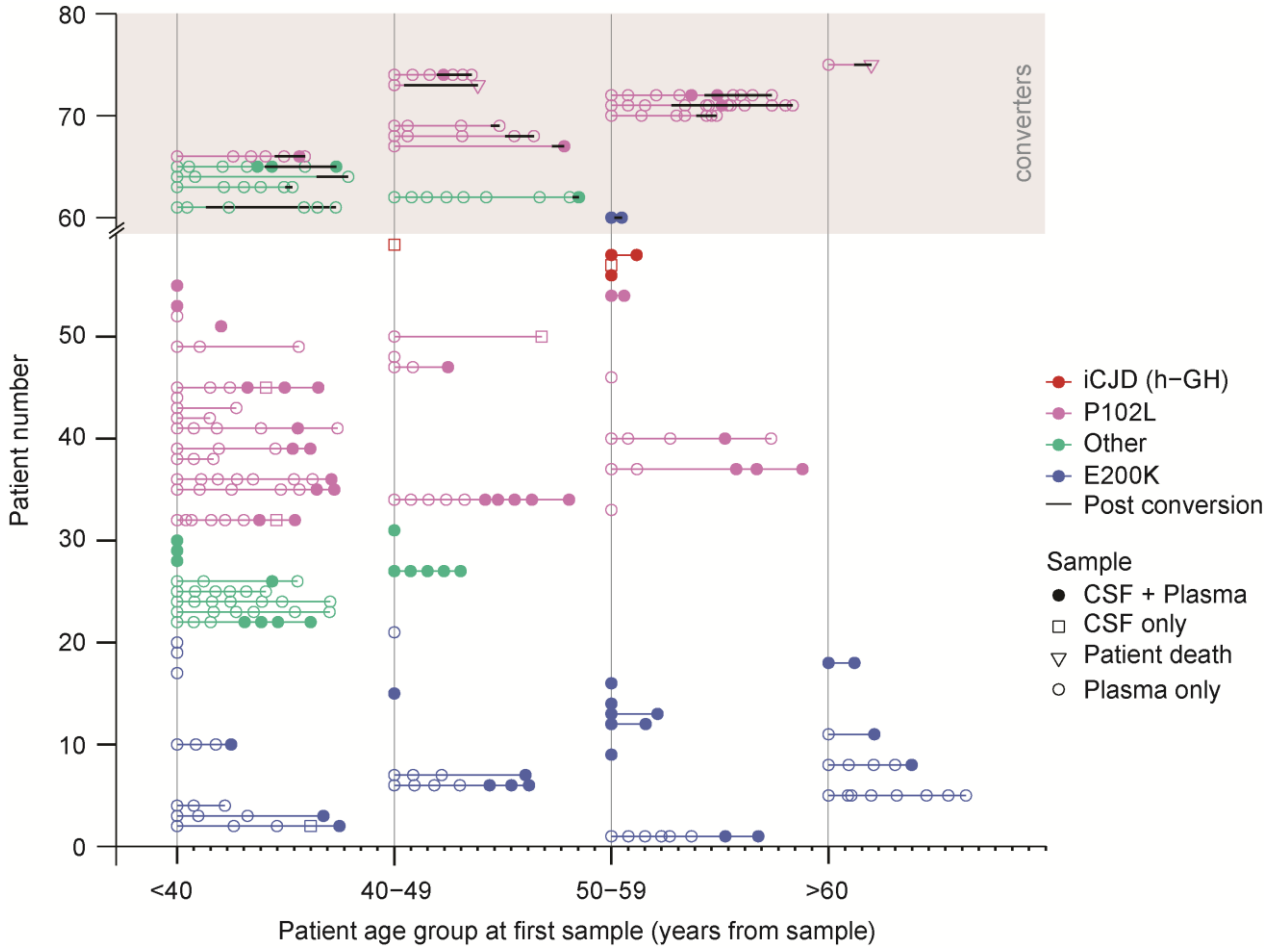

Figure 7 IPD-AR, iCJD-AR and IPD converter biofluid sample archive.

This graph plots all the samples (plasma only, CSF only or matched plasma and CSF) analysed in this study, grouped by age category (<40, 40-49, 50-59 and >60) on the *x*-axis to obscure identities, with each minor tick mark after the start of each age category reflecting an interval of one year. A total of 12 years are covered per age group as the longest follow-up is over 11 years, in order to avoid overlapped timelines. The first (or only) sample from each individual is collapsed to the start of each age category to preserve anonymity. Samples from the same individual are joined by a horizontal line if more than one sample was collected; thick black horizontal lines denote onset of clinical conversion. Converters are grouped together in the upper shaded part of the graph. For converters where only one presymptomatic sample exists without any follow-up samples, the subsequent data point (unfilled inverted triangle marker) joined by line indicates time of death. IPD mutations with fewer than five at-risk individuals were grouped as “Other” to avoid self-identification. Reproduced from Mok *et al.* 2023 (https://doi.org/10.1093/brain/awad101).

RT-QuIC prion seeding assay CSF sample cohort

Between 2015 and 2021, a total of 161 CSF samples were collected for RT-QuIC analyses from IPD-AR (n = 61; individuals = 39), IPD (n = 20; individuals = 20), sCJD/iCJD (n = 17; individuals = 17) and iCJD-AR (n = 4; individuals = 4), and non-prion controls (n = 59; individuals = 59). Notably, three pairs of CSF samples from three IPD converters (E200K = 1, P102L = 1, 6-OPRI = 1) formed part of this collection. In each of all three converters, one sample before (range -0.2 to -0.9 years), and one sample after (range 0.4 to 0.6 years) conversion was available to test.

N4PB neurodegenerative marker sample cohort

Between 2008 and 2021, we assembled at total of 416 plasma and 135 CSF samples which are available for Simoa N4PB neurodegenerative biomarker measurements. Of the plasma samples (n = 217; individuals = 69) and CSF samples (n = 67; individuals = 40) from the IPD-AR group, the greatest interest is on the plasma samples from 16 converters (range -9.9 to 7.4 years) and 7 CSF samples from three converters (range -0.9 to 4.3 years). Within these 16 converters, 8 had previous plasma NfL and tau tested on simplex Simoa platforms, and published[140]. A small collection of samples (plasma = 3; CSF = 4) from four iCJD-AR individuals was also available. All these at-risk groups were compared to IPD, CJD (sCJD, iCJD and vCJD), and HC groups.

Table 3 Sample demographics of RT-QuIC and N4PB cohorts

	Cohorts	Cohort Subgroups	Number of samples	Unique Individuals	Mean Age at Sample in yrs (SD)	Female	Male	c129 MM	c129 MV	c129 VV	*PRNP* untested/unknown
Plasma N4PB	IPD-AR		217	69	43.9 (13.3)	128	89	96	57	0	64
		IPD-AR > 2 yrs	198	66	49.0 (13.2)	115	83	82	52	0	64
		IPD-AR < 2 yrs	19	14	43.4 (13.3)	13	6	14	5	0	0
		P102L	100	33	43.7 (10.4)	68	32	26	25	0	49
		E200K	59	22	52.2 (15.9)	23	36	44	7	0	8
		Miscellaneous IPD	58	15	35.9 (9.17)	37.0	21	31	25	0	2
	c-hGH iCJD-AR		3	2	55.7 (0.6)	1	2	1	0	0	1
	Symptomatic IPD		62	26	50.9 (11.8)	40	22	33	29	0	0
	CJD		40	18	52.0 (14.5)	12	28	16	19	5	0
	Healthy controls	GFAP & NfL	132	112	49.7 (13.5)	66	66	0	0	0	127
		Tau & UCH-L1	89	63	51.3 (12.9)	38	51	0	0	0	89
CSF N4PB	IPD-AR		67	40	46.9 (12.4)	36	31	29	15	0	21
		IPD-AR > 2 yrs	64	37	47.0 (12.2)	33	31	26	15	0	21
		IPD-AR < 2 yrs	3	3	46.4 (19.2)	3	0	3	0	0	0
		P102L	30	16	46.0 (12.1)	18	12	6	5	0	19
		E200K	23	16	54.1 (10.7)	11	12	16	5	0	2
		Miscellaneous IPD	14	8	37.3 (8.4)	7	7	7	5	0	2
	c-hGH iCJD-AR		5	4	53.8 (3.0)	1	4	1	0	0	4
	Symptomatic IPD		22	21	48.4 (13.6)	14	8	14	8	0	0
	CJD		17	17	60.6 (10.7)	10	7	7	9	0	1
	Healthy controls		24	24	69.1 (6.8)	12	12	0	1	0	23
CSF RT-QuIC	IPD-AR		61	39	46.5 (12.3)	31	30	28	13	0	20
		IPD-AR > 2 yrs	58	36	46.5 (12.1)	28	30	25	13	0	20
		IPD-AR < 2 yrs	3	3	46.4 (19.2)	3	0	3	0	0	0
		P102L	27	16	45.4 (11.7)	17	10	6	5	0	16
		E200K	22	16	53.5 (10.8)	10	12	15	5	0	2
		Miscellaneous IPD	12	7	36.2 (8.6)	5	7	7	3	0	2
	c-hGH iCJD-AR		4	4	53.25 (3.1)	1	3	1	0	0	3
	Symptomatic IPD		20	20	48.9 (13.4)	13	7	12	8	0	0
	CJD		17	17	59.4 (10.5)	10	7	7	10	0	0
	Non-prion controls		59	59	65.4 (14.5)	28	31	0	1	0	58

Standard deviation (SD); codon 129 (c129); yrs (years); methionine homozygous (MM); methionine-valine heterozygous (MV); valine homozygous (VV)

Table 4 Summary of individual baseline demographics

	PRNP mutation group or CJD type	No. of individuals	Mutation status		Female	Male	Mean age at 1st sample (SD)	Mean age at disease onset (SD)	*PRNP* Codon 129			
			Carrier	Untested					MM	MV	VV	Untested/ unknown
IPD-AR & iCJD-AR	P102L-AR	33	22	11	23	10	41.3 (10.4)	x	12	9	0	12*
	E200K-AR	21	16	5	10	11	47.3 (14.7)	x	11	5	0	5
	Miscellaneous IPD-AR (5-OPRI, 6-OPRI, A117V, D178N-129M and D178N-129V)	15	12	3	9	6	32.0 (9.1)	x	7	5	0	3
	iCJD-AR	4	x	x	1	3	53.3 (3.1)	x	1	0	0	3
IPD Symptomatic at 1st Assessment	P102L	4	4	0	4	0	40.6 (12.0)	39.2 (11.4)	1	3	0	0
	E200K	3	3	0	3	0	63.0 (9.4)	62.9 (9.3)	3	0	0	0
	6-OPRI	2	2	0	1	1	33.5 (1.1)	30.8 (2.9)	2	0	0	0
	D178N-129M	1	1	0	1	0	70.3	69.5	0	1	0	0
	P105S	1	1	0	1	0	48.9	48.1	0	1	0	0
	Q212P	1	1	0	1†	0	57.6	55.0	1	0	0	0
	Y163X	1	1	0	1	0	39.4	32.9	0	1	0	0
IPD Converters	P102L	10	10	0	7	3	48.2 (6.6)	52.6 (6.3)	6	4	0	0
	D178N-129M	2	2	0	2	0	39.6 (5.9)	47.7. (8.2)	1	1	0	0
	6-OPRI	2	2	0	1	1	21.7 (3.0)	28.4 (5.1)	2	0	0	0
	E200K	1	1	0	1	0	59.2	59.4	1	0	0	0
	5-OPRI	1	1	0	1	0	37.4	39.7	1	0	0	0
CJD CSF	sCJD	16	x	x	9	6	62.1 (9.4)	61.4 (9.4)	7	8	0	1
	iCJD	2	x	x	1	1	44.2 (3.0)	43.5 (2.7)	0	2	0	0
CJD Plasma	sCJD	11	x	x	5	6	60.4 (13.2)	59.4 (13.4)	3	6	2	0
	iCJD	4	x	x	1	3	48.3 (3.5)	47.7 (3.3)	2	2	0	0
	vCJD	3	x	x	1	2	40.9 (7.7)	39.6 (6.9)	2	1	0	0
CSF-R Controls	x	59	x	x	28	31	65.4 (14.5)	x	0	1	0	58
CSF-N Controls	x	24	x	x	12	12	69.1 (6.8)	x	0	1	0	23
Plasma Controls	x	112	x	x	59	53	49.6 (14.0)	x	0	0	0	112

*includes one confirmed P102L carrier whose codon 129 status is unknown (tested elsewhere)
†male to female transgender

Exploration of optimum RT-QuIC conditions for IPD CSF samples

Due to technical, rPrP and biofluid sample resource limitations largely imposed by COVID-19 pandemic restrictions during which these experiments were carried out, a heuristic (rather than a comprehensive) approach was employed to determine the most suitable RT-QuIC conditions for detecting CSF PrP-amyloid seeding activity, guided by key findings in the literature[132-134,136]. A panel of CSF obtained from well-characterised individuals symptomatic of CJD (sCJD and iCJD), and IPD encompassing *PRNP* mutations E200K, P102L, P105S, D178N-129M, Y163X and 6-OPRI were first screened by best established IQ-CSF RT-QuIC protocol. IQ-CSF-negative IPD samples from this panel (P102L, P105S, D178N-129M, Y163X and classical 6-OPRI) were then tested repeatedly with assay variations in buffer solutions, pH, incubation temperatures, rPrP species and concentrations, salts, and CSF seeding volumes to ascertain the optimum conditions, before testing the entire IPD-AR and iCJD-AR groups. A summary of assay component permutations and outcomes is shown in Table 5.

IQ-CSF RT-QuIC in CJD phenotypes

The IQ-CSF RT-QuIC protocol proved to be highly sensitive assay for CJD-phenotype disease including sCJD (n = 15), iCJD (n = 2) and E200K fCJD (n = 4). Fifteen out of seventeen CJD CSF samples were positive (≥ 2/4 wells) while two were equivocal (1/4 wells positive) on initial survey; the two equivocal samples then tested positive when the CSF seeding volume was adjusted to 15 µl instead of 20 µl. All control CSF samples (n = 59) were negative using the 20 µl seeding volume, as were those (n = 47) using the 15 µl seeding volume. This gave an overall sensitivity and specificity of 100%; for sensitivity the 95% CI is (89.49, 100.00), while for specificity the 95% CI is (93.94, 100.00). All four out of four symptomatic E200K CSF samples were strongly positive, with all 4/4 wells from each sample exceeding fluorescence thresholds within 10 hrs from beginning.

All other IPD CSF samples were negative on IQ-CSF RT-QuIC except for a sample from a patient with 6-OPRI whose initial disease course classical of the slowly

progressive dysexecutive-apraxic syndrome of several years changed abruptly to resemble fCJD, dying within short months. The MRI Brain images obtained following his abrupt deterioration showed typical DWI changes for CJD, and CSF was also positive for protein 14-3-3. This sample tested strongly positive with IQ-CSF RT-QuIC, *vis a vis* negative results obtained from two other CSF samples from classical symptomatic 6-OPRI individuals (Figure 8).

Bespoke Hu rPrP RT-QuIC with NaI in novel P105S mutation

CSF from a patient with the novel P105S mutation, who presented with a clinical course resembling CJD and DWI abnormalities on MRI, had 1/4 positive wells on IQ-CSF RT-QuIC. Further optimisation demonstrated improved seeding activity with FL Hu rPrP RT-QuIC with 130 mM NaCl at pH 7.4 at 42°C, and even better with 130 mM NaI at similar conditions (Figure 9).

Bespoke Hu P102L rPrP RT-QuIC with NaI in P102L disease

A new iteration of RT-QuIC with bespoke conditions, using the specially designed Hu P102L rPrP construct and NaI as salt, was found to be useful in detecting seeding activity in a proportion of symptomatic P102L CSF samples. Of nine such samples, it was positive in four, all of which came from individuals with the classical GSS phenotype, though one had a late CJD-like transformation. Two other CSF samples from classical GSS individuals, and all three from those with the purely cognitive phenotype tested negative. Of note, all these P102L samples (n = 9; GSS = 5, GSS-CJD = 1, Cognitive = 3), tested negative on the standard IQ-CSF, FL Hu and FL BV RT-QuIC assays previously.

Lack of optimum RT-QuIC iterations for other IPD CSF

No optimum RT-QuIC conditions were discovered for CSF samples from symptomatic D178N-129M, Y163X and classical 6-OPRI individuals during our extensive exploration (Table 5). Certain assay conditions did produce late positives in these IPD CSF samples, but were discounted due to proximity to spontaneous fibrillisation arising from control wells (< 20 hrs apart).

Table 5 Exploratory RT-QuIC conditions for symptomatic IPD CSF panels

rPrP	rPrP (mg/L)	Temp °C	Buffer	pH	Salt	Salt (mM)	SDS %	Cut-off (hrs)	CSF (µl)	Notes
Ha90	0.1	55	PBS	7.4	NaCl	300	0.002	24	20	No spontaneous fibrillisation in Control CSF wells up to 85 hrs; highly sensitive for E200K and CJD-like 6-OPRI
Ha90	0.1	55	PBS	7.4	NaI	300	0.002	24	20	Control CSF 2/4 wells positive ≥ 25 hrs; unstable
BV	0.1	55	PBS	7.4	NaI	300	0.002	24	20	Control CSF 2/4 wells positive > 55 hrs; negative for P102L, D178-FFI, 6-OPRI, Y163X
BV	0.1	50	PBS	7.4	NaCl	300	0.002	30	20	No spontaneous fibrillisation in Control CSF wells up to 85 hrs; negative for P102L, D178-FFI 6-OPRI, Y163X
BV	0.1	50	HEPES	8	NaI	300	0.002	30	20	Control CSF 2/4 wells positive > 60 hrs; negative for P102L, D178-FFI 6-OPRI, Y163X
Ha90	0.1	50	HEPES	8	NaI	300	0.002	30	20	Control CSF 2/4 wells positive ≥ 45 hrs; unstable
BV	0.1	55	PBS	7.4	NaCl	300	0.002	24	20	Control CSF 2/4 wells positive > 50 hrs; negative for P102L, D178-FFI, 6-OPRI, Y163X
BV	0.1	55	HEPES	8	NaI	300	0.002	24	20	Control CSF 4/4 wells low positive > 54 hrs; unstable
Ha90	0.1	55	HEPES	8	NaI	300	0.002	24	20	Control CSF 2/4 wells positive > 35 hrs; unstable
Hu	0.05	37	PIPES	7	NaI	500	0	50	5	Control CSF 3/4 wells positive > 45 hrs; unstable
Hu	0.05	37	PIPES	7	NaCl	500	0	50	5	Control CSF 1/4 wells positive > 70 hrs; P102L-Cog and 6-OPRI late positives, unable to replicate
Hu	0.1	42	PBS	7.4	NaCl	130	0.002	50	20	No spontaneous fibrillisation in Control CSF wells up to 85 hrs; negative for P102L, D178-FFI, 6-OPRI, Y163X
Hu	0.1	42	PBS	7.4	NaI	130	0.002	50	20	No spontaneous fibrillisation in Control CSF wells up to 85 hrs; negative for P102L, D178-FFI, 6-OPRI, Y163X
Hu*	0.05	37	PIPES	7	NaI	500	0	50	5	Control CSF 3/4 wells positive > 45 hrs; unstable
Hu*	0.05	37	PIPES	7	NaCl	500	0	50	10	No spontaneous fibrillisation in Control CSF wells up to 85 hrs; negative for P102L, D178-FFI, 6-OPRI, Y163X
Hu*	0.05	37	PIPES	7	NaCl	500	0.001	50	10	No spontaneous fibrillisation in Control CSF wells up to 85 hrs; negative for P102L, D178-FFI 6-OPRI, Y163X
Hu*	0.05	37	PIPES	7	NaI	500	0	50	8	Control CSF 3/4 wells positive ≥ 45 hrs; unstable
Hu P102L	0.05	37	PIPES	7	NaI	150	0	50	5	Control CSF 4/4 wells positive ≥ 45 hrs; unstable
Hu P102L	0.05	37	PIPES	7	NaCl	500	0	50	5	Control CSF 4/4 wells positive ≥ 45 hrs; unstable
Hu P102L	0.1	42	PBS	7.4	NaCl	130	0.002	50	20	No spontaneous fibrillisation in Control CSF wells up to 85 hrs; positive for subset of P102L-GSS
Hu P102L	0.1	42	PBS	7.4	NaI	130	0.002	50	20	No spontaneous fibrillisation in Control CSF wells up to 85 hrs; more sensitive than NaCl for P102L-GSS
BV90	0.1	55	PBS	7.4	NaCl	300	0.002	24	20	No spontaneous fibrillisation in Control CSF (pooled) wells up to 85 hrs; inhibitory factor?
BV90	0.1	55	HEPES	8	NaI	300	0.002	24	20	No spontaneous fibrillisation in Control CSF (pooled) wells up to 85 hrs; inhibitory factor?
BV90	0.1	55	PBS	7.4	NaCl	300	0.002	24	20	Control CSF 4/4 wells positive ≥ 43 hrs; unstable
BV90	0.1	55	HEPES	8	NaI	300	0.002	24	20	Control CSF 4/4 wells positive ≥ 20 hrs; unstable
BV	0.1	55	HEPES	8	NaI	300	0.002	24	15	Control CSF 4/4 wells positive ≥ 40 hrs; unstable

Hu* use 30s/30s shake/rest cycles (vs 60s/60s for all other experiments) in BMG microplate readers at 700 rpm; shaded rows represent best assay conditions available for testing symptomatic and IPD-AR CSF collection.

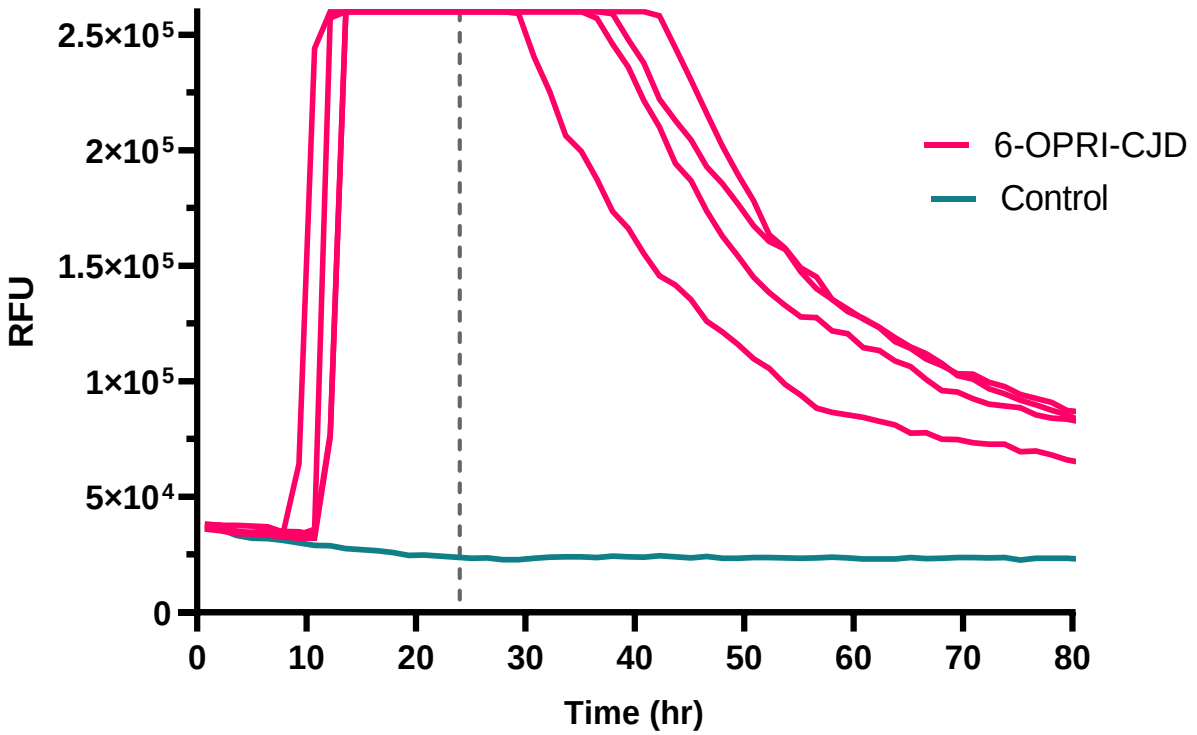

Figure 8 IQ-CSF RT-QuIC graph of CSF from 6-OPRI case with CJD-like transformation.

This figure shows the IQ-CSF RT-QuIC traces from the individuals wells seeded by CSF from one patient who had an initial classical slowly progressive 6-OPRI phenotype for several years before an abrupt CJD-like deterioration follow swiftly by death. Two other CSF samples from patients with classical 6-OPRI phenotype were negative. The dotted vertical line indicates the the cut-off time for this assay (24 hrs). Reproduced from Mok *et al.* 2023 (https://doi.org/10.1093/brain/awad101).

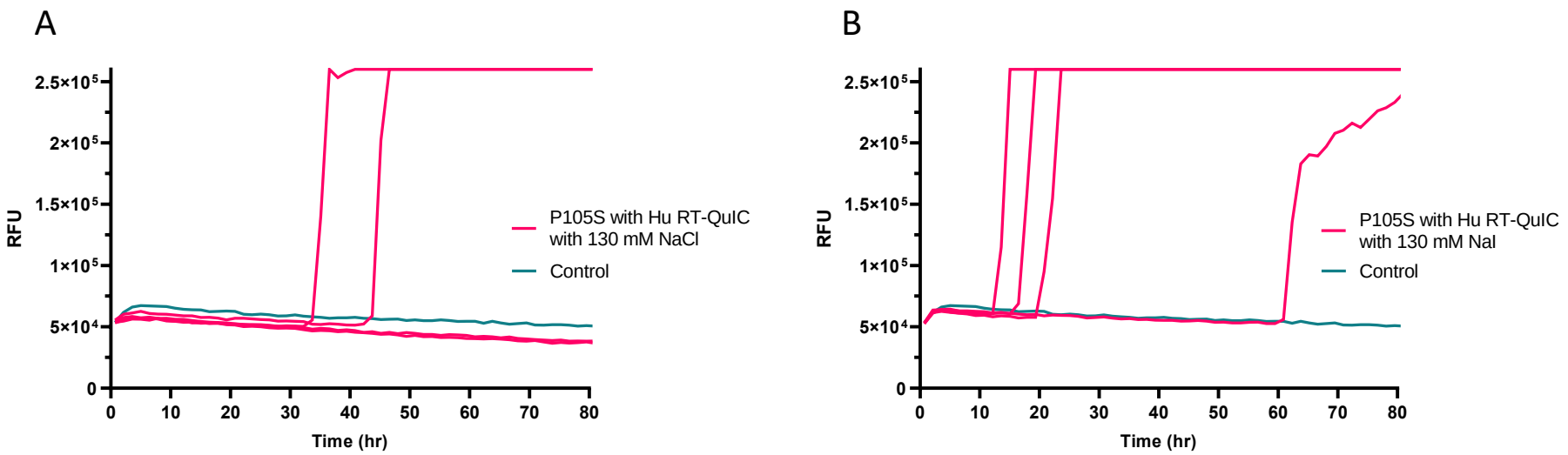

Figure 9 Comparison of FL Hu rPrP RT-QuIC responses on P105S IPD CSF sample based on salt choice.

(A) FL Hu RT-QuIC using 130 mM NaCl gave 2/4 positive wells. **(B)** In comparison, switching to 130 mM NaI resulted in shorter times to RFU threshold, and higher proportion of positive wells. The dotted vertical line denotes the cut-off time for this assay (incubated at 42°C). Reproduced from Mok *et al.* 2023 (https://doi.org/10.1093/brain/awad101).

RT-QuIC analyses of IPD-AR and iCJD-AR CSF cohorts

Based on the outcomes from the IPD CSF exploratory phase, the entire at-risk CSF sample cohort was divided into the following groups, matched to the best available RT-QuIC assay conditions:

- **E200K-AR and iCJD-AR** – Ha90 rPrP in pH 7.4 + 300 mM NaCl at 55°C (**IQ-CSF RT-QuIC**)
- **P102L-AR** – FL Hu P102L rPrP in pH 7.4 + 130 mM NaI at 42°C (**Hu P102L RT-QuIC**)
- **Other IPD-AR and P102L-AR** – FL BV rPrP in pH 7.4 + 300 mM NaCl at 50°C (**BV RT-QuIC**)

IQ-CSF RT-QuIC on E200K-AR and iCJD-AR groups

Four CSF samples from three individuals in E200K-AR group tested positive with the IQ-CSF RT-QuIC assay; all CSF samples from 11 other individuals known to carry the E200K tested negative on IQ-CSF RT-QuIC, as did CSF samples from two at-risk individuals whose mutation status is unknown. All three individuals were confirmed carriers of the E200K mutation, and one of them underwent clinical conversion 0.2 years later; this individual's post-conversion (0.4 years after) was also positive on IQ-CSF RT-QuIC.

Two of these individuals remain asymptomatic at the time of writing. One E200K-AR here had two fully positive samples (4/4 wells) about two years apart, and were drawn at 3.75 and 1.70 years from the present time (corresponding to -5.1 and -7.1 years to *predicted* onset). The other E200K-AR individual's samples was drawn at 3.37 years from the present time (-8.3 years to *predicted* onset) but only with 3/4 wells positive (Figure 10A).

The CSF SD_{50}/µl was calculated through the Spearman-Kärber as described (see Methods), revealing a rise from 1.78 to 2.34 in the converter sample pair, and a drop from 1.35 to 0.78 in the non-converter sample pair (Figure 11). The experiment was not repeated on this occasion due to limitations on sample volume resource.

Hu P102L RT-QuIC on P102L-AR group

All but one P102L-AR CSF sample (1/27) and one control sample (1/57) tested negative with the bespoke Hu P102L RT-QuIC; both samples remained positive on repeat testing (Figure 10B). All CSF samples from seven individuals known to carry the P102L mutation, as well as six at-risk individuals with unknown mutation carrier status tested negative on the Hu P102L RT-QuIC. The positive P102L-AR sample came from an untested at-risk individual over the age of 60. The one positive control CSF sample came from a set of terminally de-identified good-quality CSF samples retained from clinical referrals on the basis of neurodegenerative symptoms, further subdivided into AD and non-AD based on biomarker profiling (Figure 10C). This meant that the latter non-AD group may contain any manner of neurodegeneration other than AD. Of note, this control sample tested negative on both IQ-CSF and BV RT-QuIC assays.

BV RT-QuIC on Other IPD-AR and P102L-AR groups

Despite not being able to develop optimum RT-QuIC assays for IPD outside of E200K and P102L in the exploratory phase, the Other IPD-AR (includes 6-OPRI, D178N-129V and A117V) were tested with BV RT-QuIC on the potential of rPrP being a “universal acceptor” in BH-seeded reactions[134]. All 12/12 Other IPD-AR samples tested negative with BV RT-QuIC, as did all 27/27 P102L-AR samples; all 51/51 control samples were also negative.

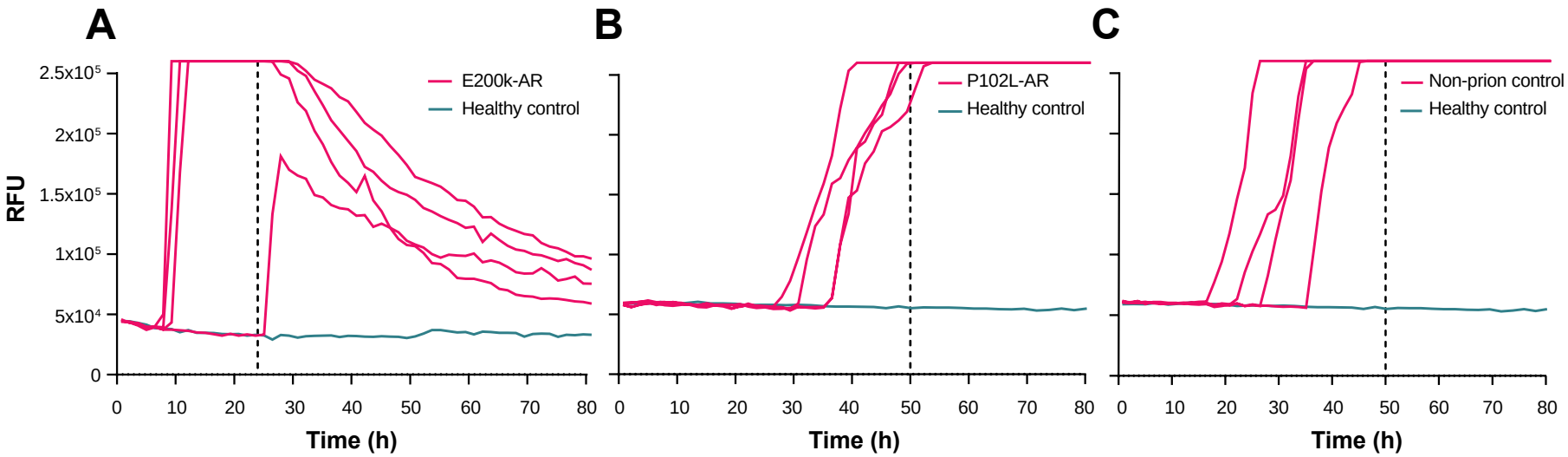

Figure 10 Graphs of select IPD-AR and control samples with positive RT-QuIC results.

(**A**) This is the sole IQ-CSF RT-QuIC positive E200K-AR sample which recorded fewer than 4/4 wells positive, drawn at 3.37 years from the present time. (**B**) This is the sole HuPrP P102L RT-QuIC positive sample in the P102L-AR set; this sample was negative when tested with BV RT-QuIC. (**C**) This non-prion disease (neurodegenerative) CSF sample tested positive with Hu P102L RT-QuIC, but tested negative with IQ-CSF RT-QuIC and BV RT-QuIC. The dotted vertical lines indicate the time cut-offs for the individual assays i.e. 24 hours for IQ-CSF RT-QuIC and 50 hours for Hu P102L RT-QuIC. Reproduced from Mok *et al.* 2023 (https://doi.org/10.1093/brain/awad101).

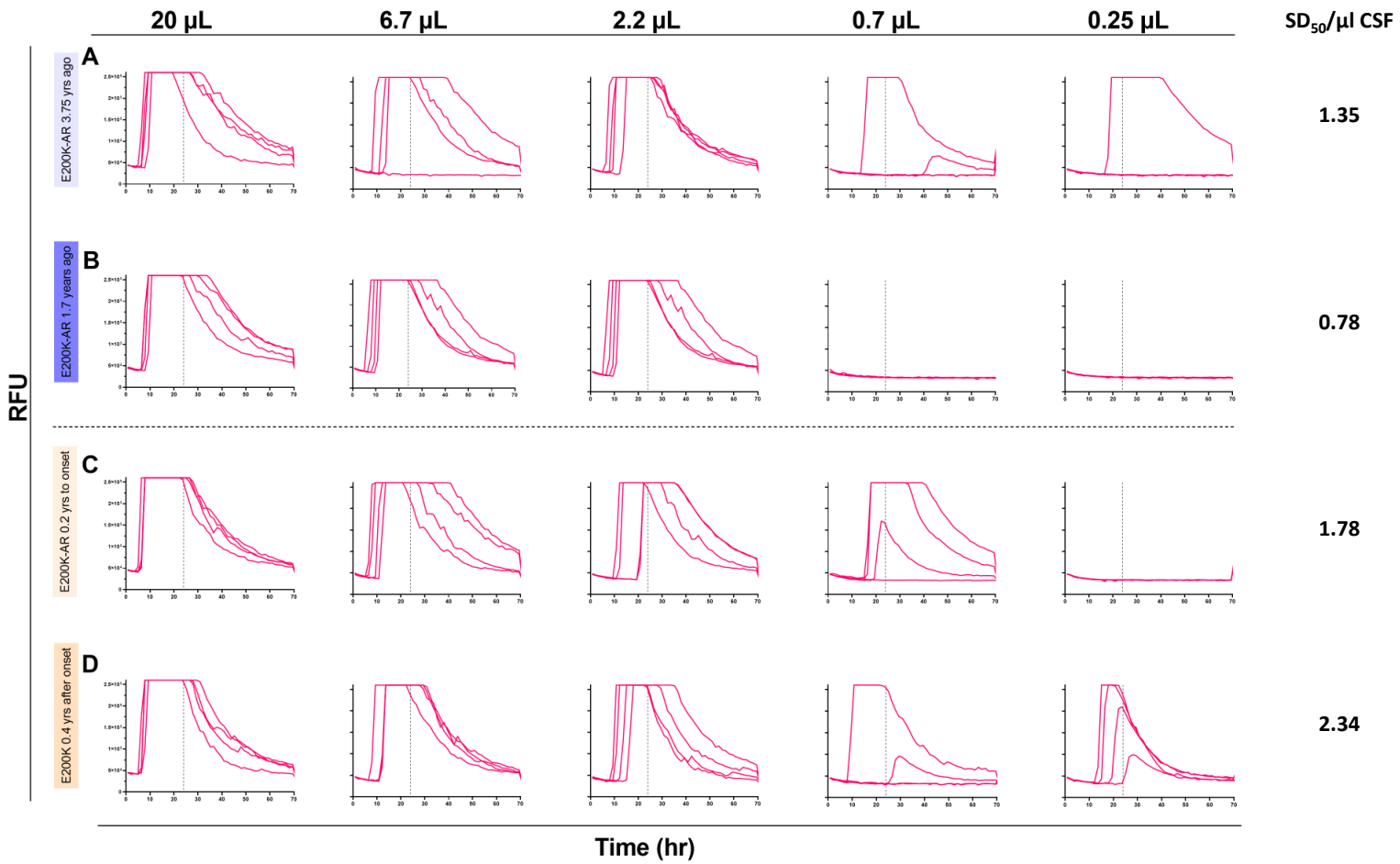

Figure 11 Dilution series calculating SD50/µl of presymptomatic E200K-AR IQ-CSF RT-QuIC positive CSF.

These panels show the CSF dilution series for the presymptomatic E200K-AR CSF samples which were positive on IQ-CSF RT-QuIC. Panels **(A)** and **(B)** depict RT-QuIC responses for the same individuals (remains asymptomatic). Panels **(C)** and **(D)** depict RT-QuIC responses for the E200K converter individual. Dotted vertical lines indicate cut-off time which is 24 hours for IQ-CSF RT-QuIC. Reproduced from Mok *et al.* 2023 (https://doi.org/10.1093/brain/awad101).

Plasma Simoa N4PB results

Of the four biomarkers assayed on the multiplexed Simoa N4PB platform, log(GFAP) and log(NfL) were found to have sequentially incremental and statistically significant mean values between IPD-AR > 2y, IPD-AR < 2y, IPD and CJD groups on single factor ANOVA with post hoc groupwise comparisons (Figure 12). For log(GFAP), IPD-AR > 2y versus IPD-AR < 2y is p = 0.0006, IPD-AR < 2y versus HC p = 0.0004, IPD-AR < 2y versus IPD is p = 0.0003; for log(NfL), IPD-AR > 2y versus IPD-AR < 2y is p = 0.002, IPD-AR < 2y versus HC is p = 0.007, and IPD-AR < 2y versus IPD is p = $3.7x10^{-6}$.

No statistically significant differences were present in the mean values of log(GFAP) and log(NfL) between HC and IPD-AR > 2y groups. The mean N4PB values for each group, and the p values from the ANOVA analyses are summarised in Table 6; the differences in mean values and p values for groupwise t-test comparisons are summarised in Table 7.

While statistically significant differences do exist between groups for log(Tau) and log(UCH-L1) which may be useful for dichotomous diagnostic segregation, these are not useful for prediction of proximity to disease onset. For example, mean log(Tau) was not statistically significant between IPD-AR > 2y versus IPD-AR < 2y (p = 0.329), HC/IPD-AR > 2y versus IPD (p = 0.1), and IPD-AR < 2y versus IPD (p = 0.849); mean log(UCH-L1) (not age-normalised) was not statistically different between IPD-AR > 2y versus IPD < 2y (p = 0.802).

In groupwise comparisons involving iCJD-AR, relevant statistically significant differences in means were noted with log(GFAP) versus CJD (2.01 vs 2.70 pg/ml; p = 0.02), and with log(Tau) versus healthy controls (0.609 vs 0.264 pg/ml; p = 0.03). The latter was driven solely by an outlier from an iCJD-AR individuals in whom there was a contemporaneous invasive pituitary craniopharyngioma.

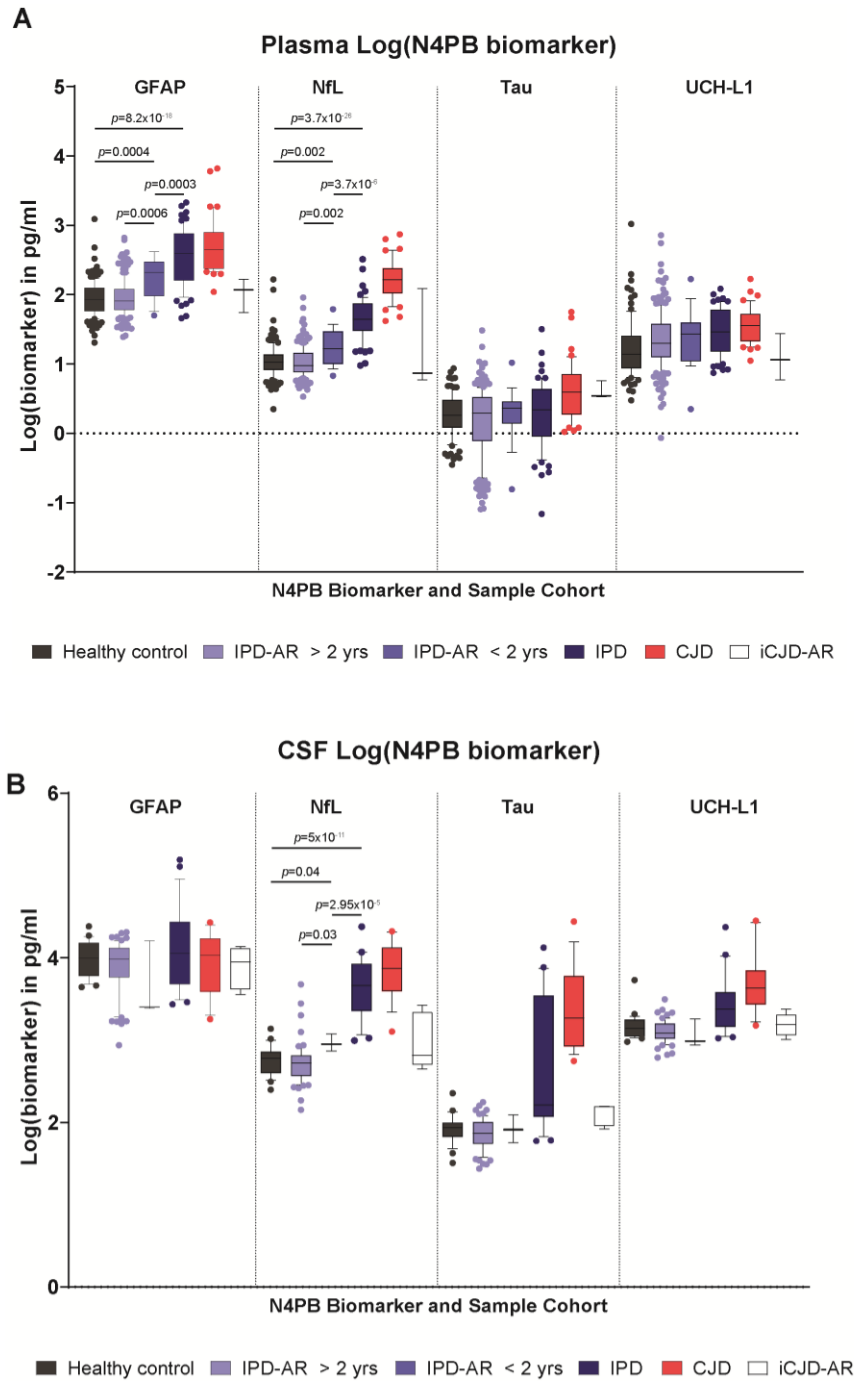

Figure 12 Simoa N4PB groupwise comparisons in Plasma and CSF.

(A) This panel shows the comparisons of means plasma N4PB values between pre-defined groups; only plasma GFAP and NfL have been found to have sequentially incremental and statistically significant differences between HC, IPD-AR > 2y, IPD-AR < 2y and IPD, with the key *p* values illustrated. **(B)** This panel shows that NfL is the only N4PB biomarker that showed similarly statistically significant incline in mean values from HC to IPD, again with the key *p* values illustrated. These figures were reproduced from Mok *et al.* 2023 (https://doi.org/10.1093/brain/awad101).

Table 6 Mean values of age-normalised N4PB biomarkers according to cohort

Plasma N4PB	Sample Number	Mean (pg/ml)	SD	ANOVA p value	CSF N4PB	Sample Number	Mean (pg/ml)	SD	ANOVA p value
Log(GFAP)				1.72629E-60	***Log(GFAP)***				0.109368
Normal Control	132	1.94	0.25		Normal Control	24	4.0	1.41	
IPD > 2yrs	198	1.95	0.26		IPD > 2yrs	64	3.9	1.40	
IPD < 2yrs	19	2.23	0.29		IPD < 2yrs	3	3.7	1.38	
IPD Symptomatic	62	2.56	0.41		IPD Symptomatic	22	4.1	1.42	
CJD	40	2.70	0.38		CJD	17	3.9	1.41	
iCJD-AR	3	2.01	0.25		iCJD-AR	5	3.9	1.40	
Log(NfL)				5.2614E-114	***Log(NfL)***				5.91E-36
Normal Control	132	1.04	0.26		Normal Control	24	2.8	1.29	
IPD > 2yrs	198	1.03	0.21		IPD > 2yrs	64	2.7	1.28	
IPD < 2yrs	19	1.26	0.27		IPD < 2yrs	3	3.0	1.31	
IPD Symptomatic	62	1.65	0.29		IPD Symptomatic	22	3.6	1.38	
CJD	40	2.22	0.29		CJD	17	3.8	1.40	
iCJD-AR	3	1.24	0.74		iCJD-AR	5	3.0	1.31	
Log(Tau)				6.99274E-06	***Log(Tau)***				6.62E-28
Normal Control	94	0.26	0.30		Normal Control	24	1.9	1.18	
IPD > 2yrs	198	0.18	0.49		IPD > 2yrs	64	1.9	1.17	
IPD < 2yrs	19	0.28	0.39		IPD < 2yrs	3	1.9	1.18	
IPD Symptomatic	62	0.30	0.48		IPD Symptomatic	22	2.6	1.27	
CJD	40	0.60	0.40		CJD	17	3.4	1.36	
iCJD-AR	3	0.61	0.13		iCJD-AR	5	2.1	1.20	
Log(UCH-L1)*				1.0087E-05	***Log(UCH-L1)****				5.84E-16
Normal Control	94	1.21	0.42		Normal Control	24	3.2	1.33	
IPD > 2yrs	198	1.35	0.40		IPD > 2yrs	64	3.1	1.33	
IPD < 2yrs	19	1.38	0.42		IPD < 2yrs	3	3.1	1.32	
IPD Symptomatic	62	1.48	0.33		IPD Symptomatic	22	3.4	1.36	
CJD	40	1.55	0.26		CJD	17	3.7	1.39	
iCJD-AR	3	1.09	0.33		iCJD-AR	5	3.2	1.34	

*not age-normalised
Standard deviation (SD)

Reproduced from Mok *et al.* 2023 (https://doi.org/10.1093/brain/awad101).

Table 7 Plasma N4PB post hoc groupwise t-test comparisons

	Group 1	Group 2	*P* value	Mean
Log(GFAP)	Healthy Control	IPD-AR > 2y	6.23E-01	1.67E-02
	Healthy Control	IPD-AR < 2y	4.28E-04	2.89E-01
	Healthy Control	IPD	1.12E-17	6.18E-01
	Healthy Control	CJD	1.77E-16	7.66E-01
	Healthy Control	iCJD-AR	6.56E-01	7.42E-02
	IPD-AR > 2y	IPD-AR < 2y	6.42E-04	2.73E-01
	IPD-AR > 2y	IPD	2.08E-17	6.01E-01
	IPD-AR > 2y	CJD	1.08E-15	7.50E-01
	IPD-AR > 2y	iCJD-AR	7.25E-01	5.75E-02
	IPD-AR < 2y	IPD	2.97E-04	3.29E-01
	IPD-AR < 2y	CJD	2.61E-06	4.77E-01
	IPD-AR < 2y	iCJD-AR	2.65E-01	2.15E-01
	IPD	CJD	6.51E-02	1.48E-01
	IPD	iCJD-AR	4.73E-02	5.44E-01
	CJD	iCJD-AR	2.41E-02	6.92E-01

	Group 1	Group 2	*P* value	Mean
Log(NfL)	Healthy Control	IPD-AR > 2y	2.98E-01	3.22E-02
	Healthy Control	IPD-AR < 2y	6.64E-03	1.96E-01
	Healthy Control	IPD	2.29E-24	5.93E-01
	Healthy Control	CJD	4.44E-32	1.16E+00
	Healthy Control	iCJD-AR	7.11E-01	1.82E-01
	IPD-AR > 2y	IPD-AR < 2y	1.57E-03	2.29E-01
	IPD-AR > 2y	IPD	3.96E-26	6.25E-01
	IPD-AR > 2y	CJD	7.82E-29	1.19E+00
	IPD-AR > 2y	iCJD-AR	6.65E-01	2.14E-01
	IPD-AR < 2y	IPD	3.67E-06	3.96E-01
	IPD-AR < 2y	CJD	2.49E-15	9.65E-01
	IPD-AR < 2y	iCJD-AR	9.76E-01	1.48E-02
	IPD	CJD	3.70E-15	5.69E-01
	IPD	iCJD-AR	4.36E-01	4.11E-01
	CJD	iCJD-AR	1.46E-01	9.80E-01

	Group 1	Group 2	*P* value	Mean
Log(Tau)	Healthy Control	IPD-AR > 2y	7.76E-02	8.28E-02
	Healthy Control	IPD-AR < 2y	8.92E-01	1.31E-02
	Healthy Control	IPD	6.21E-01	3.40E-02
	Healthy Control	CJD	1.48E-05	3.35E-01
	Healthy Control	iCJD-AR	2.87E-02	3.45E-01
	IPD-AR > 2y	IPD-AR < 2y	3.29E-01	9.59E-02
	IPD-AR > 2y	IPD	9.82E-02	1.17E-01
	IPD-AR > 2y	CJD	2.47E-07	4.18E-01
	IPD-AR > 2y	iCJD-AR	1.49E-02	4.28E-01
	IPD-AR < 2y	IPD	8.49E-01	2.09E-02
	IPD-AR < 2y	CJD	5.90E-03	3.22E-01
	IPD-AR < 2y	iCJD-AR	1.85E-02	3.32E-01
	IPD	CJD	9.28E-04	3.01E-01
	IPD	iCJD-AR	2.13E-02	3.11E-01
	CJD	iCJD-AR	9.23E-01	9.95E-03

	Group 1	Group 2	*P* value	Mean
Log(UCH-L1)	Healthy Control	IPD-AR > 2y	7.62E-03	1.39E-01
	Healthy Control	IPD-AR < 2y	1.33E-01	1.65E-01
	Healthy Control	IPD	1.50E-05	2.70E-01
	Healthy Control	CJD	5.35E-08	3.43E-01
	Healthy Control	iCJD-AR	6.02E-01	1.19E-01
	IPD-AR > 2y	IPD-AR < 2y	8.02E-01	2.58E-02
	IPD-AR > 2y	IPD	1.18E-02	1.31E-01
	IPD-AR > 2y	CJD	8.99E-05	2.04E-01
	IPD-AR > 2y	iCJD-AR	3.12E-01	2.59E-01
	IPD-AR < 2y	IPD	3.32E-01	1.05E-01
	IPD-AR < 2y	CJD	1.04E-01	1.78E-01
	IPD-AR < 2y	iCJD-AR	2.77E-01	2.85E-01
	IPD	CJD	2.15E-01	7.31E-02
	IPD	iCJD-AR	1.76E-01	3.90E-01
	CJD	iCJD-AR	1.33E-01	4.63E-01

GFAP and NfL trajectories in *converters*

A total of 16 *PRNP* mutation carriers (P102L = 10, D178N-FFI = 2, E200K = 1, 5-OPRI = 1, 6-OPRI = 2) were identified as *converters* with a median follow up of 7.8 years (IQR = 5.2 years). Of the four biomarkers tested, only log(NfL) and log(GFAP) exhibited consistent inclines in values over time through the point of conversion; log(Tau) and log(UCH-L1) trajectories were inconsistent, and hence of little use. For log(GFAP) and log (NfL), three distinct trajectory patterns were observed (Figures 13 and 14). No useful trajectories for log(Tau) and log(UCH-L1) were discerned (Figure 16).

Firstly, in clinically *fast* IPDs (E200K and D178N-129M), both log(GFAP) and log(NfL) trajectories showed largely flat lines, followed by abrupt upticks close or at the time of clinical conversion. Secondly, in clinically *slow* IPDs (P102L), slow and consistent inclines in log(GFAP) and log(NfL) towards and beyond clinical conversion were observed, with 52.6% (10/18) and 44.4% (8/18) of values above the 90th percentile of healthy controls (HC90) respectively in the 2 years before conversion. Thirdly, in the classically *slow* 5-OPRI and 6-OPRI disease, the trajectories appeared inconsistent, as values from two of three individuals lie above the HC90 pre-conversion, and in one individual all values were below the HC90 even after conversion. None of the iCJD-AR individuals converted to iCJD on follow up, but one died of invasive craniopharyngioma and another developed early onset AD.

The linear trajectories of pre-conversion log(NfL) and log(GFAP) were then modelled using mixed effects regression models with random effects for individual slopes, and with "*fast* IPD" or "*slow* IPD" as factor variables; this included data pre-conversion (up to four years pre-conversion for *slow* IPD; six months for *fast* IPD), and up to six months post-conversion. The modelling estimated slopes for plasma log(NfL) of 0.108 pg/ml/year in *slow* IPD (95% CI 0.0662, 0.149) and 1.279 pg/ml/year in *fast* IPD (1.006, 1.551) with an *x*-intercept (time pre-conversion that linear modelled trajectory crosses mean of controls) of 2.448 years; for plasma log(GFAP) 0.090 pg/ml/year in *slow* IPD (95% CI 0.040, 0.140) and 0.458 pg/ml/year in *fast* IPD (0.129, 0.787) with a *x*-intercept of 4.009 years.

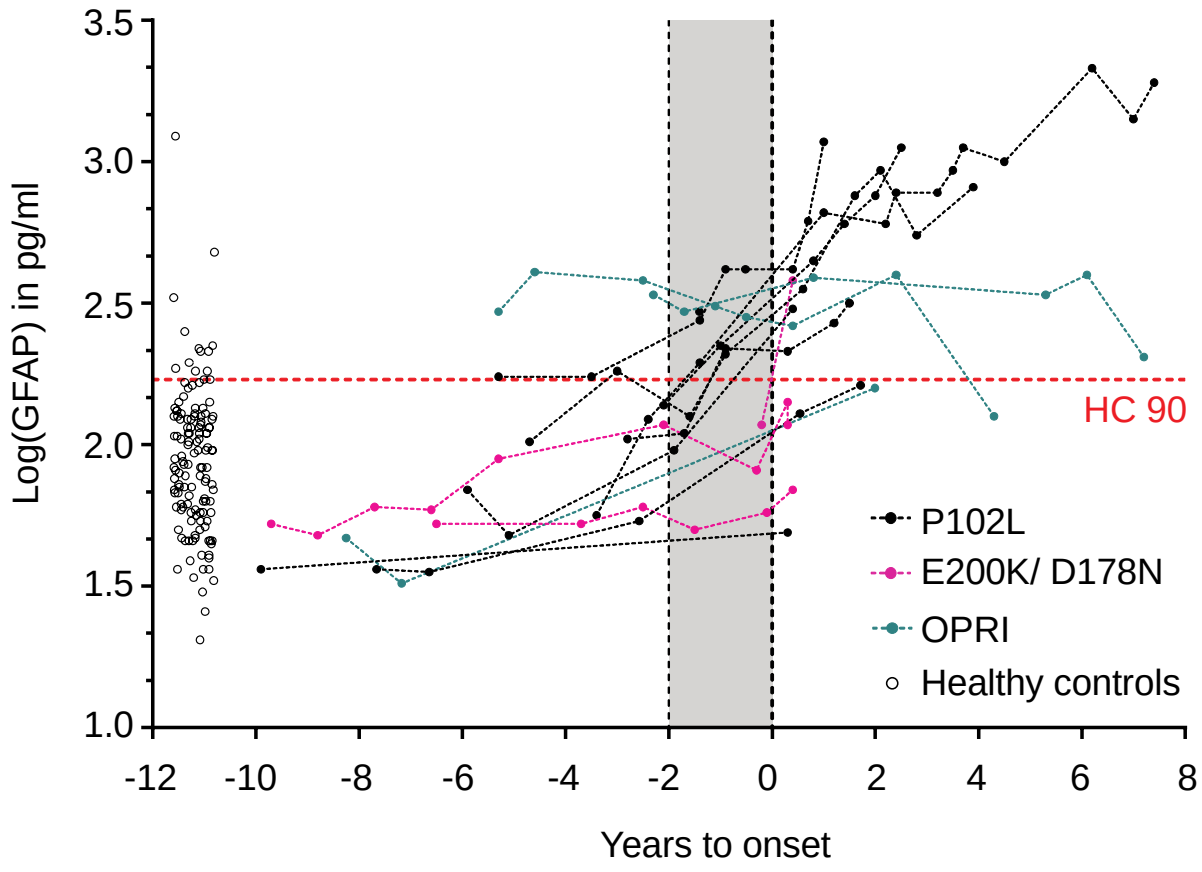

Figure 13 Plasma log(GFAP) trajectories in IPD converters

P102L converters (slow IPD) showed gradual increases in log(GFAP) from the pre-conversion phase through to the post-conversion phase with a considerable proportion of values below the HC90 thresholds respectively. Fast IPD converters (E200K and D178N-129M) had fairly flat trajectories pre-conversion but with either sudden or modest increases around the time of conversion. The dotted red horizontal line indicates the 90% percentile of the respective N4PB biomarker values; the unfilled circles to the left of the graph show the jitter plots of HC individuals; the shaded column in each graph indicates the 2-period before disease onset/clinical conversion (point 0 on x-axis). These figures were reproduced from Mok et al. 2023 (https://doi.org/10.1093/brain/awad101).

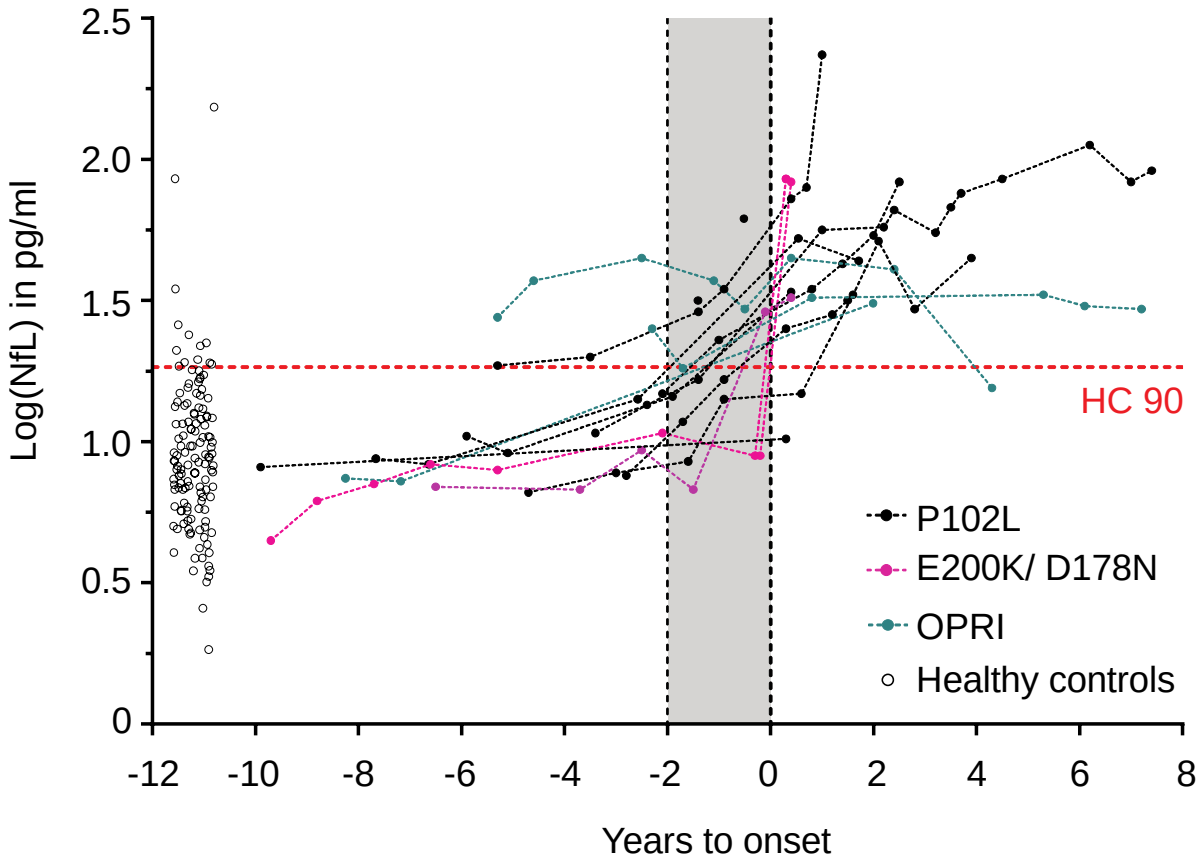

Figure 14 Plasma log(NfL) trajectories in IPD converters

P102L converters (slow IPD) showed gradual increases in log (NfL) from the pre-conversion phase through to the post-conversion phase with a considerable proportion of values below the HC90 thresholds respectively. Fast IPD converters (E200K and D178N-129M) had fairly flat trajectories pre-conversion but with a sudden increase around the time of conversion. The dotted red horizontal line indicates the 90% percentile of the respective N4PB biomarker values; the unfilled circles to the left of the graph show the jitter plots of HC individuals; the shaded column in each graph indicates the 2-period before disease onset/clinical conversion (point 0 on x-axis). These figures were reproduced from Mok et al. 2023 (https://doi.org/10.1093/brain/awad101).

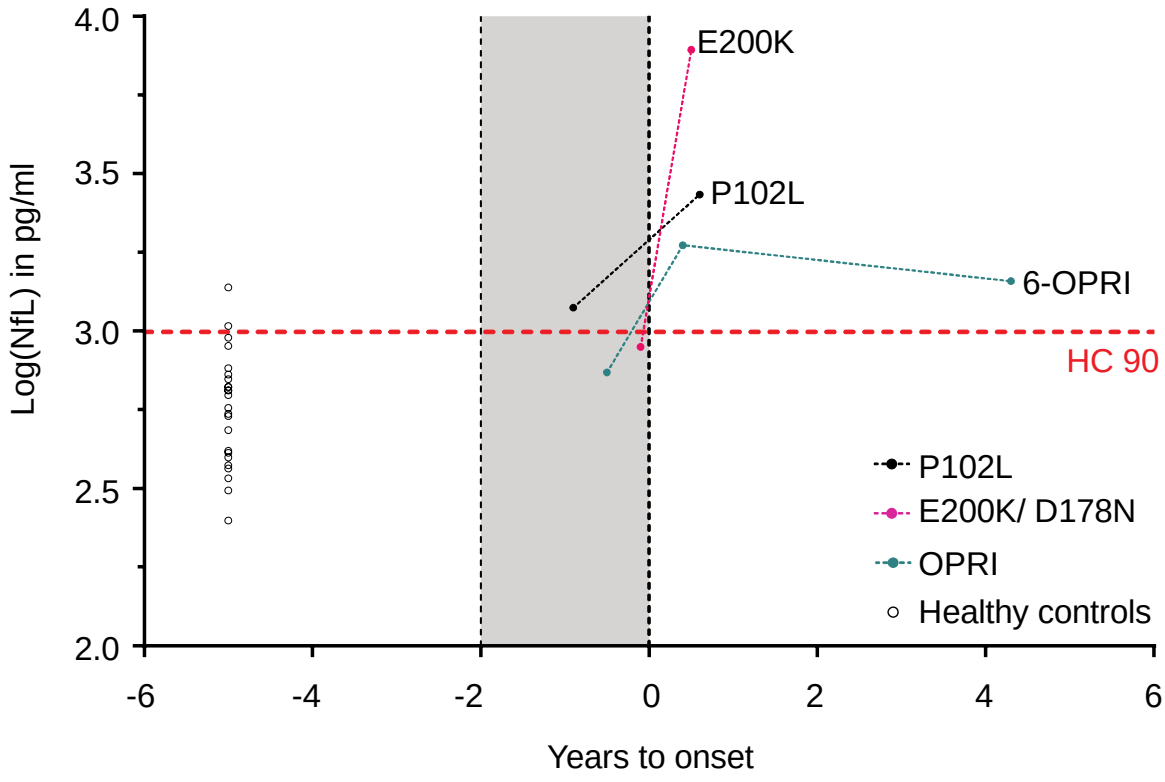

Figure 15 CSF log(NfL) trajectories in IPD-AR

This shows the CSF log(NfL) trajectories for three IPD converters; CSF NfL was elevated above HC90 only in the P102L converter within 2 years of onset. The dotted red horizontal line indicates the 90% percentile of the respective N4PB biomarker values; the unfilled circles to the left of the graph show the jitter plots of HC individuals; the shaded column in each graph indicates the 2-period before disease onset/ clinical conversion (point 0 on x-axis). These figures were reproduced from Mok *et al.* 2023 (https://doi.org/10.1093/brain/awad101).

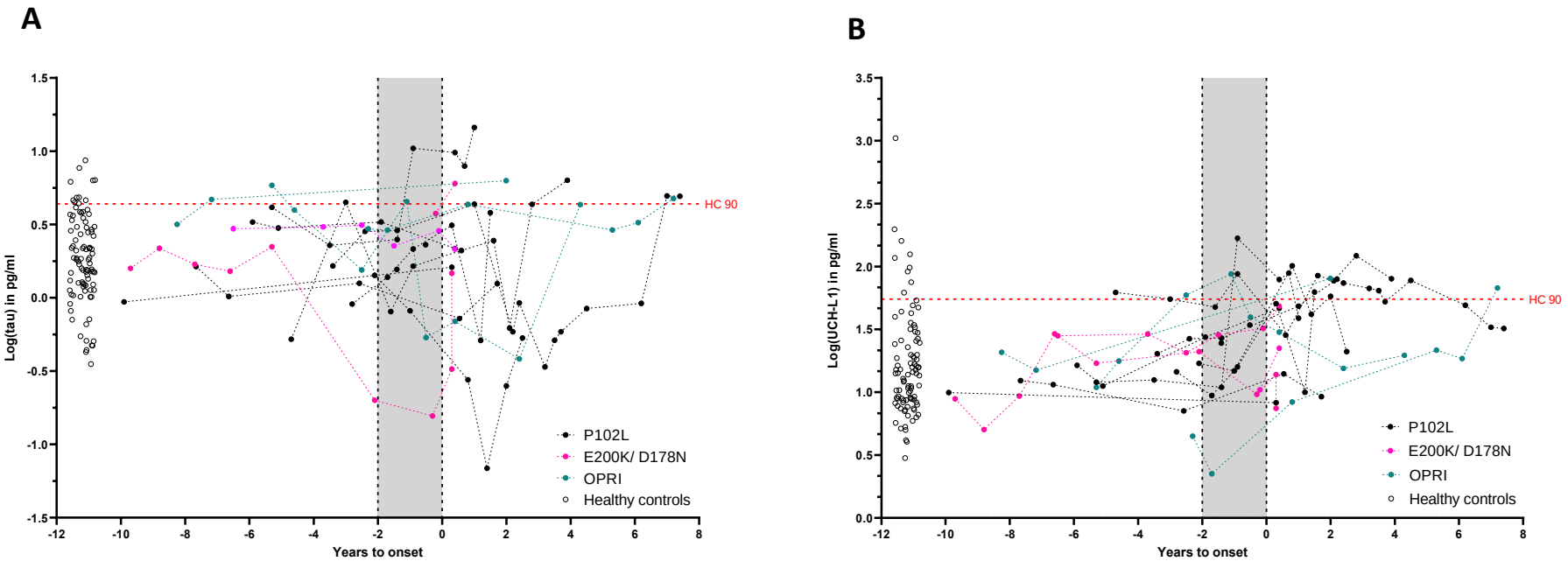

Figure 16 Plasma Tau and UCH-L1 trajectories in IPD converters.

(**A**) This panel shows the plasma log(Tau) trajectory in IPD converters. (**B**) This panel shows the plasma log(UCH-L1) trajectory in IPD converters. No consistent trends in log(Tau) nor log(UCH-L1) were appreciable for any IPD groups. In all panels, the dotted red horizontal line indicates the 90% percentile of the respective N4PB biomarker values; the unfilled circles to the left of the graph show the jitter plots of HC individuals; the shaded column in each graph indicates the 2-period before disease onset/clinical conversion (point 0 on x-axis).

CSF Simoa N4PB results

Log(NfL) was the only N4PB biomarker in CSF that demonstrated the requisite statistically significant incremental mean values between the relevant groups to be considered useful as a proximity biomarker (IPD-AR > 2y versus IPD-AR < 2y p = 0.03, IPD-AR < 2y versus HC p = 0.04, and IPD-AR < 2y versus IPD $p = 2.95 \times 10^{-5}$)(Figure 15). This pattern was not seen with CSF log(GFAP) unlike in plasma log(GFAP). Again, there were statistically significant differences seen between several groups in log(Tau) and log(UCH-L1), but crucially not in IPD-AR > 2y versus IPD-AR < 2y.

Three *PRNP* mutation carriers (P102L = 1, E200K = 1, 6-OPRI = 1) converted during the course of follow up, but the duration and number of samples were unsurprisingly small due to logistical reasons e.g. CSF collection started much later (2016) than plasma collection (2008 or earlier) in the NPMC, short interval between conversion and death in E200K *converter*, and post-conversion disability precluding travel to LP site. Only one (P102L) in three of these *converters* had a CSF log(NfL) value (3.07 pg/ml) greater than the HC90 value (2.97 pg/ml). Although N4PB values in all three IPD converters rose following disease onset, not all exceeded the HC90 thresholds respectively. Referencing the matched plasma samples, all N4PB biomarker values before conversion (0.2 years to conversion) were below the HC90 thresholds for the E200K *converter,* both plasma log(GFAP) and log(NfL) for the 6-OPRI *converter* were above the HC90 threshold 0.5 years before conversion, and only plasma log(GFAP) exceeded the HC90 threshold for the P102L *converter* 0.9 years before conversion.

Discussion

This chapter charts the sequence of accruing an extensive longitudinal biofluid archive over a decade, followed by multimodal interrogation of biomarker evolution, in individuals at risk of and in the early stages of prion disease. Efforts involved collaborations across several centres in the UK and internationally, particularly to secure sufficient control biofluid samples, in technical development and troubleshooting of RT-QuIC seed amplification assays, and Simoa analyses of candidate biomarkers of neurodegeneration. The data generated provide evidence of

two types of fluid biomarker trajectory leading up to clinical conversion. Firstly, in IPDs for which highly sensitive seed amplification assays are available (E200K), we demonstrated the existence of a presymptomatic CSF RT-QuIC seeding stage which appears considerably longer than the clinical phase itself (years vs few months respectively). Secondly, in *slow* IPDs, plasma GFAP emerged as a novel biomarker of proximity, and sequential linear increase initially in GFAP followed by NfL were detectable up to four years before conversion. In contrast, in *fast* IPDs, the neurodegenerative biomarkers (GFAP and NfL) rise at conversion with no definable presymptomatic window. These appear to mirror the distinct aspects of the two-phase kinetics model in prion propagation but it is important to note that the *bona fide* prion infectivity measured in the model may not fully represent PrP-amyloid seeding by RT-QuIC, in that non-infectious aggregates themselves may seed RT-QuIC.

A novel approach to estimating an individual's proximity to clinical conversion at any given point in time was proposed in order to address the key obstacle to meaningful biomarker data interpretation in the IPD-AR population. This does not rely on familial or parental mean ages of onset used in other inherited neurodegenerative diseases, as ages of onset are highly heterogenous in IPD with large standard deviations, and even within families with the same *PRNP* mutation. It avoids the scenario of meaninglessly assigning a mean age of onset in which an IPD-AR individual's life has exceeded. Instead this new method computes rolling estimations of age of onset relative to time of sampling in an at-risk individual until such time as the precise age of onset can be determined when conversion ensues. However, we caution that it is inherently imprecise, and should not be used counsel at-risk individuals clinically about their proximity to conversion.

Technical improvements to pre-existing Unit seed amplification assay (RT-QuIC) components were sought through a period of intensive external placement and training at the NIH RML, and then tested and implemented on return. The key interventions were successfully ensuring the purification of rPrP species which reproduced the exquisite sensitivity and specificity of the RT-QuIC assays at the Unit in line with the NIH RML, and judicious modification of existing Unit protocol to purify the novel Hu P102L rPrP. A head-to-head comparison between Unit-made and RML-made Ha90 rPrP performance in sCJD BH-seeded RT-QuIC reactions demonstrated a higher SD_{50}

and greater stability of in the RML preparation. This led to abbreviation in handling after the second NiNTA elution, thereby cutting down on repeated freeze-thaw cycles and interim storage at a potentially destabilising pH, which were felt to explain the Unit-made preparation's propensity to spontaneous fibrillisation.

E200K-AR (and iCJD-AR) biomarker trajectory

Fundamentally, any RT-QuIC assay expected to detect CSF PrP-amyloid seeding in presymptomatic IPD-AR individuals should be capable of doing so in samples from symptomatic individuals with high sensitivity. The exquisite sensitivity of the IQ-CSF RT-QuIC assay, now established at the Unit, was affirmed by testing our own panel of CJD (17/17) and symptomatic E200K (4/4) CSF panel, which then picked up four positive results from the asymptomatic E200K-AR cohort, one of which was drawn from a subsequent converter. Two of these IQ-CSF positive samples came from a single individual at 5.1 and 7.1 years to projected onset with a total of 3.75 years' follow up; the remaining sample came from an individual at 8.3 years to projected onset, with a total of 3.37 years' of actual follow-up. This would suggest that the previously detect IQ-CSF RT-QuIC positive sample from an elderly asymptomatic E200K gene carrier elsewhere was not an isolated finding[108].

The first observation of interest is that no E200K-AR individual converted without presymptomatic seeding activity. The second is that the E200K presymptomatic seeding period (as early as 8.3 years before predicted onset or 3.75 years actual follow-up) appears unexpectedly long for an illness with such an explosive onset and short duration, providing a realistic window for therapeutic intervention. The third is that none of these presymptomatic positive samples, including one drawn shortly before conversion, recorded N4PB biomarker levels above HC90, indicating that the onset of neurodegeneration is likely to be very close to conversion and potentially unrecognisable at current sampling intervals. It is hard to conceive that any follow-up interval shorter than 6 months requiring CSF examination would be acceptable to IPD-AR individuals; an informative blood biomarker (if/when discovered) might be more feasible for close monitoring.

The observation of asymptomatic seeding-positive samples without evidence of neurodegeneration, alongside seeding negative samples in the E200K-AR cohort suggest the likely sequence that gene carriers develop demonstrable CSF PrP-amyloid seeding activity at some point (being seeding negative previously) as a prerequisite herald to incipient clinical conversion. In other words, those whose CSF remain seeding-negative are not at incipient risk of conversion by up to four years, until seeding activity emerges on subsequent CSF samples. As to whether CSF SD_{50} trajectory can be used as an adjunctive proximity marker in place of neurodegenerative biomarkers, it remains to be seen with greater number of follow-ups to conversion.

Though none of the iCJD-AR CSF samples tested positive with IQ-CSF RT-QuIC, two out of two (2/2) samples from symptomatic individuals were positive. If the evolution of presymptomatic stages in iCJD mirrors that of E200K, as is expected, the IQ-CSF RT-QuIC assay remains the modality of choice in detecting presymptomatic seeding activity, and by extension those at risk of V210I and E196K. However, unlike E200K-AR, both V210I-AR and iCJD-AR are estimated to have lower penetrance at 10% or lower[49,65].

P102L-AR biomarker trajectory

P102L clinical disease can be highly heterogenous within a single pedigree or even in a single individual (see the case included here with initial GSS presentation followed by CJD-like transformation). These include the most commonly encountered GSS phenotype, the AD-like pure cognitive phenotype and the rarely seen CJD-like phenotype; molecular evidence thus far seem to suggest the clinical heterogeneity seem to be down to propagation of distinct prion strains[85,87,138]. Historically, CSF from symptomatic individuals were tested by PQ-CSF and IQ-CSF RT-QuIC assays, as a small subset of CJD surveillance cohorts dominated by sCJD, and have been found to be positive on occasions, but at low sensitivities[80-83,164,165]. Very little or no information is provided about the clinical phenotype associated with these samples, and as these cohorts usually rely on clinical referrals which are subjected CJD epidemiological case definition criteria, it is not inconceivable that these P102L subsets were enriched with the CJD-like phenotype.

The exception to these published studies on RT-QuIC sensitivity on P102L CSF is the Sano *et al.* 2013 study which reported impressive results[136]. Their assay differs substantially from the RML-based setups, and our attempts to reproduce their results were not met with success; a comparison between these assays is detailed in Table 8. One of the key differences is their use of TECAN microplate readers which have distinct shaking conditions that cannot be fully recapitulated with the BMG Labtech microplate readers used at the Unit. Correspondence with Prof Atarashi later suggested that shaking at 432 rpm on the BMG microplate readers is equivalent to their TECAN setup, but unfortunately, due to time and resource constraints, no further experiments were undertaken.

Table 8 Comparison between RML-based and Sano et al. 2013 RT-QuIC assays

Conditions	RML	Sano *et al.* 2013
Buffer	10 mM phosphate buffer pH 7.4 (per well)	50 mM PIPES buffer pH 7.0 (per well)
Salt	NaCl 300 mM or NaI 130 mM (per well)	NaCl 500 mM (per well)
EDTA	1 mM (per well)	1 mM (per well)
SDS	0.002% (per well)	NA
ThT	10 mM (per well)	10 mM (per well)
rPrP species	Ha90, BV or Hu P102L	Wild type Hu
rPrP concentration	0.1 mg/ml (per well)	0.05 mg/ml (per well)
CSF seeding volume	20 or 15 µl (per well)	5 µl (per well)
Total volume	100 µl (per well)	100 µl (per well)
Microplate reader	BMG FLUOstar or POLARstar	TECAN M200 or F200
Shaking speed	700 rpm	Maximum speed (432 rpm; 1mm amplitude)
Shaking motion	Double orbital	Circular
Shake/rest intervals (on/off)	60s/60s	30s/30s + 2 min pause
Incubation temperature	55ºC, 50 ºC or 42 ºC	37 ºC
Time cut-off	24 hrs for 55ºC; 30 hrs for 50 ºC; 50 hrs for 42ºC	53 ºC (?)

Reproduced from Mok *et al.* 2023 (https://doi.org/10.1093/brain/awad101).

Nevertheless, a novel RT-QuIC assay with bespoke conditions, using Hu P102L rPrP and NaI, was capable of detection seeding activity in a significant proportion of symptomatic P102L CSF samples that hitherto tested negative with IQ-CSF, Hu, and BV RT-QuIC assays. In addition, seeding activity was detected in an at-risk individual (> 60 years in age; asymptomatic at 3.85 years' follow-up; *PRNP* untested), and a non-prion disease control subject.

Detailed clinical profiling indicates that this assay is most successful when used to test those with the P102L-GSS and/or P102L-CJD phenotypes, as no seeding activity was detected in CSF from P102L-Cognitive cases. Given the small number of samples tested here, it remains uncertain what the true sensitivity and selectivity of this assay is when applied to larger sample sizes. Several factors are likely to influence the sensitivity of any given RT-QuIC assay, including seed-rPrP compatibility and choice of salt which have been shown to be the key elements recently. One factor which may prove to be important when considering assay sensitivity in P102L, and indeed other slowly progressive forms of IPD, is the concentration of seeding-competent prion species in the fluid compartment being tested. It is known from autopsy and molecular strain typing that a subset of clinically indistinguishable P102L-GSS individuals have a PrP-amyloid plaque predominant variant which on Western Blot solely exhibit the presence of an 8 kDa band, without the 21-30 kDa bands. One could speculate that sequestration of disease-associated PrP in amyloid plaques in brain parenchyma, and hence having very little or none in the CSF compartment, to be a possible explanation of the partial sensitivity.

With regards to the positive control sample, it is not inconceivable that this may have come from an individual with unrecognised P102L disease. This sample originated from a cohort of individuals referred with symptoms of neurodegeneration for CSF examination which was subsequently divided into those with or without biomarker evidence of AD. This sample belonged to the latter group, meaning that the source individual very likely had some form of non-AD neurodegeneration. It would certainly have been useful to know if this individual had the P102L mutation in his/her *PRNP* but the entire collection of control CSF samples here was terminally de-identified. This sample tested negative with both IQ-CSF and BV RT-QuIC assays, and hence the selectively amplification by the Hu P102L RT-QuIC assay appear to support the possibility that this individual may have had P102L-GSS. Other than the mere possibility that represented spontaneous fibrillisation of the Hu P102L rPrP under these conditions, an alternative explanation is the presence of an unknown pro-fibrillisation factor.

In this situation with P102L where only a partially sensitive RT-QuIC is available, it is unlikely that seeding activity or its dynamics will be sufficient as the sole fluid

biomarker modality for proximity monitoring, unless a universally sensitively assay iteration is found in future. The exception at present is in those whose incipient conversion is driven by assay-compatible P102L PrP isoforms. Instead, monitoring of proximity to clinical conversion can be complemented by, or solely accomplished by plasma (± CSF) neurodegenerative biomarker (GFAP first, then NfL) trajectories (rate of change) which appear to change up to 4 years before conversion. This observation in P102L (a *slow* IPD) is strikingly different from *fast* IPDs in which long seeding windows and short neurodegeneration windows exist.

Other IPD-AR biomarker trajectory

It was hoped at the conception of this study that a single universally sensitive RT-QuIC assay iteration would be available to capture seeding activity across all human disease-related PrP isoforms, and for a time, BV RT-QuIC appeared highly promising[27]. However, despite extensive optimisation efforts using BV rPrP (Table 5), no seeding activity was found in CSF samples from symptomatic 6-OPRI, P102L and D178N-129M individuals, contrary to findings when reactions were seeded by brain homogenates. Therefore, it came as no surprise that seeding activity was not detected in CSF samples collected from presymptomatic individuals at risk of classical 6-OPRI, P102L, D178N-129V, D178N-129M and A117V.

Unfortunately, no CSF samples from individuals symptomatic of 5-OPRI, A117V and D178N-129V disease were available to probe in the exploratory RT-QuIC panel. Amongst these, a single post-mortem sample from an individual with fCJD secondary to D178N-129V did test strongly positive with the previous Unit iteration of BV RT-QuIC[21]. It is not inconceivable this might be reproduced with BV RT-QuIC in ante-mortem CSF, and should be explored (as with symptomatic A117V and 5-OPRI CSF samples) when such samples become available in future. One other key RT-QuIC assay adjustment which might help in D178N and A117V is the use of Hu rPrP constructs incorporating the specific mutation, similar to that done with the Hu P102L RT-QuIC. This may or may not be tractable in OPRIs, as PrP sequence and hence conformational homogeneity could differ between different octapeptide repeat sequences.

Plasma neurodegenerative biomarkers tested did not show a sufficiently long definable presymptomatic phase in D178N-129M (FFI), but resemble the explosiveness seen in E200K, consistent with a *fast* IPDs. Trajectories for 5-OPRI and 6-OPRI appeared inconsistent in the small sample set available so little can be concluded about its utility at the present time. The prodromal stages in 5-OPRI and 6-OPRI can be notoriously long with common non-specific neuropsychiatric symptoms such as anxiety and mood problems, before a definite clinical conversion can be confidently diagnosed in practice. Indeed, some individuals with 6-OPRI disease were felt to have premorbid personality disorders which may represent unrecognised early neurodegeneration. This may explain why some two of three OPRI *converters* included in this study had plasma GFAP and NfL values above HC90 several years before conversion. Unfortunately, for the other 6-OPRI converter, there was a follow-up gap of several years during which no biomarker values were available before conversion.

Proposed presymptomatic IPD staging system

Drawing together biofluid seed amplification and neurodegenerative biomarker trajectories, alongside clinical features and disease-specific paraclinical investigations, we propose general outlines of distinct presymptomatic IPD staging systems for *fast* and *slow* IPDs (Figure 17). In *fast* IPD, there appears to be a long seeding phase of possibly up to about 4 years, without evidence of neurodegeneration until close to point of clinical conversion; in *slow* IPD, neurodegeneration (GFAP first, then NfL) begins as early as 4 years with a crescendo towards clinical conversion, while there is partial evidence for a seeding phase as early as about 4 years as well for some P102L individuals. While neurodegeneration trajectories in *slow* IPD seem evident, it ought to be pointed out that for much of the time, these biomarker values lie below the HC90. As such, there is currently insufficient confidence to enable individual prediction, particularly as information of this sort is heavily consequential. It also appears counterintuitive that plasma biomarkers seem more promising that CSF, but this may merely reflect the relative lack of sampling and follow-up data in the latter. However, it may be possible to utilise these biomarker data as outcomes/endpoints, or for enrichment in the setting of primary prevention clinical trials. Needless to say, a collaborative approach across several international centres will be required to

assemble comparable sample collections, in order to replicate and thus gain further confidence in these observed biomarker dynamics.

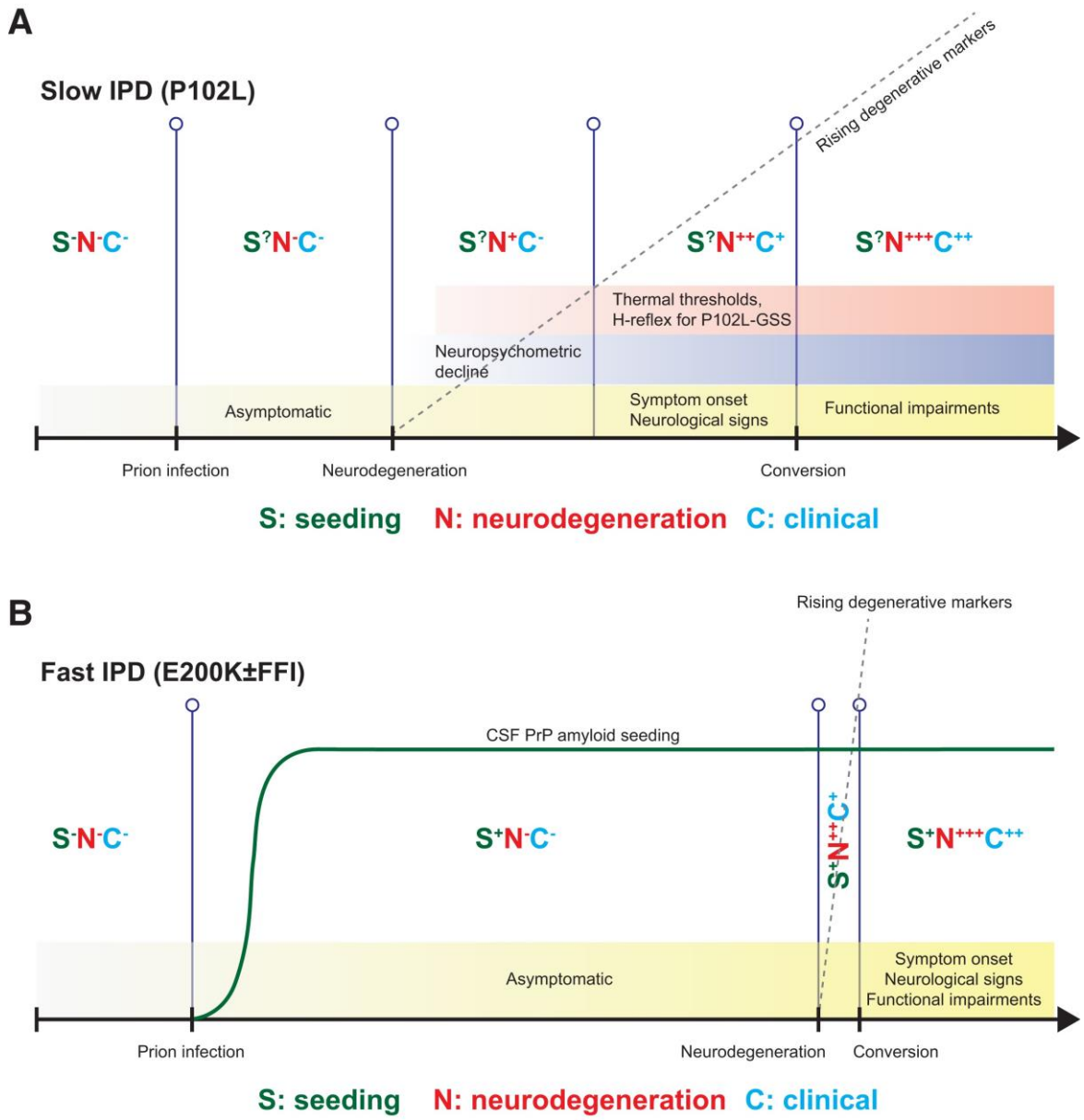

Figure 17 Proposed pre-conversion IPD staging system for fast and slow IPDs.

Each stage features graded intensities in prion seeding activity, neurodegeneration markers and clinical aspects, along with ancillary investigations known to herald the onset of conversion (neuropsychometry, and neurophysiology in P102L). (**A**) *Slow* IPDs are likely to have an extended window for neurodegenerative markers, making it easier to capture and follow at 6-12 monthly sampling intervals; however we only have partially sensitive RT-QuIC seeding assays for *slow* IPDs. (**B**) *Fast* IPDs are likely to have a very short and explosive neurodegeneration window, which means it might not be easy to capture and follow at similar sampling intervals; this may be offset by the existence of highly sensitive RT-QuIC assays. These figures were reproduced from Mok *et al.* 2023 (https://doi.org/10.1093/brain/awad101).

Conclusion

This study underscores how fundamental understanding of prion propagation derived from animal transmission studies (two-phase kinetics model) can be applied to probe biomarker evolution and discovery in the presymptomatic stage in individuals at risk of prion disease. However, this is only possible through the painstaking assembly a longitudinal biofluid sample resource that included at-risk individuals who were recruited prior to disease onset, and followed through to clinical conversion. The results in turn highlights distinct and likely sequential biomarker dynamics (seeding and neurodegeneration) which can be exploited as proximity markers to influence design of primary prevention therapies in selection, enrichment and endpoint determination, pending consolidation with larger cohorts down the line.

Fluid, neuropsychometric and imaging biomarkers are already very well characterised in individuals at risk of familial AD and FTD[115,148,166]. Increasing recognition that these diseases, both familial and sporadic, share key aspects of prion disease mechanisms including proteopathic seed propagation, transmissibility and strain biology suggest that successful adaptation of seed amplification assays to other proteopathic neurodegenerative diseases may uncover a new, and possibly earlier targets for therapeutic strategies[101,102,167-169]. Indeed, the relatively recently adapted α-synuclein RT-QuIC assay has proved successful in probing the pre-motor phase of Parkinson's disease, dementia with Lewy Bodies and Multiple system atrophy, while similar seed amplification assays are being honed for 3-repeat, 4-repeat and AD-tau, and transactive response DNA-binding protein-43[170-177].

In general, if proteopathic seeding does indeed precede neurodegeneration, it can be easily envisaged that a seeding-only phase without neurodegeneration will extend the presymptomatic window in which therapeutic interventions may be administered. This will have profound implications in timing and study design for therapeutic strategies against neurodegenerative disease as a whole. In individuals at risk of prion disease, this may revive interest in previously trialled drugs which failed to cure disease in the symptomatic phase or repurposed molecules[178-183], but more importantly, shift focus

to rationally-designed strategies such as PrP depletion through monoclonal antibodies and ASOs[53,184].

CHAPTER 3

Implications of vCJD in a *PRNP* c129 MV patient

Publication:

Mok T, Jaunmuktane Z, Joiner S, et al. ***Variant Creutzfeldt–Jakob Disease in a Patient with Heterozygosity at PRNP Codon 129.*** *New England Journal of Medicine. 2017/01/18/ 2017; 376(3): 292-294. doi:10.1056/NEJMc1610003*

Introduction

Dietary transmission of prion disease historically occurred in outbreaks in defined populations, and have been the subject of intense study. Once the offending source had been identified and its practice ceased, the incidence usually dwindled steadily[185-187]. However, the emergence of further cases following long incubation times decades down the line, strongly influenced by genetic determinants of susceptibility, have renewed interest in, and raised concerns over the initial scale of exposures with the possibility of ensuing “waves”. The first of these was kuru, arising from ritualistic cannibalism in the Fore linguistic group of the Eastern Highlands of Papua New Guinea, although observation of disproportionately prevalent *PRNP* codon 129 heterozygosity (c129 MV) in elderly survivors (and worldwide) was thought result from balancing selection, suggesting that outbreaks of either human-to-human (cannibalism) or animal-to-human transmissions have taken place throughout history[188].

BSE, the epizootic prion disease of cattle, crossed the species barrier and infected humans causing variant Creutzfeldt-Jakob disease (vCJD), provoking an animal and public health crisis. vCJD was first recognised in humans in 1995, affecting young adults in the UK, and reached peak incidence in the early 2000s. Three individuals were subsequently identified to have died from vCJD after receiving blood transfusions sourced from vCJD-affected individuals, while another had proven peripheral lymphoreticular system only infection. Overall, a total of 67 recipients were recorded to have been exposed from blood products from vCJD patients but no further cases of vCJD arising from this group of at-risk individuals have since been reported. Following discovery of its source, the implicated agricultural practices were stopped, and further infection control measures such as leucodepletion of blood products were introduced, resulting in a decline in its incidence. By 2015, about 10 years from peak incidence, a total of 225 deaths were recorded worldwide, with 177 in the UK[189].

Distinguishing clinical features from sCJD include young age at onset, distal limb sensory symptoms (pain, numbness, and paraesthesia), prominent neuropsychiatric symptoms, chorea, and early cerebellar ataxia. Clinical diagnosis can be supported

by the presence of thalamic “pulvinar sign” on MRI Brain, positive Direct Detection Assay in blood, and demonstration of disease-related PrP immunoreactivity in tonsillar biopsy. Brain histology and immunocytochemistry typically show “florid” PrP amyloid “cluster” plaques, while molecular strain typing through immunoblot shows PrP^{Sc} type 4 (London classification), as in peripheral lymphoid tissue including tonsils.

However, the typicity of these “characteristic” clinical and pathological features are predicated on the basis that virtually all affected individuals up to 2016 have been methionine homozygous at *PRNP* c129. vCJD was clinically suspected in an individual with *PRNP* c129 MV, but no confirmatory tissue diagnosis was available; the blood transfusion related infection restricted to the peripheral lymphoreticular system was from a c129 MV individual[190]. Given that *PRNP* c129 polymorphism is recognised to exert profound influence on prion disease susceptibility, incubation period, clinical phenotype, and molecular pathology, it is uncertain whether the typicity associated with methionine homozygosity at c129 will be recapitulated in individuals either heterozygous or valine homozygous at c129 if/when cases arise. Indeed, transmission of BSE prions to transgenic mice expressing human homozygous PrP 129M has been shown not only to propagate type 4 PrP^{Sc}, but also type 2 which is associated with sCJD[191]. Furthermore, transgenic mice expressing human PrP 129V, when challenged by either vCJD or BSE prions, can propagate up to four distinct disease phenotypes[192]. This is of concern considering the scale of BSE exposure in the UK population (i.e. anyone alive today, but born before 1996), and the subsequently estimated prevalence of vCJD prions of up to 1 in 2000 from examination of archived appendiceal tissue[193]. Given the prevalence of *PRNP* c129 heterozygosity (46%) and c129 valine homozygosity (12%) in the general population, there has been considerable speculation about whether further waves of vCJD might occur in these groups, associated with longer incubation times and perhaps more variable and even unrecognisable clinicopathological phenotypes. Long incubation periods of up to 40 and 50 years have been observed in c-hGH iCJD and kuru respectively attributed to *PRNP* c129 heterozygosity and presumably its effects on homotypic PrP interactions[49,194]. As such, it is not unreasonable to expect that cases in individuals either MV or VV at c129 will arise after a period of latency.

Case history

In August 2015, a 36-year-old right hand dominant man, who worked as a scaffolder was referred to the UK NHS National Prion Clinic (NPC) with a history of behavioural change, cognitive impairment, gait ataxia and myoclonus. His illness was felt to have begun in October 2014 with emergence of uncharacteristic irascible and argumentative behaviour, coupled with failure to complete work-related projects to his previous standards. In the 4 years prior, he had been afflicted by persistent low mood, then attributed to a prolonged grief reaction following the death of his fiancée due to an unrelated illness. In the ensuing months after October 2014, he became progressively abulic and ataxic, and developed memory impairment, disinhibition, sweet craving, dysarthria, and reduplicative para-amnesia sequentially. At no point did he complain of numbness, paraesthesia, or pain in his limbs.

By the time I assessed him in August 2015, he had a Mini Mental State Examination score of 25/30, losing points in orientation for time, memory and copying intersecting pentagons. In the bedside cognitive test battery specially designed for prion disease, he scored poorly on verbal and visual recognition memory, phonological processing, calculation, spelling, information processing, Luria 3-step, and verbal fluency. Identification of line drawings, praxis, letter cancellation, recognition of fragmented letters and reading irregular words remained intact.

Cranial nerve examination revealed abnormal convergence, broken visual smooth pursuit, and cerebellar dysarthria. Limb examination revealed multifocal myoclonus, general hyperreflexia, sustained ankle clonus, extensor plantar responses and cerebellar gait ataxia; bilateral grasp reflexes but no other primitive reflexes, were present. Sensory examination revealed diminution of vibration perception in his distal lower limbs below his knees; all other modalities were intact.

This patient had no previous potential medical exposures such as blood transfusion, neurosurgery or c-hGH; he had never donated blood. In his family, both parents and

his younger sister were well. A paternal uncle had dementia and died in his 60s. He was born and lived entirely in the UK, and had an omnivorous diet.

PRNP sequencing showed no mutations; his c129 was methionine-valine heterozygous (MV). MRI brain showed restricted diffusion in the basal ganglia, hypothalamus, insular cortex, and medial thalami but not in the pulvinar (Figure 18). The electro-encephalogram [97] was encephalopathic, without any evidence of periodic complexes. His CSF was acellular, with normal protein and glucose levels; 14.3.3 protein was not detected, s100b was 0.39 (normal < 0.41 ng/L) and the RT-QuIC was negative (National CJD Research and Surveillance Unit). vCJD blood test (Direct Detection Assay) was negative. The clinical features and investigations satisfied the criteria for a diagnosis of probable sporadic CJD.

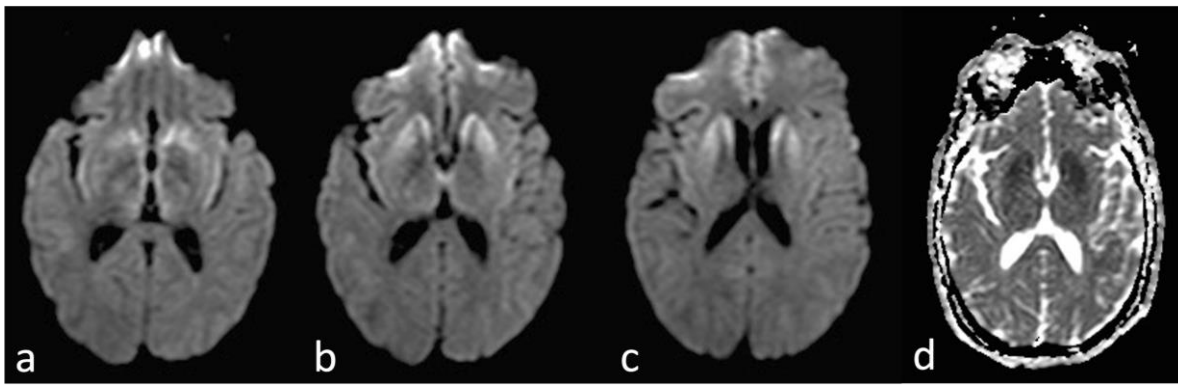

Figure 18 Magnetic Resonance Imaging features of PRNP c129 MV vCJD.

Trace-weighted diffusion weighted images (DWI) (**a-c**) and apparent diffusion coefficient (ADC) map (**d**). The trace-weighted DWI images demonstrate high signal intensity in the insular cortex, hypothalamus, medial thalamus as well as the caudate nucleus and putamen bilaterally but not in the pulvinar. These structures appear dark on the ADC map confirming true diffusion restriction. Reproduced from Mok *et al.* 2017 (doi: 10.1056/NEJMc1610003).

The patient was discharged to a local care home, and was reviewed on 3 occasions over the next 12 weeks by the NPC. He died in February 2016, but in the intervening time developed confabulation, visual hallucinations, optic ataxia, restricted upgaze, upper limb ataxia, prosopagnosia, and progressive daytime somnolence. In the short weeks before death, he became bedbound, had severe agitation and dysphagia.

Neuropathology and molecular strain typing

The fresh whole brain weighed 1490 g. Haematoxylin and eosin (H&E) staining on histological examination disclosed widespread amyloid plaques, including “florid” and “cluster” plaque morphologies in both cerebral and cerebellar cortices; microplaques were observed in the basal ganglia (Figure 19). Microvacuolar degeneration was seen with the greatest severity in the neuropil region of the caudate nuclei and putamina, but to a lesser extent in the thalami, and even milder in the cerebral and cerebellar cortices. The amyloid plaques were labelled with abnormal PrP immunoreactivity; a widespread but distinct stellate pericellular and perivascular PrP immunolabelling was seen in the cerebellar cortical molecular layer and in the cerebral cortex. Linear PrP deposition along the neuronal processes were noted in the basal ganglia and thalami.

Minute amounts of abnormal PrP was detected in the lymphoid tissue of the spleen, while none was found in the appendix and mesenteric lymph nodes. Immunoblotting of brain homogenates from the patient’s frontal and parietal cortices, and thalamus and cerebellum demonstrated the presence of London type 4 PrP^{Sc} pathognomonic of vCJD.

The spleen contained only minute amounts of abnormal prion protein in lymphoid tissue, whilst no prion protein could be reliably detected in the appendix and mesenteric lymph nodes. Immunoblot analyses of patient brain homogenates (frontal cortex, parietal cortex, thalamus, and cerebellum) demonstrated the presence of type 4 PrP^{Sc} by the London classification scheme (Figure 20) pathognomonic of vCJD.

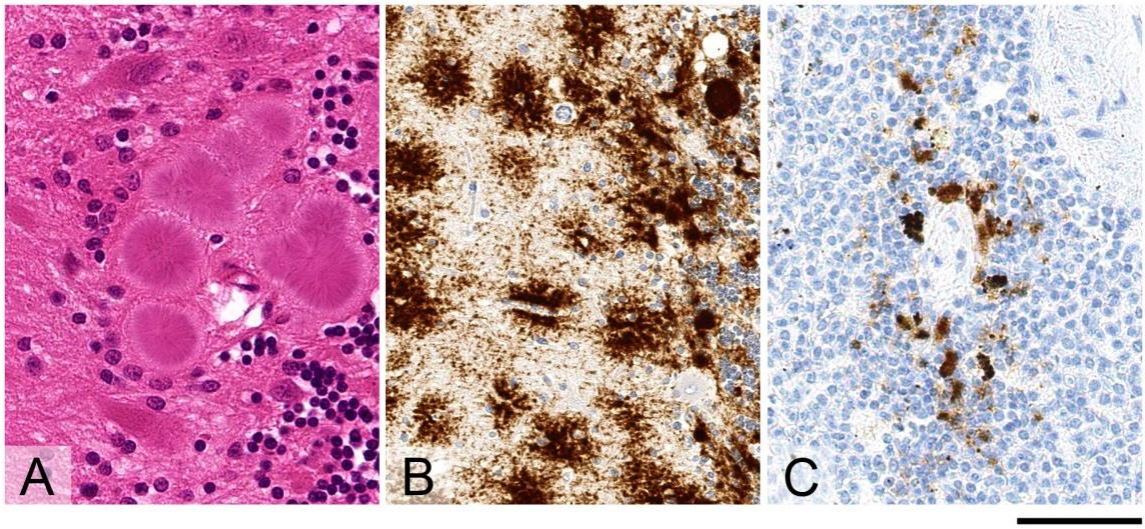

Figure 19 Neuropathology of vCJD with *PRNP* c129 MV genotype.

(**A**) frequent florid plaques and cluster plaques throughout the cerebellar cortex (H&E). (**B**) immunostaining for abnormal PrP (ICSM35 antibody) highlights amyloid plaques and shows widespread stellate pericellular and perivascular deposits. (**C**) Focal abnormal PrP deposits are seen in the spleen. Scale bar: 50 µm. Reproduced from Mok *et al.* 2017 (doi: 10.1056/NEJMc1610003).

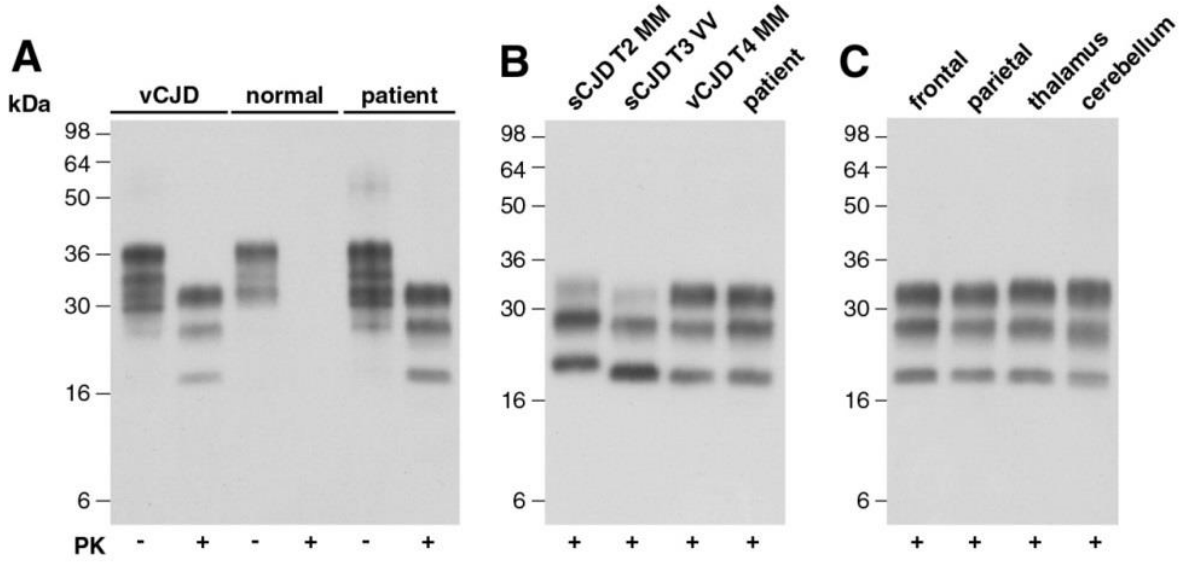

Figure 20 Immunoblotting of *PRNP* c129 MV vCJD.

Panels (**A**)-(**C**) are immunoblots of brain homogenate analysed with anti-PrP monoclonal antibody 3F4 and high sensitivity enhanced chemiluminescence to characterise PrP^{Sc}. (A) Equivalent aliquots of 10% (w/v) brain homogenate (frontal cortex) from a normal human control case, a reference vCJD case or the patient analysed before (-) or after (+) digestion with PK. (B) PK-digested 10% (w/v) brain homogenate (frontal cortex) from the patient or reference cases of sCJD and vCJD. The provenance of the brain sample is designated above each lane. For the reference cases the PrP^{Sc} type (types 2, 3 or 4 designated T2, T3 or T4; London classification) and *PRNP* c129 genotype are shown. (C) PK-digested 10 % (w/v) homogenates prepared from different regions of the patient's brain; frontal cortex, parietal cortex, thalamus and cerebellum. The volumes of samples loaded for immunoblots shown in panels B and C were varied to give equivalent levels of total PrP signal intensity. Reproduced from Mok *et al.* 2017 (doi: 10.1056/NEJMc1610003).

Discussion

This case, reported by in 2017 in the *New England Journal of Medicine* was the very first and only autopsy-proven vCJD case thus far, in an individual heterozygous at *PRNP* codon 129[30]. Its detection affirmed some of the concerns that had been harboured even in the previous decade during which the incidence was dwindling. This first of these was whether further waves of vCJD particularly in individuals who possessed c129 genotype other than methionine homozygous would be observed, and secondly if this does happen, whether the disease phenotype/pathology could be easily recognisable as vCJD. Indeed, the clinical course in this case did not resemble classical vCJD in that disease attribution of the prodromal long bereavement phase was debatable, the onset of cognitive decline was earlier than expected, and that he did not have chorea or limb pain. Furthermore, his MRI Brain did not show the "pulvinar sign", but had features most consistent with sCJD; from the point view of epidemiological case definition, he met criteria for sCJD, rather than vCJD. Without autopsy examination, this case would have been erroneously classified in national surveillance statistics.

This was by no means the first time that criteria used for epidemiological case definition (without tissue confirmation) had failed to capture vCJD cases, nor the first time sCJD-like MRI features had been seen in vCJD. A review of 106 pathologically proven vCJD cases found 12 cases which did not satisfy criteria for possible or probably vCJD in life; 8 of these had the "pulvinar sign" on MRI but did not have the requisite clinical features, while the remaining 4 had suboptimal MRI investigation[195]. In the initial *PRNP* c129 MM driven wave of vCJD infections, sCJD-like changes on MRI were seen in older affected individuals[196,197].

Considering how indispensable autopsy was in clinching the diagnosis here, this case would have been expected to kindle efforts in public health and epidemiology to intensify autopsy surveillance. On the contrary, in reality, autopsy rates have plummeted despite a concomitant rise in CJD incidence[57]. This means that year-on-year, the number of new cases of sCJD have risen, but only very small proportion <10% of these cases have tissue confirmation. Advances in diagnostic tools such as

DWI MRI and CSF RT-QuIC assay have been invoked to explain the rise in CJD incidence, but without a high autopsy rate, the true incidence of vCJD in *PRNP* 129 MV (and possibly VV) individuals is likely to remain obscure.

The scale of BSE exposure in humans and the estimated prevalence of vCJD prion carriers (1 in 2000), are several magnitudes higher than combined total for IPD and iCJD, and as such represents the largest group of individuals at risk of prion disease. Unlike IPD and iCJD though, this population remains unfeasible to study and define for several reasons. Firstly, it is impossible identify and track exposed individuals as this practically includes the entire UK population alive today born before 1996, and also because the source was so ubiquitous. Secondly, the penetrance of vCJD in the at-risk population is so far unknown, not helped by the extremely low autopsy rate. Even with high autopsy rates the number of cases identified would be likely only to represent a small proportion of the annual sCJD incidence, and as such the penetrance would be extremely low *vis a vis* number of individuals theoretically exposed. Thirdly, except for one report in which vCJD prions were demonstrated in presymptomatic plasma samples from eventual vCJD sufferers by PMCA[198], no further fluid biomarkers or assays have proved to be useful for preclinical detection of vCJD prions. Interestingly, the CSF of this MV patient tested positive for vCJD prions by PMCA in a subsequent publication[199]. It would be difficult to envisage PMCA, being labour intensive to perform, could be used to medium to large scale screening purposes without significant investment in funding and logistics, particularly the requirement for Category 3 containment laboratories. A blood Direct Detection Assay has been shown to have reasonably high sensitivity and specificity for symptomatic individuals, but was found to be negative here in this MV case, and has yet to be applied to presymptomatic human samples.

Conclusion

The detection of this first autopsy-proven case of vCJD in an individual heterozygous at *PRNP* codon 129 affirmed long held suspicions that BSE prions are not only able to propagate in non-MM individuals and manifest after long incubation times, but also

that further cases may be challenging to recognise clinically in life due to altered strain characteristics. This is a highly though-provoking situation considering the sheer scale of BSE exposure in the UK population born prior to 1996. If the estimated prevalence of vCJD prions from the appendix study is in any way accurate (worst case scenario), it implies that the number of at-risk individuals in the UK could exceed 30,000. This argues strongly for more robust autopsy surveillance in prion disease, which currently lingers abysmally at < 10%, despite increasing annual incidence of “sCJD” across several age categories. Fundamentally, without accurate case ascertainment, the true incidence of vCJD will remain obscure, effectively precluding any meaningful definition of risk.

CHAPTER 4

Determining the penetrance of novel *PRNP* variants of uncertain significance

Publications:

Mok TH, Koriath C, Jaunmuktane Z, et al. ***Evaluating the Causality of Novel Sequence Variants in the Prion Protein Gene by Example.*** *Neurobiology of Aging. 2018/05// 2018; doi:10.1016/j.neurobiolaging.2018.05.011*

&

Brennecke N, Cali I, Mok TH, et al. ***Characterization of Prion Disease Associated with a Two-Octapeptide Repeat Insertion.*** *Viruses. Sep 8 2021;13(9)doi:10.3390/v13091794*

Introduction

A great deal has been learnt about the variation of *PRNP* sequence in different populations in the last two decades[65,200]. On one end of the spectrum lies the commonly occurring benign polymorphisms, some of which can modify prion disease susceptibility and clinical phenotype; on the other end are the highly penetrant autosomal dominant variants associated with well-characterised clinical phenotypes, such as large octapeptide repeat insertions (OPRIs), P102L, D178N, E200K and Y163X. In between lie the partially penetrant variants such as V210I found in both control and patient populations which confer significant higher risk of, but not inevitable disease; then there are variants such as the relatively common V180I and M232R in the Far East, smaller OPRIs (<4), and extremely rare variants, where penetrance is not fully resolved.

A combination of decades-long single gene sequencing efforts, followed by the recent advent of low-cost high-throughput next generation sequencing have helped to assemble large-scale genomic databases[201], which on one hand has generated greater number of variants of uncertain significance, but on the other can be leveraged to estimate penetrance of such gene variants. This approach has led to reclassification of several *PRNP* variants previously thought to be pathogenic in the literature, as either benign polymorphisms or low-risk variants[65].

Extremely rare variants are exceedingly difficult to classify, as they are found in very few affected individuals and in the normal population, and sometimes none in the latter; this can be made even more challenging in the absence of a family history or distinctive neuropathological markers. Causal analyses of these rare variants observed in CJD had historically been inclined towards overcalling in terms of pathogenicity and penetrance, and the ensuing erroneous assignation would have had profound impact on areas of personal life such as genetic counselling, family planning, and psychological burden. Moreover, with the increasing availability of preimplantation genetic diagnosis, and opportunities for prevention strategies, it is becoming even more vital that rigorous methods are developed for accurate *PRNP* variant appraisal.

In the course of this MD(res) project, I first encountered the T201S *PRNP* variant in an individual diagnosed with sporadic CJD. This led to an international collaboration with Danish colleagues who possessed a historic case of a CJD patient with this variant in whom archived brain tissue was available for further examination. We assessed multiple lines of evidence including clinical features, neuropathology, molecular strain typing, large-scale genomic databases, PrP structure and *in silico* prediction, in order to estimate the causality of this variant. Following this, I saw a CJD patient whose *PRNP* sequencing demonstrated the presence of 2-OPRI, which although not extremely rare, was at that point a variant of uncertain significance. Together with collaborators in the USA and Australia, led by the US group, we applied a very similar approach to evaluate 2-OPRI. The outcomes of these evaluations were expected to have significant implications not only on the risk of disease in blood relatives of the index cases, but also downstream matters such as threshold for predictive gene testing, and eligibility for inclusion into research or clinical trials in primary prevention studies.

Methods

Ethical approval

Research consent for use of brain tissue from the Danish T201S case was granted under the Danish Health Act (paragraph 187) pre-2009. For the cases included in the 2-OPRI study, ethical approvals were obtained through Institutional review board from University Hospitals Cleveland Medical Center (STUDY20201625), the Scotland A Research Ethics Committee (05/MRE00/63), and the University of Melbourne Human Research Ethics Committee (ethics approval number 1341074).

Neuropathology, immunoblotting and molecular strain typing

Neuropathological examination, immunoblotting and molecular strain typing for the T201S case were performed at the MRC Prion Unit at UCL. Formalin-fixed and formic

acid pre-treated paraffin-embedded post mortem brain tissue samples obtained from the Danish T201S case were prepared and examined as previously described[202]. Of note, anti-PrP antibodies ICSM35 (D-Gen Ltd, London, UK, 1:1000) and KG9 (University of Edinburgh, 1:500) were used for PrP immunohistochemistry. Immunoblotting was undertaken with frozen frontal cortex according to previously protocols[151]. Molecular strain typing of PrP^{Sc} was performed by comparison to reference cases of sporadic CJD (sCJD) and IPD of known PrP^{Sc} type according to the London classification. For quantitation and analysis of PrP^{Sc} glycoform ratios, blots were developed in chemifluorescent substrate (AttoPhos; Promega) and visualized on a Storm 840 phosphorimager (Molecular Dynamics). Quantitation of PrP^{Sc} glycoforms was performed using ImageQuaNT software (Molecular Dynamics), again following established protocols at the MRC Prion Unit at UCL[43].

The molecular and histopathological studies for US 2-OPRI cases were done at the National Prion Disease Pathology Surveillance Center (NPDPSC) in Cleveland, Ohio. Brain regions examined by western blotting included the frontal cortex, cerebellum and/or occipital cortex. For the USA cases, the formalin-fixed brain was treated as previously described; PrP immunohistochemistry was done using the 3F4 antibody at 1:1000[203]. Brain tissue blocks from the only UK-autopsied case were from 1985 and not suitable for modern immunocytochemistry. Tissues were prepared for homogenisation and PK digestion, and western blotting was carried out according to previously established protocols[204,205]. For the 2-OPRI cases, the "Parchi" PrP^{Sc} typing system was used instead of the London classification as this body of work was led by collaborators at the NPDPSC in the USA; the solitary UK case was converted to its equivalent in the Parchi classification system to facilitate comparisons[59].

Penetrance Estimation

The large-scale databases used to estimate the penetrance of T201S and 2-OPRI included different versions of the Broad Institute's Genomic Association Database (gnomAD), and for 2-OPRI exclusively, the UK 100,000 Genomes Project. The total allele count (denominator) used in the calculation for T201S was 246,250 from gnomAD v1, while the upper ranges from gnomAD v2.1.1 (range 247,484–**279,320**)

and gnomAD v3 (range 141,382–**142,740**) were used for 2-OPRI; the total allele count from the 100,000 Genomes Project was 66,670. Within these datasets, assertion of unaffected status is secure in the 100,000 Genomes Project, as both 2-OPRI alleles originate from individuals within non-neurological cohorts. However, this is not the case for the gnomAD datasets as variant–phenotype data are not routinely available and unfortunately not shareable following official enquiry. The list of contributing cohorts to the gnomAD datasets include Alzheimer's disease, migraine, and psychiatry cohorts, which cannot be deemed strictly non-neurological.

The central estimate of disease penetrance for a given variant is equal to the proportion of individuals with the disease who have the gene variant (number of variant alleles found in CJD cases ÷ all *PRNP*-sequenced CJD cases) multiplied by the prevalence of the disease (lifetime risk of CJD (0.02%)), and divided by the frequency of the gene variant in the general population (number of variant alleles found in a specific dataset ÷ number of *PRNP* alleles sequenced in that particular dataset). The Wilson Interval is best used to calculate the 95% confidence interval here as the central estimate is close to zero.

$$\boldsymbol{Penetrance = lifetime\ risk\ of\ CJD\ x\ \frac{variant\ allele\ frequency\ in\ CJD\ cases}{variant\ allele\ frequency\ in\ normal\ population}}$$

Results

T201S

Clinical details

Genetic sequencing of CJD cases at the MRC Prion Unit on patients reviewed by the NHS National Prion Clinic in the UK revealed a 76-year-old British Caucasian woman with the T201S *PRNP* gene variant in 2017. Subsequently, literature search identified another case of CJD associated with the *PRNP* T201S gene variant in a 63-year-old Danish woman presented as a poster in the the 19th European Stroke Conference in 2010[206]. Both women had abrupt clinical onsets, and rapid neurological and cognitive

decline featuring early non-fluent dysphasia. Within 8-10 weeks, both progressed to akinetic mutism with myoclonus and died. An autopsy was performed on the Danish woman.

Neither women possessed a family history of a similar illness, nor were there any individuals in their families who had neurological or cognitive problems. The family history in the British case was censored with the death of her mother at 57 from lung cancer.

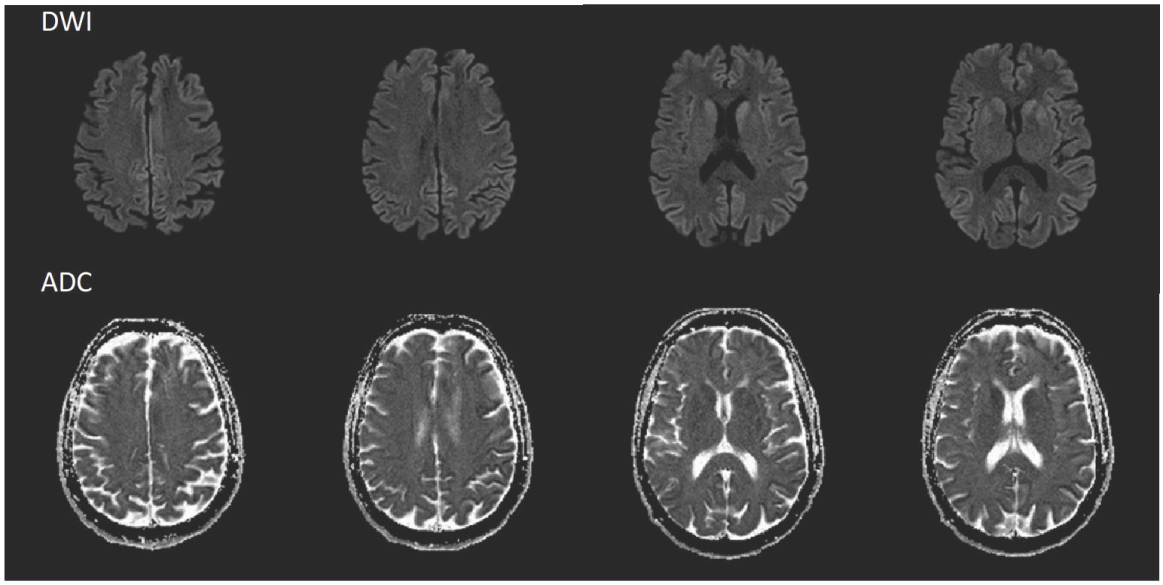

Figure 21 DWI sequences from MRI Brain of British case.

The upper panel shows the axial DWI sequence, while the lower panel shows the ADC maps. Signal hyperintensity in the caudate heads and anterior putamina is seen on DWI with corresponding low signal on ADC indicating truly restricted diffusion; similar signal mismatch is widespread over the cortices.

MRI Brain studies in both cases revealed characteristic DWI findings consistent with CJD such as restricted diffusion in the basal ganglia, and cortical ribboning either exclusively or predominantly on the left cerebral hemisphere; DWI and ADC sequences from the British case are shown in Figure 21. EEG done early in the clinical course of the Danish case showed frontotemporal slowing at 1-2 Hz, while generalised periodic complexes were seen on the EEG done late in the course of the British case. CSF examination in both cases had cell counts and routine biochemistry were normal; only the CSF sample from the Danish case was analysed for prion-specific markers in

which the protein 14-3-3 was positive and the neuron-specific enolase was elevated at 101 ng/ml (<35).

Sequencing of the entire *PRNP* open reading frame in both patients demonstrated a threonine to serine missense substitution at codon 201 (T201S); the underlying nucleotide change was c.602C>G (CCDS 13080.1) in both cases. Their c129 genotypes were both methionine homozygous (MM).

Neuropathology

Routine H&E–stained sections revealed widespread microvacuolar degeneration in the neocortex, deep grey nuclei and to a lesser extent in the molecular layer of the cerebellar cortex. Immunostaining for abnormal PrP showed diffuse synaptic (punctate or granular) labelling throughout grey matter regions but no kuru or multicentric plaques or other plaque-like deposits (Figure 22). In the white matter, there were no filamentous deposits, which have been reported in a proportion of IPD cases[70]. The histological appearances were indistinguishable from sCJD patients with *PRNP* 129MM genotype and type 2 PrP^{Sc} (London Classification) which corresponds to type 1 PrP^{Sc} of the Parchi classification.

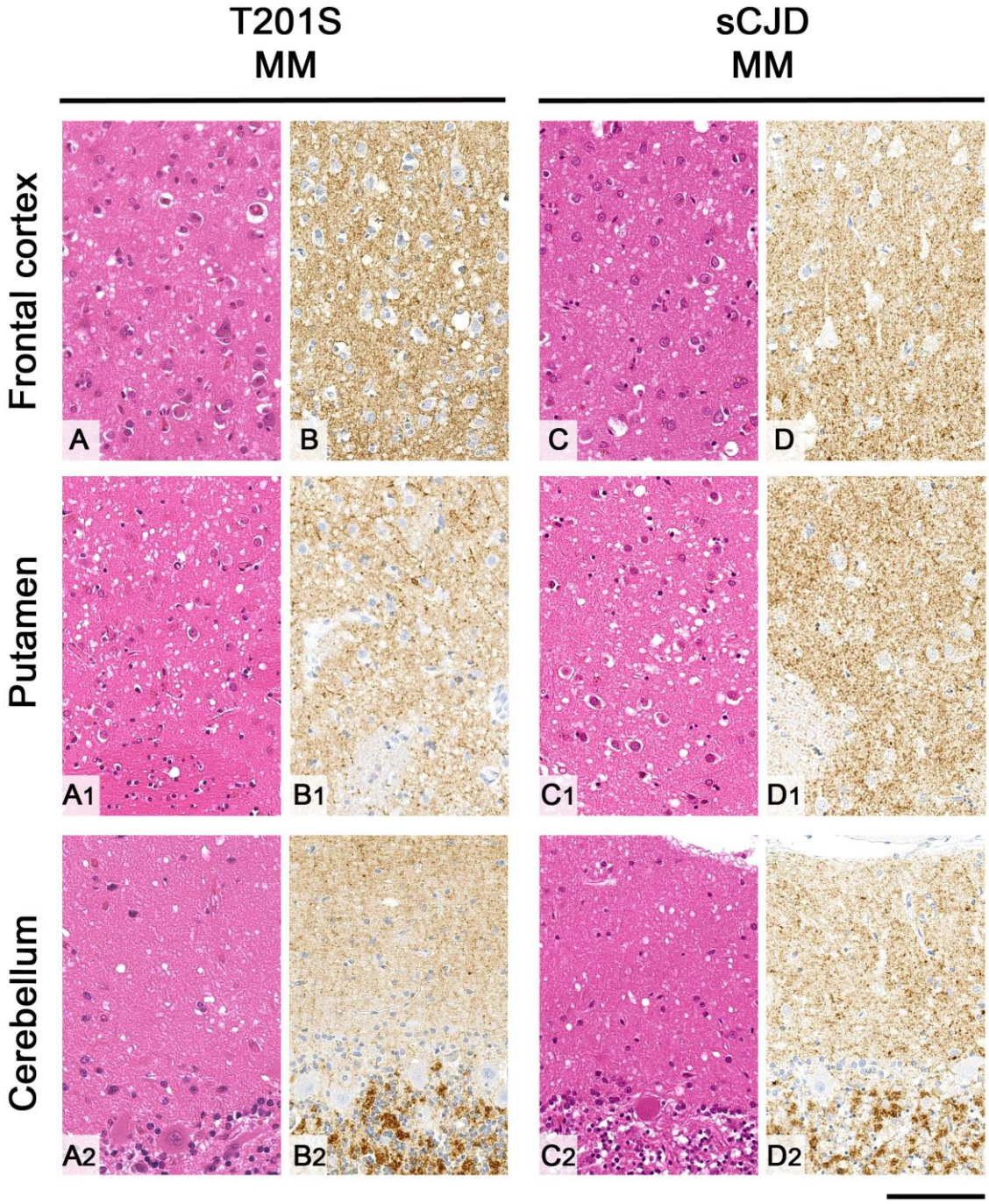

Figure 22 Comparison of prion pathology between a T201S patient (Danish case) and a classical sCJD case, both with *PRNP* codon 129MM genotype.

Prion pathology in T201S patient (A-A2 and B-B2) is similar to that seen in *PRNP* c129 MM sCJD case (C-C2 and D-D2): H&E stained sections from the frontal cortex (A and C), putamen (A1 and C1) and cerebellar cortex (A2 and C2) show widespread microvacuolar degeneration in the neuropil. The same regions immunostained for abnormal prion protein with KG9 antibody (B-B2) and ICSM35 antibody (D-D2) show diffuse synaptic (punctate or granular) labelling (B and D, frontal cortex), (B1 and D1, putamen) and (B2 and D2, cerebellar cortex). Scale bar: 100 µm. Reproduced from Mok *et al.* 2018 (https://doi.org/10.1016/j.neurobiolaging.2018.05.011).

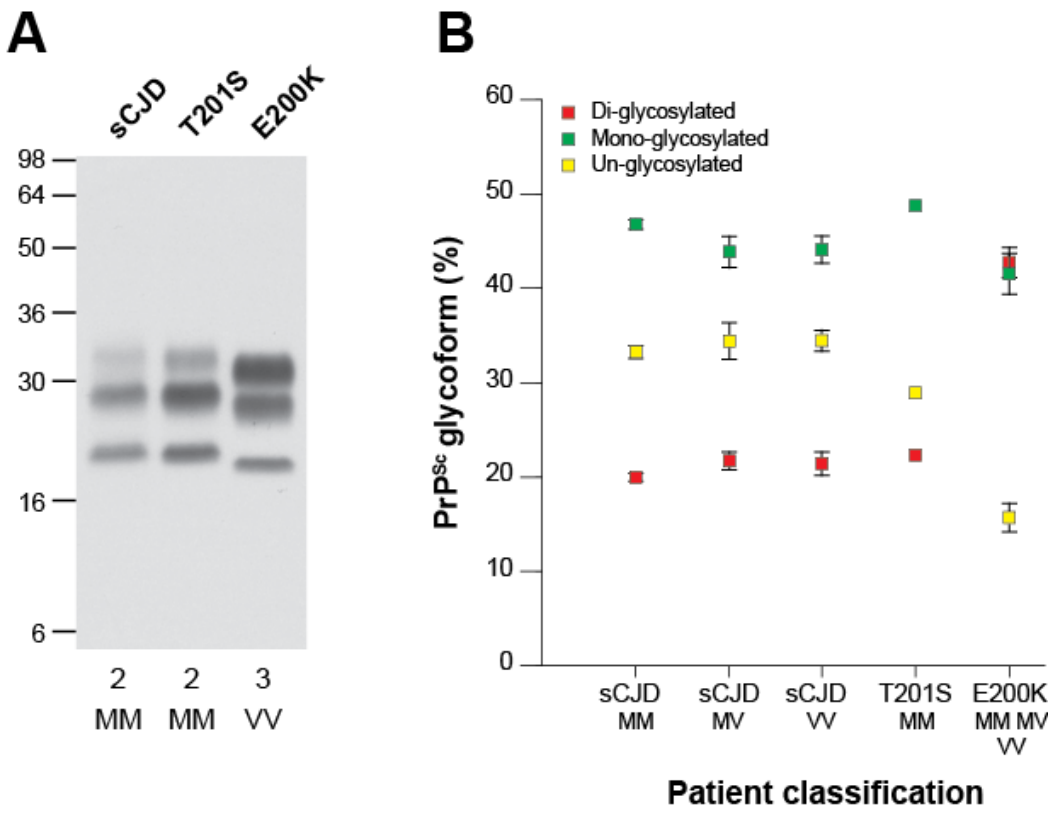

Figure 23 PrP^{Sc} typing in T201S patient brain.

(**A**) Immunoblot of PK-digested 10% (w/v) brain homogenates (frontal cortex) from the Danish T201S case, and reference cases of sCJD or IPD E200K using anti-PrP monoclonal antibody 3F4 and high sensitivity enhanced chemiluminescence. The provenance of the brain sample is designated above each lane and the PrP^{Sc} type (London classification) and *PRNP* c129 genotype of the patient are shown below. (**B**) Ratios of the three principal protease-resistant PrP glycoforms seen in PrP^{Sc} from the Danish T201S case in comparison to PrP^{Sc} from patients with classical CJD or IPD E200K. Data points for the reference cases represent the mean relative proportions of di-, mono- and unglycosylated PrP as percentage ± SEM. In some cases the error bars were smaller than the symbols used. The number of reference cases analysed were: sCJD 129MM with type 2 PrP^{Sc} (n = 37), sCJD c129 MV with type 2 PrP^{Sc} (n = 8), sCJD c129 VV with type 2 PrP^{Sc} (n = 9) and IPD E200K (n=6; three c129 MM with type 1 PrP^{Sc} fragment size, two c129 MV with type 2 PrP^{Sc} fragment size and one c129 VV with type 3 PrP^{Sc} fragment size).

Reproduced from Mok *et al.* 2018 (https://doi.org/10.1016/j.neurobiolaging.2018.05.011).

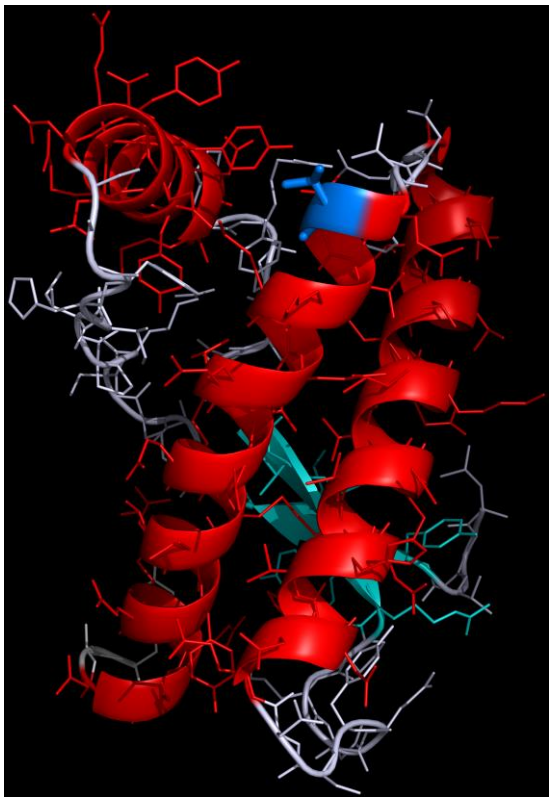

Figure 24 Location of the T201S variant in the structure of human PrP^C.

PrP^C is displayed as a "ribbon" representation of its secondary structure, together with sidechain groups. α-helices are coloured red and β-strands coloured cyan (residues 125-225 are displayed). Residue 201 is located at the start of the third α-helix, and is coloured in blue with its threonine sidechain displayed in stick representation. This figure was prepared using PyMOL (PyMOL Molecular Graphics System, Schrödinger, LLC). Reproduced from Mok *et al.* 2018 (https://doi.org/10.1016/j.neurobiolaging.2018.05.011).

Immunoblot and molecular strain typing

Immunoblot analyses of brain homogenate from T201S case 1 demonstrated a PrP^{Sc} type corresponding to type 2 PrP^{Sc} of the London classification seen in patients with sCJD (Figure 23). Type 2 PrP^{Sc} shows a predominance of monoglycosylated PrP, which contrasts markedly with the distinctive glycoform ratio of mutant PrP^{Sc} seen in IPD E200K (Figure 23B)[43]. These findings indicate that the T201S missense coding change does not impart conformational preferences to PrP^{Sc} in the same way that E200K does.

Effect of T201S on PrP structure

The threonine to serine substitution studied here is considered conservative, as both these amino acids are uncharged, polar, and of similar size; serine being slightly smaller due to the substitution of a proton for the methyl group found in the threonine side chain. Furthermore, X-ray and nuclear magnetic resonance studies of recombinant PrP^{C} [207,208] show that T201 is situated at the start of helix 3 of the PrP, with its side chain predominantly solvent exposed rather than within the protein core; thus, unlikely to destabilize PrP^{C} (Figure 24).

Computational (*in silico*) predictions

A range of sequence- and structure-based *in silico* tools are available to assist the interpretation of novel missense variants. It is however recognised that these computational algorithms are inclined to overestimate the damaging effect of missense variants, particularly in the context of variants of milder impact.

Here, Polymorphism Phenotyping version 2 (PolyPhen-2)[209] and Sorting Intolerant From Tolerant (SIFT)[210] predicted that the T201S mutation to be *possibly damaging* or *deleterious*, respectively; its Combined Annotation Dependent Depletion (CADD)[211] score of 26 ranks it within 1% of the most deleterious mutations. While these in silico tools are unanimous in their predictions for highly penetrant mutations such as P102L, D178N, and E200K (*probably damaging* by PolyPhen-2, *deleterious* by SIFT, and score > 30 by CADD), predictions for other *PRNP* missense variants, both benign and pathogenic, are somewhat mixed. For example, the benign V209M is predicted to be *benign* by PolyPhen-2, *deleterious* by SIFT, and a CADD score of 20.2; the incompletely penetrant V210I is predicted to be *benign* by PolyPhen-2, *tolerated* by SIFT, and a CADD score of 13.53; the highly penetrant A117V is predicted to be *probably damaging* by PolyPhen-2 and CADD score 23.3, but *tolerated* by SIFT. Hence, this illustrates why gene variants of *PRNP* should not be evaluated solely by *in silico* tools.

Estimating the penetrance of T201S

T201S was found in a single individual in gnomAD v1 of 123,125 individuals (1 in 246,250 alleles). By leveraging this large-scale population database, we then used

methods for calculating the baseline risk of CJD previously described in Minikel *et al.* 2016 and computed the upper bound of the 95% confidence interval (CI) using the Wilson Interval[65]. The total CJD alleles from sequenced *PRNP* are derived from the sum of alleles in sequenced CJD cases in Minikel *et al.* 2016 (years 1990–2013) and additional alleles (n = 844) from sequenced CJD cases at the Medical Research Council Prion Unit (years 2014 to present). The estimated penetrance of T201S using this approach is 0.45% (95% CI 0.02%, 9.35%).

2-OPRI

Clinical details

A total of three prion disease research and surveillance centres worldwide responded to a call put out by the NPDPSC in Cleveland, Ohio for cases of CJD associated with the presence of 2-OPRI in the *PRNP*, resulting in eight cases being identified; five of these were from the USA, two from the UK and one from Australia (Table 9). All eight cases were of Caucasian ethnicity, of which half were males. The age at onset was known for six of these, with the median being 75 (range 58–84 years, mean 71 years ± 8.1). Unsurprisingly, heterozygosity at *PRNP* c129 was associated with a significantly later age of onset (64.3 ± 5.5 and 78.0 ± 5.3, respectively, *t*-test, $p = 0.036$). All individuals with known age at onset had disease durations of 10 months or less, with the exception of the Australian case who went on for 21 months. The clinical features, while heterogenous from case to case, were consistent with what one usually observes in CJD, including dementia, ataxia, pyramidal signs, visual symptoms, and myoclonus.

Table 9 Clinical features of CJD cases associated with 2-OPRI

Case	Origin	Diagnosis	*PRNP* c129	PrP^{Sc} Type[a]	Age at Onset (Years)	Disease Duration (Months)	Sex	14-3-3 Protein	Tau (pg/mL)[b]	RT-QuIC	PSWC on EEG	MRI c/w CJD	Family History	Clinical Phenotype
1	US	Definite	MM	1	67	2	Male	Pos.	17,727	NA	NA	Yes	None	Slurred speech, then a fulminant course including cognitive and cerebellar symptoms and myoclonus
2	US	Probable	MM	1	NA	NA	Male	Pos.	8848	NA	NA	Yes	None	NA
3	US	Definite	MM	1	68	7	Female	Pos.	7990	NA	Yes	Yes	Mother with several year slowly progressive dementia in her 60s, thought to be AD	Absence-like episodes, followed 5 months later by cognitive symptoms, personality change, and myoclonus
4	US	Probable	MV	1–2	84	3	Female	Unk.	Unk.	NA	NA	Yes	None	Myoclonus, unilateral weakness/spasticity, late cognitive symptoms
5	US	Definite	MM	1–2	NA	NA	Female	Pos.	15,046	Pos.	NA	Yes	None	NA
6	UK	Probable	MV	NA	76	10	Male	Neg.	Unk.	Pos.	No	Yes	Sister with 2-year history of Alzheimer's dementia starting at age 89; sister with mild dementia in her 80s.	Gait ataxia, followed by cognitive symptoms, visual hallucinations, and myoclonus
7	UK	Definite	MM	1	58	7	Male	Unk.	Unk.	NA	No	NA	Unknown	Right hand paresthesia followed by unilateral weakness/spasticity
8	AU	Probable	MV	NA	74	21	Female	Pos.	Unk.	Pos.	No	Yes	Brother with 5-year history of dementia in his 60s.	Visual disturbances, followed by gait disturbance, Parkinsonian features, apraxia, and visuospatial difficulties

[a]Parchi classification; [b]tau levels >1,150 pg/mL are suggestive of prion disease; PrP^{Sc}: PK-resistant disease-associated PrP; Codon 129 polymorphism in cis with the 2-OPRI mutation is underlined if known. US: United States; UK: United Kingdom; AU: Australia; RT-QuIC: real-time quaking-induced conversion; Pos.: positive; Neg.: negative; Unk.: unknown; PSWC: periodic sharp wave complexes; NA: not available; AD: Alzheimer's disease. Adapted from Brennecke et al. 2021 (doi: 10.3390/v13091794).

None of the cases had a confirmed family history of CJD, although three cases had a family history of poorly characterised long duration (> 2 years) neurodegenerative disease. None of the blood relatives of the cases had their *PRNP* sequenced.

All but one of these cases had MRI Brain scans which demonstrated restricted diffusion in the cortex; three had, in addition, restricted diffusion in the deep nuclei. The only case without MRI Brain imaging hailed from 1985 when the technology was unavailable; CJD was confirmed in this case by autopsy. Five of six cases in which protein 14-3-3 in the CSF was tested returned positive results; all three cases tested for CSF RT-QuIC were positive. Repeat sequences in the OPRI region of the *PRNP* were available for all but one, and are shown in Table 10. Five were methionine homozygous at c129, three were methionine-valine heterozygous.

Table 10 Molecular features and histotype of 2-OPRI cases

Case number	*PRNP* c129 genotype	Repeat Sequence	PrP^{Sc}	sCJD histotype[b]
1	MM	R1-R2-R2-**R2-R2**-R3-R4	1	MM(MV)1
2	MM	R1-R2-R2-R3-**R2-R3**-R4	1	MM(MV)1
3	MM	R1-R2-R2-**R2-R2**-R3-R4	1	MM(MV)1
4	MV	R1-R2-R2-**R2-R2**-R3-R4	1-2	MV2C+1[c]
5	MM	R1-R2-R2-R3-**R2a-R2a**-R4	1	MM1-2[c]
6 (UK)	MV	R1-R2-R2-**R2-R2**-R3-R4	NA	NA
7 (UK)	MM	R1-R2-R2-R3-**R2a-R2a**-R4	1	MM(MV)1
8 (AUS)	MV	NA	NA	NA

[b]Parchi classification; c Minor sCJDMM2 component affecting the temporal cortex; Codon 129 polymorphism in cis with the 2-OPRI mutation is underlined if known. PrP^{Sc}: PK-resistant disease-associated PrP; MM: methionine homozygosity; MV: methionine/valine heterozygosity; NA: not available. Adapted from Brennecke et al. 2021 (doi: 10.3390/v13091794).

Neuropathology

Neuropathology was available in six out of eight cases and were analysed according to the Parchi classification, as this study was led by the US collaborators. Four cases demonstrated classic spongiform degeneration and reactive astrocytosis, and had a synaptic pattern of PrP deposition on immunohistochemical examination (cases 1–3 and 7 from Table 10) (Figure 25). These were consistent with histopathological

features associated with sCJDMM(MV)1. Case 5 demonstrated the sCJDMM1-2 histotype with a minor type 2 component, characterised by large vacuoles and perivacuolar PrP deposition in the temporal cortex. Case 4, carrying the c129 MV genotype and PrP^{Sc} type 1–2, showed mild spongiform degeneration with small and large vacuoles, and diffuse and coarse PrP deposits within the neocortex. No features suggestive of IPD, such as filamentous PrP deposits in the subcortical white matter or "striped" cerebellar PrP staining characteristic of some OPRIs, were observed in the

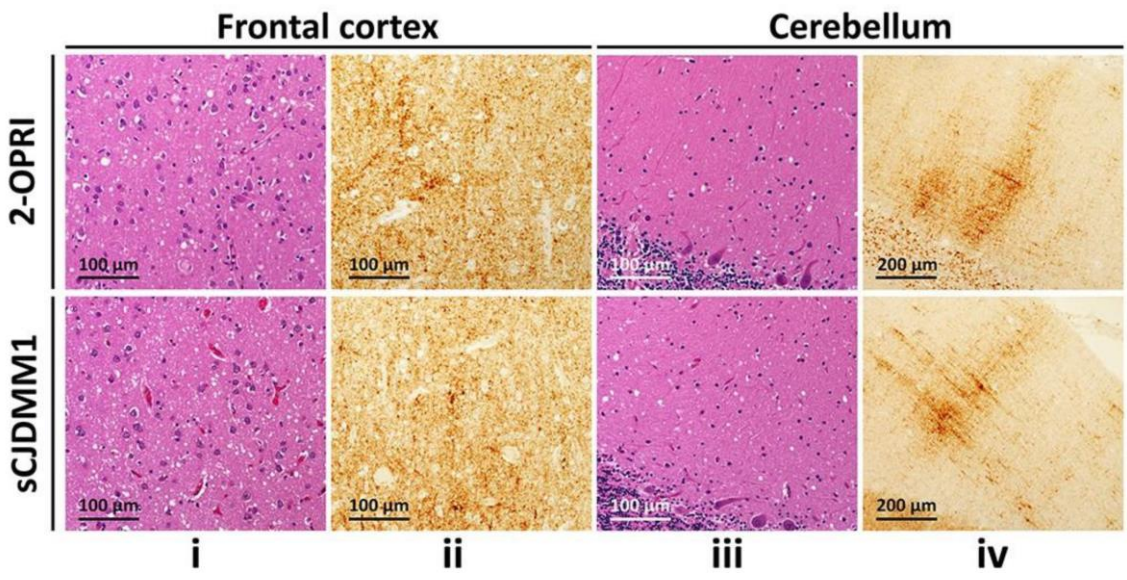

Figure 25 Histological determination of 2-OPRI and sCJDMM1.

(**i**,**iii**) H&E staining. (**ii**,**iv**) PrP immunohistochemistry. (**i**,**iii**) Fine spongiform degeneration. (**ii**,**iv**) Diffuse PrP immunostaining (**ii**,**iv**) with the typical "brush stroke-like" deposits in the cerebellar molecular layer (**iv**); antibody: 3F4. Reproduced from Brennecke *et al.* 2021 (doi: 10.3390/v13091794).

autopsied brains[70].

Immunoblot and molecular strain typing

On Western blotting, PK-undigested and detergent-insoluble PrP fragments from 2-OPRI brains showed different motility patterns and additional bands when compared to sCJD (Figure 26A & 26B). Comparison was also made with a 7-OPRI case where the ~34–35 kDa doublet appeared as a triplet in the 7-OPRI case, while a band with the molecular weight of ~42–44 kDa was not detected in 2-OPRI (Figure 26C). Following digestion with PK, the Western blot profile of PrP^{Sc} from the OPRI and sCJD cases became virtually indistinguishable (Figure 26D). Glycoform ratio analyses per

Hill *et al.* 2006 were not performed on this occasion but the UK case (Case 7) was included in the OPRI group in Hill *et al.* 2006 which demonstrated a pattern indistinguishable from sCJD (Figure 27).

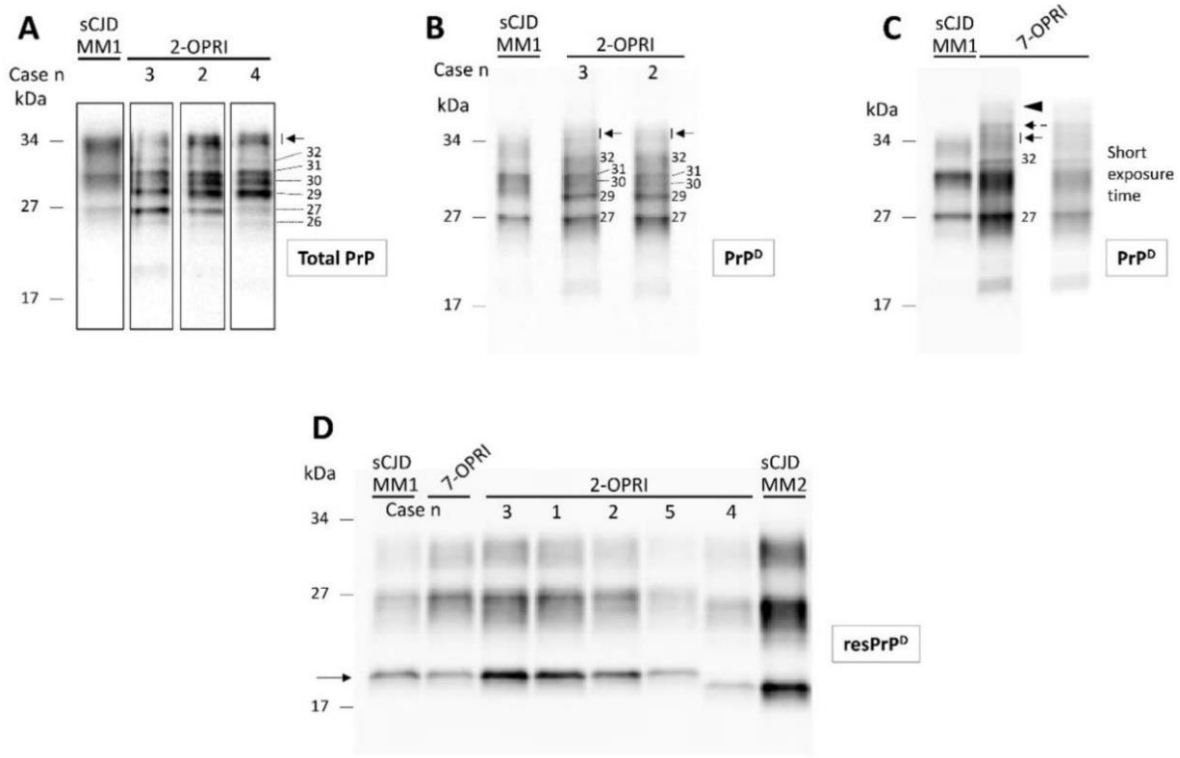

Figure 26 Western blot (WB) profiles of total PrP, detergent-insoluble PrP^D and $resPrP^D$ (Parchi classification).

Samples harvested from the cerebral cortex were probed with the anti-PrP antibody 3F4. (A): Total PrP showing a complex PrP profile in 2-OPRI cases but not in sCJDMM1. The approximate molecular size of each band is indicated by the numbers on the right; arrow: PrP doublet of ~34–35 kDa. (B): Western blot profile of detergent-insoluble PrPD harvested from 2-OPRI resembles that of total PrP except for the absence and weak presence of the ~26 and ~30 kDa fragments, respectively. (C): Insoluble PrPD WB profile of a 7-OPRI features a sharp band of ~32 kDa, a PrPD triplet in the ~34–36 kDa region, and a PrPD smear of ~42–44 kDa, whereas the PrPD region of ~31 to 27 kDa resembles that of sCJD MM1. (D): The unglycosylated isoform of resPrPD (arrow) in 2-OPRI-MM1 (cases 1–3), 2-OPRI-MM1-2 (case 5), and 7-OPRI-MM1 migrates to ~20 kDa, matching the gel mobility of resPrPD type 1 (sCJD MM1). The unglycosylated resPrPD of 2-OPRI-MV1-2 (case 4) migrates to ~19 kDa, thus matching the gel mobility of sCJDMM2 resPrPD type 2. Reproduced from Brennecke et al. 2021 (doi: 10.3390/v13091794).

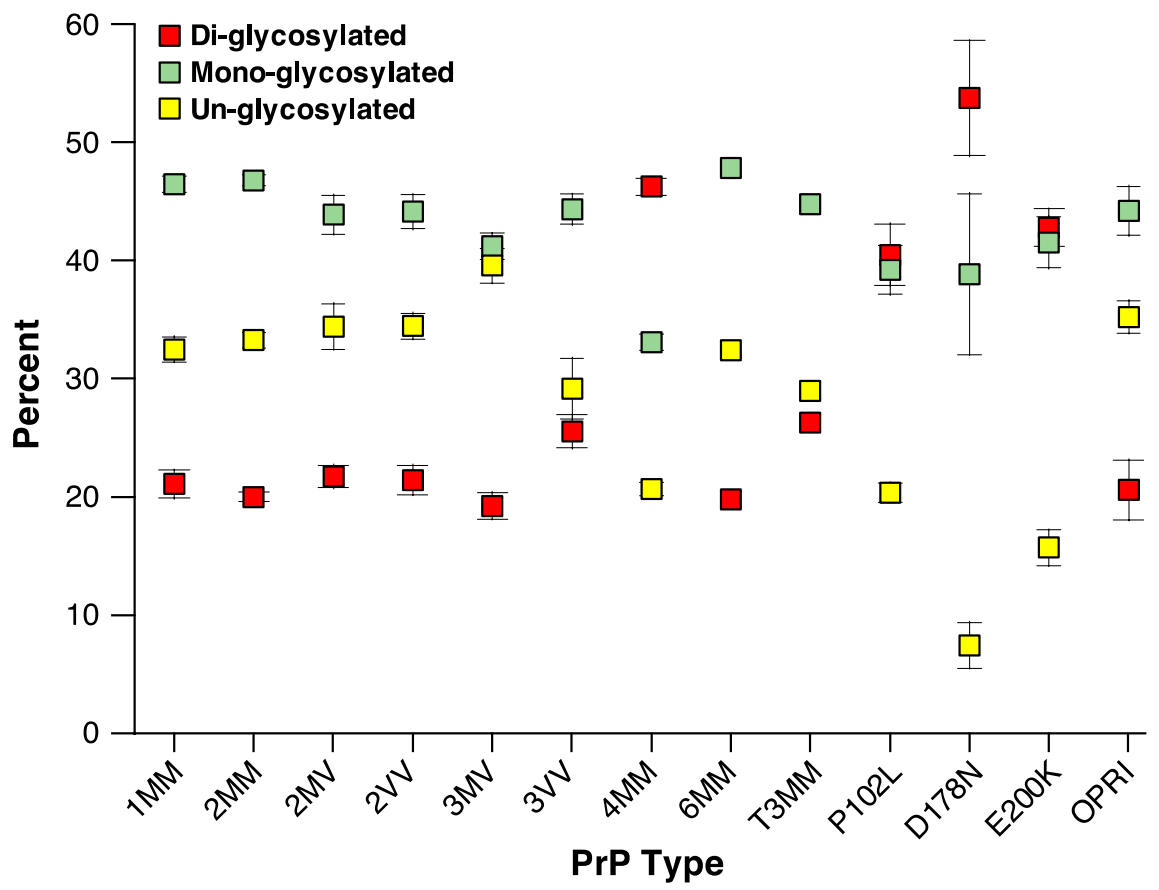

Figure 27 Ratio of three principal PrP^{Sc} glycoforms of ~21–30 kDa seen in classical sCJD, vCJD and cases of IPD.

Data points represent the mean relative proportions of di-, mono- and unglycosylated PrP as percentage ± SEM. In some cases the error bars were smaller than the symbols used. The number of cases analysed were: sCJD type 1 PrP^{Sc} 129MM (n = 17), sCJD type 2 PrP^{Sc} 129, MM,MV,VV (n = 57), sCJD type 3 PrP^{Sc} 129MM (n = 1), sCJD type 3 PrP^{Sc} 129MV (n = 8), vCJD type 4 129MM (n = 30), P102L 129MM (n = 4), D178N 129MM (n = 2), E200K 129, MM,MV,VV (n = 5), OPRI mutations 129 MM, MV (n = 5). For *PRNP* point mutations P102L, E200K and D178N, there is a statistically significant difference in the proportions of di- and un-glycosylated PrP glycoforms when compared with PrP^{Sc} types 1–3 in classical CJD ($P < 0.0001$ for the di- and un-glycosylated bands; unpaired t-test) and in the proportions of mono- and un-glycosylated PrP glycoforms compared with type 4 PrP^{Sc} seen in vCJD ($P < 0.004$ for either glycoform; unpaired t-test). The PrP glycoform ratio in OPRI cases (***including the British 2-OPRI case from 1985***) shows no significant difference from PrP^{Sc} seen in sporadic CJD cases of the same codon 129 genotype ($P > 0.1$). Reproduced from Hill *et al.* 2006 (doi: 10.1093/brain/awl013).

Estimating the penetrance of 2-OPRI

Interrogation of a number of available large-scale population genetic datasets identified a total of sixteen 2-OPRI alleles in presumably unaffected individuals. Within these 16 alleles, six (five exomic, one genomic) were from gnomAD v2.1.1 (USA), eight from gnomAD v3 (USA), and two from the 100,000 Genomes Project (UK)[212]. Of the 14 alleles from the gnomAD datasets, seven were non-Finnish Europeans, four were Finnish Europeans, one was South Asian, one was African and one was Latino/admixed American; eight were male and six were female. Age range data was available for five of six gnomAD v2.1.1 cases only, with two cases in the 55–60 years range, two cases in the 60–65 year range, one case in the 65–70 years age range, and unknown for one; age range data for gnomAD v3.1.1 is available for two of eight cases, with one case in the 65-70 years age range and one case in the 70-75 years age range. Estimation of 2-OPRI penetrance and 95% CI using a Bayesian approach and the Wilson interval, respectively, revealed an extremely low penetrance of 0.34% and below, and upper bounds of 95% CI below 2%[65]. Specifically, the estimated penetrance by leveraging the gnomAD v2.1.1 was 0.34% (95% CI 0.08, 1.46), gnomAD v3 was 0.13% (95%CI 0.03, 0.51), and, for the 100,000 Genomes Project, it was 0.24% (95%CI 0.03, 1.75).

Discussion

Assignation of penetrance/pathogenicity are fairly straightforward for *PRNP* gene variants, such as P102L, D178N, E200K and Y163X, where canonical clinical syndromes, clear segregation within affected kindreds, or where pathognomonic neuropathological and molecular strain typing patterns exist. The challenge arises when *PRNP* gene variants are discovered in association with common prion disease clinical phenotypes without any of the distinguishing features listed above. Such was the situation with the unexpected discovery of the extremely rare T201S variant in an individual classified as *probable* sCJD in life according to national surveillance criteria, without a family history of CJD and in whom no brain tissue was available to examine. Efforts to resolve this led to an international collaboration with Danish colleagues, and subsequent interrogation of multiple lines of evidence including neuropathology and molecular strain typing, PrP structural analysis, computational (*in silico*) predictions,

and use of large-scale genomic databases to provide a guidance framework to apply to other *PRNP* variants of unknown significance.

Relative to the rarity of T201S, a handful of publications from as early as the 1990s had attempted to ascertain the penetrance of 2-OPRI, but were limited by the lack of autopsy confirmation. The very first and only report of autopsy-proven CJD in association with 2-OPRI prior Brennecke *et al.* 2021[213] was by Goldfarb *et al.* 1993; this report identified several 2-OPRI carriers in blood relatives, of whom two had long-duration dementias, but without autopsy diagnosis[214]. Two other publications found 2-OPRI in individuals (and relatives) with long-duration dementias but again neither had autopsy-proven prion disease[97,215]. As such it came as no surprise that the issue remained unresolved until we attempted a more comprehensive examination in 2021[213].

The common features shared by both T201S and 2-OPRI are, other than being associated with CJD, include the absence of a family history of similar illness and the lack of unique neuropathological features pointing towards IPD. It was determined that *in silico* prediction tools frequently used to assign pathogenicity in other diseases cannot be used to make reliable predictions prion disease. Highly-penetrant *PRNP* gene variants cause disease by unknown mechanisms that result in a conformational structural change, rather than by simple loss- or gain-of-function mechanisms in which functional and computational data can be more tractable to study in cellular models. This lack of applicability was crystallised through the exploration of a number of established benign and highly-penetrant *PRNP* gene variants.

In terms of PrP structural considerations, T201S and 2-OPRI differ in that T201S is a missense point mutation in the carboxy-terminal, while 2-OPRI is a repeat insertion located in the amino-terminal of the protein. T201S is felt only to cause minor perturbation of the native PrP^{C} structure by virtue of its additional methyl group but its pathogenicity cannot be completely ruled out. Analyses of *PRNP* missense variants have focussed on stabilisation/destabilisation of native PrP^{C}, but these studies use recombinant unglycosylated PrP, which may not recapitulate all of the folding problems encountered in vivo[216]. Alternatively, the disease-associated mutations may

primarily affect the stability of more relevant on-pathway folding intermediates[217]. The disease-causing mechanism of OPRIs in general remain obscure as this section of the protein is unfolded and highly mobile in the normal cellular form of PrP and is rapidly digested by PK[18]. It is possible that this may relate to its binding of divalent cations including Cu^{2+} and Zn^{2+}, by the histidine residues in the OPRI region, which in turn may have an influence in controlling oligomerisation *in vivo*[218]. While it was by no means conclusive, the PrP structural analyses suggest that neither T201S nor 2-OPRI are unlikely to impart a significant change in PrP conformation. However, it is possible that the observations above may modified, refined or even completely superseded by near atomic resolution visualisation of prion structure. This was recently accomplished in rodent prion strains, and if/when applicable to human prion strains/species, could be highly illuminating[44-46]. For example, it is possible that a otherwise minor change to the amino acid sequence such as that seen in T201S might in reality result in significant effects on its secondary and tertiary structure, and hence its pathogenicity[219,220].

Thus far, it has not possible to apply practice guidelines such as the American College of Medical Genetics and Genomics for T201S and 2-OPRI due to insufficient data to combine criteria for stratification[221]. There is lack of segregation, functional, de novo, and computational and predictive data to satisfy the stipulated American College of Medical Genetics and Genomics criteria[202]. Moreover, computational prediction has been proven to be unreliable for classifying *PRNP* gene variants, and PrP structural analyses have failed to provide any clear pathogenic role.

Nevertheless, we showed that it is possible to produce both qualitative and quantitative estimates of pathogenicity and penetrance for both T201S and 2-OPRI, by harnessing data from multiple lines of evidence specific for prion disease. Different prion strains can propagate in the same host to produce different disease phenotypes and appear to be encoded by distinct abnormal PrP conformations and assembly states[41]. Different human PrP^{Sc} isoforms associated with phenotypically distinct forms of human prion disease (molecular strain types) have considerable diagnostic utility and are classified by both the fragment size and ratio of the 3 principal PrP bands seen after partial PK digestion[42,43]. Variations in the primary sequence of human PrP profoundly affect the ability of the expressed protein to propagate particular prion

strains through conformational selection. The c129 polymorphism determines the ability of wild-type human PrP to propagate particular prion strains in patients with sporadic or acquired forms of prion disease while highly penetrant missense mutations that cause IPD[72], for example, P102L, E200K, and D178N, impose additional conformational preferences for PrP assemblies, resulting in PrP^{Sc} molecular strain types that are distinct from those propagated in patients with sporadic or acquired aetiologies[43,87,138,222,223]. Immunoblot analyses showed that PrP^{Sc} from T201S brain tissue resembled that of type 2 sCJD 129MM rather than that seen in highly-penetrant carboxy-terminal *PRNP* point mutations such as E200K. However, glycoform ratio analysis is non-discriminative for 2-OPRI as perturbations in the *PRNP* octapeptide repeat region do not seem to impart distinct PrP conformational assembly preferences that are reflected in identifiable glycoform ratio signatures.

Neither T201S nor 2-OPRI produced any neuropathological characteristics that are distinct from the gamut of observed findings in sporadic CJD. More specifically, no filamentous PrP deposits nor “striped” cerebellar PrP staining were found in T201S or 2-OPRI brains, though the significance of these deposits applies more to 2-OPRI than T201S[70,224]. For 2-OPRI, a possible source ascertainment bias remains, arising from the sole focus in obtaining detailed clinical *PRNP* sequencing and autopsied brain material from those presenting with CJD phenotypes to prion disease surveillance centres. The dichotomous phenotypes of CJD and long-duration dementia syndromes are well-described even within the same pedigrees in larger OPRIs, most notably in 4- and 5-OPRI families[99,225]; furthermore, the penetrance in these pedigrees are notoriously incomplete, and ages of onset can be extremely variable. In the 2-OPRI case series, three patients had immediate blood relatives with long-duration neurodegenerative disease presumed to be non-prion diseases such as Alzheimer’s disease, but none of them underwent *PRNP* sequencing, and no autopsied brain material was examined to exclude prion pathology. If prion disease neuropathology was identified in these relatives with long-duration neurodegenerative disease syndromes, this line of evidence would have influenced our conclusions.

Finally, the central estimates for the lifetime risks of CJD from T201S [0.45% (95% CI 0.02%, 9.35%)] and 2-OPRI (0.13-0.24%; uppermost bound of 95%CI is 1.75%), produced by leveraging large-scale genomic databases, are extremely low (close to

zero) and with reasonably narrow confidence intervals; for comparison the lifetime risk of CJD in the UK is 1 in 5000 or 0.02% This suggest that both these *PRNP* gene variants are either benign or at worst low-risk variants, the latter resulting in ~15-23 fold increase on the background risk. This method of estimating penetrance comes with different risks of inaccuracy, two of which are exemplified separately by T201S and 2-OPRI. With singletons of extremely low frequency such as T201S, the true population allele count represent by genomic databases can not only be imprecise, but also biased towards underestimation. This is exemplified by the shift in calculated penetrance from 0.22% (95% CI 0.01%, 4.56%) to 0.45% (95% CI 0.02%, 9.35%), when the original Exome Aggregation Consortium database expanded into the gnomAD in which the allele count doubled from 121,384 to 246,250 alleles. Even more strikingly, it was pointed out that 69% of very rare singletons for Europeans (6503 exomes) in the Exome Sequencing Project were not identified again in the Exome Aggregation Consortium database, despite a 10-fold expansion. Hypothetically, if this holds true for gnomAD, the true allele frequency of a rare singleton such as T201S could be 1 in 2.5 million or lower, raising the upper limit of the 95% CI to 94% (or higher) and rendering the estimation meaningless. The risk with 2-OPRI pertains to the use of short-read sequencing technologies, with read lengths of up to 150 base pairs, which may not be able to fully resolve the spectrum of 2-OPRI alleles present given that 2-OPRIs are 171 base pairs long. It is likely therefore that the 2-OPRI allele frequency is underestimated in the population, although use of more recent sequencing probes with read lengths of up to 300 base pairs will address this issue.

Conclusion

Precise estimates of penetrance for T201S and 2-OPRI continue to elude us at the present time on account of the limitations detailed above. T201S may turn out to be a completely benign or at most a very low-risk variant, while 2-OPRI is likely to be a low-risk variant leading to only very modest increase above the background risk of CJD. Multiple lines of evidence, the key being molecular strain typing for T201S, and low penetrance estimations for both clearly indicate that these are not highly-penetrant variants associated with inevitable or high lifetime risks. In fact the central estimations of less that 0.5%, and upper bound of 95% confidence intervals of less than 10%

means that routine predictive testing for blood relatives cannot be justified. Following our analyses, we met with the surviving blood relatives of the British patients to explain the results, and we were able to reassure them. The daughter of the lady with the T201S variant had sought advice from her local clinical genetics service who agreed with our conclusions.

Estimation of penetrance for novel or rare variants is the requisite step to determine eligibility of blood relatives for inclusion into research cohorts for studying individuals. Naturally, gene variants with estimated penetrance considered to be below the threshold for predictive genetic testing, should not be enrolled into at-risk research cohorts. Further expansion of large-scale population genomic databases in tandem with assiduous autopsy surveillance and high rates of *PRNP* sequencing in CJD cases will further hone the precision in estimating true penetrance of rare variants.

CHAPTER 5

Summary and future directions

This thesis sums up our efforts in tackling an assortment of challenges and unmet needs faced by healthy individuals at risk of prion disease, broadly covering areas of risk/penetrance estimation, recognising altered disease phenotypes after long incubation periods and most importantly predicting clinical onset. For the IPD-AR population, we discovered evidence of PrP-amyloid seeding and distinct trajectories of neurodegenerative markers up to four years prior to clinical onset. This allowed us to propose preclinical staging system depending on the speed of clinical evolution i.e. fast versus slow IPDs, which may be used to stratify individuals' proximity to clinical onset. Description of the first autopsy-proven case of vCJD in an individual heterozygous at *PRNP* c129 highlights the inadequacies of currently available ante mortem diagnostic tools, raises questions about the true incidence of vCJD, and the possibility of further epidemics. For rare or novel *PRNP* variants of uncertain significance, we now have a framework of interrogation which can be applied to determine their penetrance, with downstream implications on genetic counselling, family planning, inclusion into research studies and preventative trials.

With regards to vCJD, it can be argued that a "second wave" is already afoot with the description of this *PRNP* c129 MV case here, though the extent of it will likely remain obscure as long as the autopsy rate in CJD surveillance is low. Since our publication in 2017, no further cases have been detected but this could be completely spurious as the national autopsy rate has since declined to less than 10% of suspected CJD cases per annum. The stark reality is that if its true incidence is not captured, neither brain nor biofluid samples with unimpeachable provenance will be available for diagnostic assay development, and hence similarly any hope for risk stratification in the at-risk population. In order to achieve reasonably high autopsy rates, we believe that sufficient funding needs to be allocated to facilitate the logistics of performing autopsies including availability of high-risk pathology suites, transport of bodies, and maintaining storage facilities for brain tissue. Sustainable funding of this scale is really only possible through commitments from central government.

In tandem, modelling of vCJD in transgenic mice expressing different human *PRNP* c129 genotype, with serial passages of brain from this 129MV vCJD case may help isolate the different strains contained within. One of the most exciting recent

developments in the prion field is the visualisation of the prion structure down to near-atomic resolution, allowing for discrimination of mouse-adapted prion strains[46]. If or when this technology is applicable to human prion strains, identification of distinct ultrastructural signatures in these new vCJD related prion strains could very well be used not only to “fish out” unrecognised cases retrospectively in “sCJD” brain tissue archives, but also for diagnostic purposes prospectively. High-resolution Cryo-EM is neither widely available nor tractable as yet because of the laborious purification protocols and infection control logistics.

Accurate evaluation of penetrance for *PRNP* variants of uncertain significance is important for several reasons already mentioned, but for the purpose of this thesis, it is highly consequential because it determines whether blood relatives of carriers should be recruited to studies of at-risk individuals. In the former, it will help avoid the masking or dilution of any genuine and informative biomarker effects by erroneous inclusion of control subjects. The framework proposed here is by no means definitive, and requires further refinement. Similar to vCJD above, visualisation of prion structure may have a major impact on how we understand the structural implications of these variants, especially in those that are felt at present not to destabilise PrP^C significantly. These new insights could prove extremely useful for variants whose penetrance or pathogenicity remain uncertain even after applying our framework in the present form.

While we now know a great deal more about preclinical biomarker evolution in the IPD-AR population, significant gaps in knowledge will need to be filled before the data can be leveraged as pharmacodynamic endpoints or for enrichment in upcoming preventative strategies. For the purposes of individual feedback, even greater certainty over the length of prodromal biomarker change, and its inevitability and proximity to clinical onset, is required given how consequential information like this could be on life decisions. Needless to say, all the above requires access to much greater number of samples particularly from converters, but researchers in this area are faced by a twofold disadvantage – a very rare disease with low annual conversion rates.

Despite possessing one of the largest cohorts of IPD-AR individuals (and biofluid sample archive) to date, our experience also lays bare the utter impossibility of

accruing sufficient volume and range of biofluid samples required to address the outstanding questions in a timely manner, if our Unit were to press on independently. For context, it took our Unit over 15 years to recruit this cohort and assemble this biofluid archive, which contains merely 16 converters. The only feasible strategy forward is to enlist fellow researchers worldwide in collaboration to build and share sample resources, further develop seed amplification assays and expand range of tested neurodegenerative biomarkers, and to apply for ambitious funding streams to finance these efforts. Of these, we believe the most critical but most immediately realisable measure is the ability to share sample resources, which requires agreement to harmonise sample collection, processing and storage protocols. We envisage that, if successful in this regard, collaborators working on different assay developments will have access to the necessary samples for required for exploration, optimisation, screening, and validation. This will be particularly useful in *PRNP* mutations with tendency for geographical clustering e.g. E200K in Slovakia and Israel, V210I in Italy, D178N in Germany, France and Italy[75,109,226,227]. In our Cohort, for example, we were not able to study RT-QuIC assay compatibility for D178N-129V (fCJD phenotype), because we did not possess any CSF samples from symptomatic individuals. Sample resource pooling will also generate sufficient numbers required for more confident interpretation of data. An oral platform presentation of this work at Prion 2022 in Göttingen stimulated ample interest in European and Israeli researchers to meet for a preliminary discussion. It is hoped the recent publication of this work in *Brain* will inspire further momentum to find the necessary common ground to reach an agreement, and to expand collaborations with fellow researchers in other regions e.g. North America, South America, Asia, and potentially Africa further down the line.

Our work here demonstrates the presence of a presymptomatic PrP amyloid seeding-only phase, further extending the IPD prodromal period beyond that of the silent neurodegeneration phase. However, this can only be fully appreciated if a highly sensitive RT-QuIC assay exists for a particular mutation, such as IQ-CSF RT-QuIC for E200K. Although we were not as successful in doing so for P102L with the novel bespoke Hu P102L rPrP RT-QuIC, we showed that it is possible to customise assay conditions for certain prion strains or species, which hitherto have failed to be picked up by existing assays. Amongst the possible modifications, we anticipate that the use of specific mutant rPrP constructs may lead to favourable seed-substrate

compatibilities for mutations such as D178N and A117V, with sensitivity further boosted by switching salts along the Hofmeister series. Ideally, RT-QuIC assay optimisation should be as comprehensive as possible but the huge number of permutations in assay conditions e.g. rPrP species, salts, reaction mix components, and shaking kinetics, will require considerable sample and human resource, and funding, again highlighting the need for a multicentre collaborative approach. This applies similarly to interrogation of neurodegenerative and non-neurodegenerative biomarkers where the list of novel markers grows rapidly with each passing month. It is worth noting that certain biomarker measurements, the prime example being CSF total PrP level are highly sensitive to small variations in sample handling, underlining the importance to harmonise these protocols. Additionally some potential also lies in enlisting complementary measures such as using data-driven computational methods to unravel the sequence of neurodegenerative biomarker progression to help refine disease staging in the prodromal period[166].

Finally, at the close of this thesis, I wish to quote directly from Eric Minikel's CureFFI blog piece on the *bioRxiv* preprint of our biomarker study from November 2022. On a personal level, I confess that I have been deeply touched by Eric and his wife Sonia's courage, resolve, dedication, kindness and seemingly undimmable optimism in their quest for a cure. Their narrative has been a great motivation for me to take up and continue this project, and I am sure they have had similar effects on other researchers worldwide. While they did write an editorial comment in *Brain* to accompany our article, I often find myself coming back to this clarion extract:

"What remains to be done then? For one, we all need to follow a greater number of mutation carriers, for longer into the future, and collaborate more closely with one another to look at more markers in the samples collected. My wish is that everyone following pre-symptomatic PRNP mutation carriers can get plenty of funding to increase, expand, intensify. If grant reviewers say, "but it's been done", you send them to talk to me. Meanwhile, even if, as this report suggests, RT-QuIC does prove sensitive to prodromal E200K and NfL/GFAP sensitive to prodromal P102L, there's still a big gap we need to fill. For D178N and probably a handful of other mutations, we still really have no *plausible prodromal markers to turn to. Even at the symptomatic stage, D178N people's CSF is only occasionally positive by RT-QuIC [Sano*

2013, Cramm 2015, Franceschini 2017, Foutz 2017, Rhoads 2020] and their plasma often has only a modest increase in NfL [Zerr 2018, Hermann 2022]. ***For all you methods development / biomarker discovery people out there, this is your call to action.****”*

REFERENCES

1. Brown P, Bradley R. 1755 and all that: a historical primer of transmissible spongiform encephalopathy. *BMJ*. Dec 19-26 1998;317(7174):1688-92. doi:10.1136/bmj.317.7174.1688
2. Cuillé J CP-L. La maladie dite “tremblante” du mouton; est-elle inoculable? *Compte Rend Acad Sci*. 1936;203:1552.
3. Gordon WS. Advances in veterinary research. *Vet Rec*. Nov 23 1946;58(47):516-25.
4. Hadlow WJ. Kuru likened to scrapie: the story remembered. *Philos Trans R Soc Lond B Biol Sci*. Nov 27 2008;363(1510):3644. doi:10.1098/rstb.2008.4013
5. Klatzo I, Gajdusek DC, Zigas V. Pathology of Kuru. *Lab Invest*. Jul-Aug 1959;8(4):799-847.
6. Gajdusek DC, Gibbs CJ, Alpers M. Experimental transmission of a Kuru-like syndrome to chimpanzees. *Nature*. Feb 19 1966;209(5025):794-6. doi:10.1038/209794a0
7. Gibbs CJ, Jr., Gajdusek DC, Asher DM, et al. Creutzfeldt-Jakob disease (spongiform encephalopathy): transmission to the chimpanzee. *Science*. Jul 26 1968;161(3839):388-9. doi:10.1126/science.161.3839.388
8. Crick F. Central dogma of molecular biology. *Nature*. Aug 8 1970;227(5258):561-3. doi:10.1038/227561a0
9. Sigurdsson B. RIDA, A Chronic Encephalitis of Sheep: With General Remarks on Infections Which Develop Slowly and Some of Their Special Characteristics. *British Veterinary Journal*. 1954/09/01/ 1954;110(9):341-354. doi:https://doi.org/10.1016/S0007-1935(17)50172-4
10. Griffith JS. Self-replication and scrapie. *Nature*. Sep 2 1967;215(5105):1043-4. doi:10.1038/2151043a0
11. Gibbons RA, Hunter GD. Nature of the scrapie agent. *Nature*. Sep 2 1967;215(5105):1041-3. doi:10.1038/2151041a0
12. Pattison IH, Jones KM. The possible nature of the transmissible agent of scrapie. *Vet Rec*. Jan 7 1967;80(1):2-9. doi:10.1136/vr.80.1.2
13. Hunter GD, Millson GC. Studies on the Heat Stability and Chromatographic Behaviour of the Scrapie Agent. *J Gen Microbiol*. Nov 1964;37:251-8. doi:10.1099/00221287-37-2-251
14. Pattison IH. Resistance of the Scrapie Agent to Formalin. *J Comp Pathol*. Apr 1965;75:159-64. doi:10.1016/0021-9975(65)90006-x
15. Alper T, Cramp WA, Haig DA, Clarke MC. Does the agent of scrapie replicate without nucleic acid? *Nature*. May 20 1967;214(5090):764-6. doi:10.1038/214764a0
16. Prusiner SB. Novel proteinaceous infectious particles cause scrapie. *Science*. Apr 9 1982;216(4542):136-44. doi:10.1126/science.6801762
17. Basler K, Oesch B, Scott M, et al. Scrapie and cellular PrP isoforms are encoded by the same chromosomal gene. *Cell*. Aug 1 1986;46(3):417-28. doi:10.1016/0092-8674(86)90662-8
18. Prusiner SB, Groth DF, Bolton DC, Kent SB, Hood LE. Purification and structural studies of a major scrapie prion protein. *Cell*. Aug 1984;38(1):127-34. doi:10.1016/0092-8674(84)90533-6
19. Oesch B, Westaway D, Walchli M, et al. A cellular gene encodes scrapie PrP 27-30 protein. *Cell*. Apr 1985;40(4):735-46. doi:10.1016/0092-8674(85)90333-2

20. Locht C, Chesebro B, Race R, Keith JM. Molecular cloning and complete sequence of prion protein cDNA from mouse brain infected with the scrapie agent. *Proc Natl Acad Sci U S A*. Sep 1986;83(17):6372-6. doi:10.1073/pnas.83.17.6372
21. Kretzschmar HA, Stowring LE, Westaway D, Stubblebine WH, Prusiner SB, Dearmond SJ. Molecular cloning of a human prion protein cDNA. *DNA*. Aug 1986;5(4):315-24. doi:10.1089/dna.1986.5.315
22. Prusiner SB. Prions. *Proc Natl Acad Sci USA*. 1998/11/10/ 1998;95(23):13363-13383.
23. Zahn R, Liu A, Luhrs T, et al. NMR solution structure of the human prion protein. *Proc Natl Acad Sci U S A*. Jan 4 2000;97(1):145-50. doi:10.1073/pnas.97.1.145
24. Hosszu LLP, Jackson GS, Trevitt CR, et al. The residue 129 polymorphism in human prion protein does not confer susceptibility to Creutzfeldt-Jakob disease by altering the structure or global stability of PrPC. *J Biol Chem*. 2004/07/02/ 2004;279(27):28515-28521. doi:10.1074/jbc.M313762200
25. Palmer MS, Dryden AJ, Hughes JT, Collinge J. Homozygous prion protein genotype predisposes to sporadic Creutzfeldt-Jakob disease. *Nature*. Jul 25 1991;352(6333):340-2. doi:10.1038/352340a0
26. Pocchiari M, Puopolo M, Croes EA, et al. Predictors of survival in sporadic Creutzfeldt-Jakob disease and other human transmissible spongiform encephalopathies. *Brain*. Oct 2004;127(Pt 10):2348-59. doi:10.1093/brain/awh249
27. Mead S, Poulter M, Uphill J, et al. Genetic risk factors for variant Creutzfeldt-Jakob disease: a genome-wide association study. *Lancet Neurol*. Jan 2009;8(1):57-66. doi:10.1016/S1474-4422(08)70265-5
28. Bishop MT, Diack AB, Ritchie DL, Ironside JW, Will RG, Manson JC. Prion infectivity in the spleen of a PRNP heterozygous individual with subclinical variant Creutzfeldt-Jakob disease. *Brain*. Apr 2013;136(Pt 4):1139-45. doi:10.1093/brain/awt032
29. Kaski D, Mead S, Hyare H, et al. Variant CJD in an individual heterozygous for PRNP codon 129. *Lancet*. Dec 19 2009;374(9707):2128. doi:10.1016/S0140-6736(09)61568-3
30. Mok T, Jaunmuktane Z, Joiner S, et al. Variant Creutzfeldt–Jakob Disease in a Patient with Heterozygosity at PRNP Codon 129. *New England Journal of Medicine*. 2017/01/18/ 2017;376(3):292-294. doi:10.1056/NEJMc1610003 10.1056/NEJMc1610003</p>
31. McLean CA, Storey E, Gardner RJ, Tannenberg AE, Cervenakova L, Brown P. The D178N (cis-129M) "fatal familial insomnia" mutation associated with diverse clinicopathologic phenotypes in an Australian kindred. *Neurology*. Aug 1997;49(2):552-8. doi:10.1212/wnl.49.2.552
32. Monari L, Chen SG, Brown P, et al. Fatal familial insomnia and familial Creutzfeldt-Jakob disease: different prion proteins determined by a DNA polymorphism. *Proc Natl Acad Sci U S A*. Mar 29 1994;91(7):2839-42. doi:10.1073/pnas.91.7.2839
33. Brown P, Goldfarb LG, Kovanen J, et al. Phenotypic characteristics of familial Creutzfeldt-Jakob disease associated with the codon 178Asn PRNP mutation. *Ann Neurol*. Mar 1992;31(3):282-5. doi:10.1002/ana.410310309
34. Shibuya S, Higuchi J, Shin RW, Tateishi J, Kitamoto T. Protective prion protein polymorphisms against sporadic Creutzfeldt-Jakob disease. *Lancet*. Feb 7 1998;351(9100):419. doi:10.1016/S0140-6736(05)78358-6

35. Asante EA, Smidak M, Grimshaw A, et al. A naturally occurring variant of the human prion protein completely prevents prion disease. *Nature*. Jun 25 2015;522(7557):478-81. doi:10.1038/nature14510
36. Mead S, Whitfield J, Poulter M, et al. A novel protective prion protein variant that colocalizes with kuru exposure. *N Engl J Med*. Nov 19 2009;361(21):2056-65. doi:10.1056/NEJMoa0809716
37. Lukic A, Beck J, Joiner S, et al. Heterozygosity at polymorphic codon 219 in variant creutzfeldt-jakob disease. *Arch Neurol*. Aug 2010;67(8):1021-3. doi:10.1001/archneurol.2010.184
38. Jones E, Hummerich H, Vire E, et al. Identification of novel risk loci and causal insights for sporadic Creutzfeldt-Jakob disease: a genome-wide association study. *Lancet Neurol*. Oct 2020;19(10):840-848. doi:10.1016/S1474-4422(20)30273-8
39. Bolton DC, McKinley MP, Prusiner SB. Identification of a protein that purifies with the scrapie prion. *Science*. Dec 24 1982;218(4579):1309-11. doi:10.1126/science.6815801
40. Meyer RK, McKinley MP, Bowman KA, Braunfeld MB, Barry RA, Prusiner SB. Separation and properties of cellular and scrapie prion proteins. *Proc Natl Acad Sci U S A*. Apr 1986;83(8):2310-4. doi:10.1073/pnas.83.8.2310
41. Collinge J, Clarke AR. A general model of prion strains and their pathogenicity. *Science*. 2007/11/09/ 2007;318(5852):930-936. doi:10.1126/science.1138718
42. Hill AF, Joiner S, Wadsworth JDF, et al. Molecular classification of sporadic Creutzfeldt-Jakob disease. *Brain*. 2003/06// 2003;126(Pt 6):1333-1346.
43. Hill AF, Joiner S, Beck JA, et al. Distinct glycoform ratios of protease resistant prion protein associated with PRNP point mutations. *Brain*. 2006/03// 2006;129(Pt 3):676-685. doi:10.1093/brain/awl013
44. Kraus A, Hoyt F, Schwartz CL, et al. High-resolution structure and strain comparison of infectious mammalian prions. *Mol Cell*. Nov 4 2021;81(21):4540-4551 e6. doi:10.1016/j.molcel.2021.08.011
45. Manka SW, Zhang W, Wenborn A, et al. 2.7 A cryo-EM structure of ex vivo RML prion fibrils. *Nat Commun*. Jul 13 2022;13(1):4004. doi:10.1038/s41467-022-30457-7
46. Manka SW, Wenborn A, Betts J, et al. A structural basis for prion strain diversity. *Nat Chem Biol*. May 2023;19(5):607-613. doi:10.1038/s41589-022-01229-7
47. Hill AF, Collinge J. Subclinical prion infection. *Trends Microbiol*. Dec 2003;11(12):578-84. doi:10.1016/j.tim.2003.10.007
48. Collinge J, Whitfield J, McKintosh E, et al. A clinical study of kuru patients with long incubation periods at the end of the epidemic in Papua New Guinea. *Philos Trans R Soc Lond, B, Biol Sci*. 2008/11/27/ 2008;363(1510):3725-3739. doi:10.1098/rstb.2008.0068
49. Rudge P, Jaunmuktane Z, Adlard P, et al. Iatrogenic CJD due to pituitary-derived growth hormone with genetically determined incubation times of up to 40 years. *Brain*. 2015/11// 2015;138(Pt 11):3386-3399. doi:10.1093/brain/awv235
50. Sandberg MK, Al-Doujaily H, Sharps B, Clarke AR, Collinge J. Prion propagation and toxicity in vivo occur in two distinct mechanistic phases. *Nature*. 2011/02/24/ 2011;470(7335):540-542. doi:10.1038/nature09768
51. Sandberg MK, Al-Doujaily H, Sharps B, et al. Prion neuropathology follows the accumulation of alternate prion protein isoforms after infective titre has peaked. *Nat Commun*. 2014 2014;5:4347. doi:10.1038/ncomms5347

52. White AR, Enever P, Tayebi M, et al. Monoclonal antibodies inhibit prion replication and delay the development of prion disease. *Nature*. Mar 6 2003;422(6927):80-3. doi:10.1038/nature01457
53. Raymond GJ, Zhao HT, Race B, et al. Antisense oligonucleotides extend survival of prion-infected mice. *JCI Insight*. 2019/08/22/ 2019;4(16):e131175. doi:10.1172/jci.insight.131175
54. Uttley L, Carroll C, Wong R, Hilton DA, Stevenson M. Creutzfeldt-Jakob disease: a systematic review of global incidence, prevalence, infectivity, and incubation. *Lancet Infect Dis*. Jan 2020;20(1):e2-e10. doi:10.1016/S1473-3099(19)30615-2
55. Urwin PJ, Mackenzie JM, Llewelyn CA, Will RG, Hewitt PE. Creutzfeldt-Jakob disease and blood transfusion: updated results of the UK Transfusion Medicine Epidemiology Review Study. *Vox Sang*. May 2016;110(4):310-6. doi:10.1111/vox.12371
56. Urwin P. *Evidence for sporadic Creutzfeldt-Jakob disease being an acquired disease*. The University of Edinburgh; 2019. http://hdl.handle.net/1842/35774
57. The National CJD Research & Surveillance Unit. The 30th Annual Report 2021: Creutzfeldt-Jakob Disease Surveillance in the UK. https://www.cjd.ed.ac.uk/sites/default/files/report30.pdf
58. Mead S, Rudge P. CJD mimics and chameleons. *Pract Neurol*. Apr 2017;17(2):113-121. doi:10.1136/practneurol-2016-001571
59. Parchi P, Giese A, Capellari S, et al. Classification of sporadic Creutzfeldt-Jakob disease based on molecular and phenotypic analysis of 300 subjects. *Annals of Neurology*. 1999/08// 1999;46(2):224-233.
60. McGuire LI, Peden AH, Orrú CD, et al. Real time quaking-induced conversion analysis of cerebrospinal fluid in sporadic Creutzfeldt-Jakob disease. *Annals of Neurology*. 2012/08// 2012;72(2):278-285. doi:10.1002/ana.23589
61. McGuire LI, Poleggi A, Poggiolini I, et al. Cerebrospinal fluid real-time quaking-induced conversion is a robust and reliable test for sporadic creutzfeldt-jakob disease: An international study. *Annals of Neurology*. 2016/07// 2016;80(1):160-165. doi:10.1002/ana.24679
62. Orru CD, Groveman BR, Foutz A, et al. Ring trial of 2nd generation RT-QuIC diagnostic tests for sporadic CJD. *Ann Clin Transl Neurol*. Nov 2020;7(11):2262-2271. doi:10.1002/acn3.51219
63. Zerr I, Kallenberg K, Summers DM, et al. Updated clinical diagnostic criteria for sporadic Creutzfeldt-Jakob disease. *Brain*. 2009/10// 2009;132(Pt 10):2659-2668. doi:10.1093/brain/awp191
64. Keuss SE, Ironside JW, O'Riordan J. Gerstmann-Straussler-Scheinker disease with atypical presentation. *BMJ Case Rep*. Nov 1 2017;2017doi:10.1136/bcr-2017-220907
65. Minikel EV, Vallabh SM, Lek M, et al. Quantifying prion disease penetrance using large population control cohorts. *Science Translational Medicine*. 2016/01/20/ 2016;8(322):322ra9. doi:10.1126/scitranslmed.aad5169
66. Mead S, Lloyd S, Collinge J. Genetic Factors in Mammalian Prion Diseases. *Annu Rev Genet*. 2019/09/19/ 2019;doi:10.1146/annurev-genet-120213-092352
67. Collinge J, Brown J, Hardy J, et al. Inherited prion disease with 144 base pair gene insertion. 2. Clinical and pathological features. *Brain*. 1992/06// 1992;115 (Pt 3):687-710.
68. Hainfellner JA, Brantner-Inthaler S, Cervenakova L, et al. The original Gerstmann-Straussler-Scheinker family of Austria: divergent clinicopathological

phenotypes but constant PrP genotype. *Brain Pathol*. Jul 1995;5(3):201-11. doi:10.1111/j.1750-3639.1995.tb00596.x
69. Reiniger L, Lukic A, Linehan J, et al. Tau, prions and Aβ: the triad of neurodegeneration. *Acta Neuropathologica*. 2011/01// 2011;121(1):5-20. doi:10.1007/s00401-010-0691-0
70. Reiniger L, Mirabile I, Lukic A, et al. Filamentous white matter prion protein deposition is a distinctive feature of multiple inherited prion diseases. *Acta Neuropathologica Communications*. 2013/05/09/ 2013;1:8. doi:10.1186/2051-5960-1-8
71. Mead S, Gandhi S, Beck J, et al. A novel prion disease associated with diarrhea and autonomic neuropathy. *N Engl J Med*. 2013/11/14/ 2013;369(20):1904-1914. doi:10.1056/NEJMoa1214747
72. Mead S. Prion disease genetics. *Eur J Hum Genet*. 2006/03// 2006;14(3):273-281. doi:10.1038/sj.ejhg.5201544
73. Windl O, Giese A, Schulz-Schaeffer W, et al. Molecular genetics of human prion diseases in Germany. *Hum Genet*. Sep 1999;105(3):244-52. doi:10.1007/s004399900124
74. Laplanche JL, Delasnerie-Laupretre N, Brandel JP, et al. Molecular genetics of prion diseases in France. French Research Group on Epidemiology of Human Spongiform Encephalopathies. *Neurology*. Dec 1994;44(12):2347-51. doi:10.1212/wnl.44.12.2347
75. Mitrova E, Belay G. Creutzfeldt-Jakob disease with E200K mutation in Slovakia: characterization and development. *Acta Virol*. 2002;46(1):31-9.
76. Goldfarb LG, Brown P, Mitrova E, et al. Creutzfeldt-Jacob disease associated with the PRNP codon 200Lys mutation: an analysis of 45 families. *Eur J Epidemiol*. Sep 1991;7(5):477-86. doi:10.1007/BF00143125
77. Minikel EV, Vallabh SM, Orseth MC, et al. Age at onset in genetic prion disease and the design of preventive clinical trials. *Neurology*. 2019/07/09/ 2019;93(2):e125-e134. doi:10.1212/WNL.0000000000007745
78. Breithaupt M, Romero C, Kallenberg K, et al. Magnetic Resonance Imaging in E200K and V210I Mutations of the Prion Protein Gene. *Alzheimer Disease & Associated Disorders*. 2013 2013;27(1):87-90. doi:10.1097/WAD.0b013e31824d578a
79. Jarius C, Kovacs GG, Belay G, Hainfellner JA, Mitrova E, Budka H. Distinctive cerebellar immunoreactivity for the prion protein in familial (E200K) Creutzfeldt-Jakob disease. *Acta Neuropathol*. May 2003;105(5):449-54. doi:10.1007/s00401-002-0664-z
80. Foutz A, Appleby BS, Hamlin C, et al. Diagnostic and prognostic value of human prion detection in cerebrospinal fluid. *Annals of Neurology*. 2017/01// 2017;81(1):79-92. doi:10.1002/ana.24833
81. Bongianni M, Orrù C, Groveman BR, et al. Diagnosis of Human Prion Disease Using Real-Time Quaking-Induced Conversion Testing of Olfactory Mucosa and Cerebrospinal Fluid Samples. *JAMA neurology*. 2017/02/01/ 2017;74(2):155-162. doi:10.1001/jamaneurol.2016.4614
82. Franceschini A, Baiardi S, Hughson AG, et al. High diagnostic value of second generation CSF RT-QuIC across the wide spectrum of CJD prions. *Sci Rep*. 2017/09/06/ 2017;7(1):10655. doi:10.1038/s41598-017-10922-w
83. Groveman BR, Orrú CD, Hughson AG, et al. Extended and direct evaluation of RT-QuIC assays for Creutzfeldt-Jakob disease diagnosis. *Ann Clin Transl Neurol*. 2017/02// 2017;4(2):139-144. doi:10.1002/acn3.378

84. Hsiao K, Baker HF, Crow TJ, et al. Linkage of a prion protein missense variant to Gerstmann-Straussler syndrome. *Nature*. Mar 23 1989;338(6213):342-5. doi:10.1038/338342a0
85. Webb T, Poulter M, Beck J, et al. Phenotypic heterogeneity and genetic modification of P102L inherited prion disease in an international series. *Brain*. 2008/10/01/ 2008;131(10):2632-2646. doi:10.1093/brain/awn202
86. Rudge P, Jaunmuktane Z, Hyare H, et al. Early neurophysiological biomarkers and spinal cord pathology in inherited prion disease. *Brain*. 2019/03/01/ 2019;142(3):760-770. doi:10.1093/brain/awy358
87. Wadsworth JDF, Joiner S, Linehan JM, et al. Phenotypic heterogeneity in inherited prion disease (P102L) is associated with differential propagation of protease-resistant wild-type and mutant prion protein. *Brain*. 2006/06// 2006;129(Pt 6):1557-1569. doi:10.1093/brain/awl076
88. Chen SG, Parchi P, Brown P, et al. Allelic origin of the abnormal prion protein isoform in familial prion diseases. *Nat Med*. Sep 1997;3(9):1009-15. doi:10.1038/nm0997-1009
89. Gabizon R, Telling G, Meiner Z, Halimi M, Kahana I, Prusiner SB. Insoluble wild-type and protease-resistant mutant prion protein in brains of patients with inherited prion disease. *Nat Med*. Jan 1996;2(1):59-64. doi:10.1038/nm0196-59
90. Silvestrini MC, Cardone F, Maras B, et al. Identification of the prion protein allotypes which accumulate in the brain of sporadic and familial Creutzfeldt-Jakob disease patients. *Nat Med*. May 1997;3(5):521-5. doi:10.1038/nm0597-521
91. Kretzschmar HA, Neumann M, Stavrou D. Codon 178 mutation of the human prion protein gene in a German family (Backer family): sequencing data from 72-year-old celloidin-embedded brain tissue. *Acta Neuropathol*. 1995;89(1):96-8. doi:10.1007/BF00294264
92. Goldfarb LG, Haltia M, Brown P, et al. New mutation in scrapie amyloid precursor gene (at codon 178) in Finnish Creutzfeldt-Jakob kindred. *Lancet*. Feb 16 1991;337(8738):425. doi:10.1016/0140-6736(91)91198-4
93. Medori R, Tritschler HJ, LeBlanc A, et al. Fatal familial insomnia, a prion disease with a mutation at codon 178 of the prion protein gene. *N Engl J Med*. Feb 13 1992;326(7):444-9. doi:10.1056/NEJM199202133260704
94. Lugaresi E, Provini F. Fatal familial insomnia and agrypnia excitata. *Rev Neurol Dis*. Summer 2007;4(3):145-52.
95. Owen F, Poulter M, Lofthouse R, et al. Insertion in prion protein gene in familial Creutzfeldt-Jakob disease. *Lancet*. Jan 7 1989;1(8628):51-2. doi:10.1016/s0140-6736(89)91713-3
96. Mead, Poulter M, Beck J, et al. Inherited prion disease with six octapeptide repeat insertional mutation--molecular analysis of phenotypic heterogeneity. *Brain*. Sep 2006;129(Pt 9):2297-317. doi:10.1093/brain/awl226
97. Croes EA, Theuns J, Houwing-Duistermaat JJ, et al. Octapeptide repeat insertions in the prion protein gene and early onset dementia. *J Neurol Neurosurg Psychiatry*. Aug 2004;75(8):1166-70. doi:10.1136/jnnp.2003.020198
98. Mok TH, Nihat A, Majbour N, et al. Seed amplification and neurodegeneration marker trajectories in individuals at risk of prion disease. *Brain*. Mar 28 2023;doi:10.1093/brain/awad101
99. Kaski DN, Pennington C, Beck J, et al. Inherited prion disease with 4-octapeptide repeat insertion: disease requires the interaction of multiple genetic risk factors. *Brain*. Jun 2011;134(Pt 6):1829-38. doi:10.1093/brain/awr079

100. Ae R, Hamaguchi T, Nakamura Y, et al. Update: Dura Mater Graft-Associated Creutzfeldt-Jakob Disease - Japan, 1975-2017. *MMWR Morb Mortal Wkly Rep*. Mar 9 2018;67(9):274-278. doi:10.15585/mmwr.mm6709a3
101. Purro SA, Farrow MA, Linehan J, et al. Transmission of amyloid-beta protein pathology from cadaveric pituitary growth hormone. *Nature*. Dec 2018;564(7736):415-419. doi:10.1038/s41586-018-0790-y
102. Jaunmuktane Z, Mead S, Ellis M, et al. Evidence for human transmission of amyloid-β pathology and cerebral amyloid angiopathy. *Nature*. 2015/09/10/ 2015;525(7568):247-250. doi:10.1038/nature15369
103. Banerjee G, Samra K, Adams ME, et al. Iatrogenic cerebral amyloid angiopathy: an emerging clinical phenomenon. *J Neurol Neurosurg Psychiatry*. May 16 2022;doi:10.1136/jnnp-2022-328792
104. Kaushik K, van Etten ES, Siegerink B, et al. Iatrogenic Cerebral Amyloid Angiopathy Post Neurosurgery: Frequency, Clinical Profile, Radiological Features, and Outcome. *Stroke*. May 2023;54(5):1214-1223. doi:10.1161/STROKEAHA.122.041690
105. Owen J, Beck J, Campbell T, et al. Predictive testing for inherited prion disease: report of 22 years experience. *Eur J Hum Genet*. 2014/12// 2014;22(12):1351-1356. doi:10.1038/ejhg.2014.42
106. Thompson AGB, Lowe J, Fox Z, et al. The Medical Research Council prion disease rating scale: a new outcome measure for prion disease therapeutic trials developed and validated using systematic observational studies. *Brain*. 2013/04// 2013;136(Pt 4):1116-1127. doi:10.1093/brain/awt048
107. Corbie R, Campbell T, Darwent L, Rudge P, Collinge J, Mead S. Estimation of the number of inherited prion disease mutation carriers in the UK. *Eur J Hum Genet*. Jun 27 2022;doi:10.1038/s41431-022-01132-8
108. Vallabh SM, Minikel EV, Williams VJ, et al. Cerebrospinal fluid and plasma biomarkers in individuals at risk for genetic prion disease. *BMC Med*. Jun 18 2020;18(1):140. doi:10.1186/s12916-020-01608-8
109. Noa B, Tamara S, Gitit K, et al. The natural history study of preclinical genetic Creutzfeldt-Jakob Disease (CJD): a prospective longitudinal study protocol. *BMC Neurol*. Apr 14 2023;23(1):151. doi:10.1186/s12883-023-03193-8
110. Brown P, Gibbs CJ, Rodgers-Johnson P, et al. Human spongiform encephalopathy: the National Institutes of Health series of 300 cases of experimentally transmitted disease. *Annals of Neurology*. 1994/05// 1994;35(5):513-529. doi:10.1002/ana.410350504
111. Brown P, Brandel JP, Preece M, Sato T. Iatrogenic Creutzfeldt-Jakob disease: the waning of an era. *Neurology*. Aug 8 2006;67(3):389-93. doi:10.1212/01.wnl.0000231528.65069.3f
112. Brown P, Brandel JP, Sato T, et al. Iatrogenic Creutzfeldt-Jakob disease, final assessment. *Emerg Infect Dis*. Jun 2012;18(6):901-7. doi:10.3201/eid1806.120116
113. Swerdlow AJ, Higgins CD, Adlard P, Jones ME, Preece MA. Creutzfeldt-Jakob disease in United Kingdom patients treated with human pituitary growth hormone. *Neurology*. 2003/09/23/ 2003;61(6):783-791. doi:10.1212/01.WNL.0000084000.27403.15
114. Banerjee G, Adams ME, Jaunmuktane Z, et al. Early onset cerebral amyloid angiopathy following childhood exposure to cadaveric dura. *Ann Neurol*. Feb 2019;85(2):284-290. doi:10.1002/ana.25407

115. Preische O, Schultz SA, Apel A, et al. Serum neurofilament dynamics predicts neurodegeneration and clinical progression in presymptomatic Alzheimer's disease. *Nat Med*. Feb 2019;25(2):277-283. doi:10.1038/s41591-018-0304-3
116. Cortelli P, Perani D, Montagna P, et al. Pre-symptomatic diagnosis in fatal familial insomnia: serial neurophysiological and 18FDG-PET studies. *Brain*. Mar 2006;129(Pt 3):668-75. doi:10.1093/brain/awl003
117. Fox NC, Freeborough PA, Mekkaoui KF, Stevens JM, Rossor MN. Cerebral and cerebellar atrophy on serial magnetic resonance imaging in an initially symptom free subject at risk of familial prion disease. *BMJ*. Oct 4 1997;315(7112):856-7. doi:10.1136/bmj.315.7112.856
118. Ncjdrsu E. Diagnostic criteria for human prion diseases.
119. Thompson AGB, Mead SH. Review: Fluid biomarkers in the human prion diseases. *Mol Cell Neurosci*. Jun 2019;97:81-92. doi:10.1016/j.mcn.2018.12.003
120. Mok TH, Mead S. Preclinical biomarkers of prion infection and neurodegeneration. *Curr Opin Neurobiol*. Apr 2020;61:82-88. doi:10.1016/j.conb.2020.01.009
121. Kocisko DA, Come JH, Priola SA, et al. Cell-free formation of protease-resistant prion protein. *Nature*. Aug 11 1994;370(6489):471-4. doi:10.1038/370471a0
122. Saborio GP, Permanne B, Soto C. Sensitive detection of pathological prion protein by cyclic amplification of protein misfolding. *Nature*. 2001/06/14/ 2001;411(6839):810-813. doi:10.1038/35081095
123. Atarashi R, Wilham JM, Christensen L, et al. Simplified ultrasensitive prion detection by recombinant PrP conversion with shaking. *Nat Methods*. Mar 2008;5(3):211-2. doi:10.1038/nmeth0308-211
124. Atarashi R, Satoh K, Sano K, et al. Ultrasensitive human prion detection in cerebrospinal fluid by real-time quaking-induced conversion. *Nature Medicine*. 2011/02// 2011;17(2):175-178. doi:10.1038/nm.2294
125. Colby DW, Zhang Q, Wang S, et al. Prion detection by an amyloid seeding assay. *Proceedings of the National Academy of Sciences*. 2007/12/26/ 2007;104(52):20914-20919. doi:10.1073/pnas.0710152105
126. Saa P, Castilla J, Soto C. Ultra-efficient replication of infectious prions by automated protein misfolding cyclic amplification. *J Biol Chem*. Nov 17 2006;281(46):35245-52. doi:10.1074/jbc.M603964200
127. Zanusso G, Monaco S, Pocchiari M, Caughey B. Advanced tests for early and accurate diagnosis of Creutzfeldt-Jakob disease. *Nat Rev Neurol*. 2016/06// 2016;12(6):325-333. doi:10.1038/nrneurol.2016.65
128. Orrú CD, Yuan J, Appleby BS, et al. Prion seeding activity and infectivity in skin samples from patients with sporadic Creutzfeldt-Jakob disease. *Science Translational Medicine*. 2017/11/22/ 2017;9(417)doi:10.1126/scitranslmed.aam7785
129. Schmitz M, Silva Correia S, Hermann P, et al. Detection of Prion Protein Seeding Activity in Tear Fluids. *N Engl J Med*. May 11 2023;388(19):1816-1817. doi:10.1056/NEJMc2214647
130. Orrú CD, Bongianni M, Tonoli G, et al. A test for Creutzfeldt-Jakob disease using nasal brushings. *N Engl J Med*. 2014/08/07/ 2014;371(6):519-529. doi:10.1056/NEJMoa1315200
131. Orrù CD, Hughson AG, Race B, Raymond GJ, Caughey B. Time course of prion seeding activity in cerebrospinal fluid of scrapie-infected hamsters after intratongue and intracerebral inoculations. *J Clin Microbiol*. Apr 2012;50(4):1464-6. doi:10.1128/jcm.06099-11

132. Orrú CD, Hughson AG, Groveman BR, et al. Factors That Improve RT-QuIC Detection of Prion Seeding Activity. *Viruses*. 2016/05/23/ 2016;8(5)doi:10.3390/v8050140
133. Metrick MA, do Carmo Ferreira N, Saijo E, et al. Million-fold sensitivity enhancement in proteopathic seed amplification assays for biospecimens by Hofmeister ion comparisons. *Proceedings of the National Academy of Sciences*. 2019/10/22/ 2019:201909322. doi:10.1073/pnas.1909322116
134. Orrú CD, Groveman BR, Raymond LD, et al. Bank Vole Prion Protein As an Apparently Universal Substrate for RT-QuIC-Based Detection and Discrimination of Prion Strains. *PLoS pathogens*. 2015/06// 2015;11(6):e1004983. doi:10.1371/journal.ppat.1004983
135. Mok TH, Nihat A, Luk C, et al. Bank vole prion protein extends the use of RT-QuIC assays to detect prions in a range of inherited prion diseases. *Sci Rep*. 2021/12// 2021;11(1):5231. doi:10.1038/s41598-021-84527-9
136. Sano K, Satoh K, Atarashi R, et al. Early detection of abnormal prion protein in genetic human prion diseases now possible using real-time QUIC assay. *PLoS ONE*. 2013 2013;8(1):e54915. doi:10.1371/journal.pone.0054915
137. Asante EA, Linehan JM, Smidak M, et al. Inherited prion disease A117V is not simply a proteinopathy but produces prions transmissible to transgenic mice expressing homologous prion protein. *PLoS pathogens*. 2013 2013;9(9):e1003643. doi:10.1371/journal.ppat.1003643
138. Asante EA, Grimshaw A, Smidak M, et al. Transmission Properties of Human PrP 102L Prions Challenge the Relevance of Mouse Models of GSS. *PLoS pathogens*. 2015/07// 2015;11(7):e1004953. doi:10.1371/journal.ppat.1004953
139. Rissin DM, Kan CW, Campbell TG, et al. Single-molecule enzyme-linked immunosorbent assay detects serum proteins at subfemtomolar concentrations. *Nat Biotechnol*. Jun 2010;28(6):595-9. doi:10.1038/nbt.1641
140. Thompson AGB, Anastasiadis P, Druyeh R, et al. Evaluation of plasma tau and neurofilament light chain biomarkers in a 12-year clinical cohort of human prion diseases. *Molecular Psychiatry*. 2021/03/05/ 2021;doi:10.1038/s41380-021-01045-w
141. Blennow K, Diaz-Lucena D, Zetterberg H, et al. CSF neurogranin as a neuronal damage marker in CJD: a comparative study with AD. *Journal of Neurology, Neurosurgery & Psychiatry*. 2019/08// 2019;90(8):846-853. doi:10.1136/jnnp-2018-320155
142. Llorens F, Kruse N, Schmitz M, et al. Evaluation of α-synuclein as a novel cerebrospinal fluid biomarker in different forms of prion diseases. *Alzheimer's & Dementia*. 2017/06// 2017;13(6):710-719. doi:10.1016/j.jalz.2016.09.013
143. Abu-Rumeileh S, Steinacker P, Polischi B, et al. CSF biomarkers of neuroinflammation in distinct forms and subtypes of neurodegenerative dementia. *Alzheimers Res Ther*. Dec 31 2019;12(1):2. doi:10.1186/s13195-019-0562-4
144. Llorens F, Thüne K, Tahir W, et al. YKL-40 in the brain and cerebrospinal fluid of neurodegenerative dementias. *Mol Neurodegeneration*. 2017/12// 2017;12(1):83. doi:10.1186/s13024-017-0226-4
145. Villar-Piqué A, Schmitz M, Lachmann I, et al. Cerebrospinal Fluid Total Prion Protein in the Spectrum of Prion Diseases. *Molecular Neurobiology*. 2019/04// 2019;56(4):2811-2821. doi:10.1007/s12035-018-1251-1
146. Vallabh SM, Nobuhara CK, Llorens F, et al. Prion protein quantification in human cerebrospinal fluid as a tool for prion disease drug development. *Proceedings of the National Academy of Sciences*. 2019/04/16/ 2019;116(16):7793-7798. doi:10.1073/pnas.1901947116

147. Minikel EV, Kuhn E, Cocco AR, et al. Domain-specific Quantification of Prion Protein in Cerebrospinal Fluid by Targeted Mass Spectrometry. *Mol Cell Proteomics*. 2019/12// 2019;18(12):2388-2400. doi:10.1074/mcp.RA119.001702
148. Rohrer JD, Nicholas JM, Cash DM, et al. Presymptomatic cognitive and neuroanatomical changes in genetic frontotemporal dementia in the Genetic Frontotemporal dementia Initiative (GENFI) study: a cross-sectional analysis. *Lancet Neurol*. 2015/03// 2015;14(3):253-262. doi:10.1016/S1474-4422(14)70324-2
149. Ryman D, Morris J, Bateman R. PREDICTING SYMPTOM ONSET IN AUTOSOMAL DOMINANT ALZHEIMER'S DISEASE: A SYSTEMATIC REVIEW AND META-ANALYSIS. *Alzheimer's & Dementia*. 2014/07// 2014;10(4):P218-P219. doi:10.1016/j.jalz.2014.04.299
150. Webb TE, Whittaker J, Collinge J, Mead S. Age of onset and death in inherited prion disease are heritable. *Am J Med Genet B Neuropsychiatr Genet*. Jun 5 2009;150b(4):496-501. doi:10.1002/ajmg.b.30844
151. Wadsworth JDF, Powell C, Beck JA, et al. Molecular diagnosis of human prion disease. *Methods Mol Biol*. 2008 2008;459:197-227. doi:10.1007/978-1-59745-234-2_14
152. Orrù CD, Groveman BR, Hughson AG, et al. RT-QuIC Assays for Prion Disease Detection and Diagnostics. (1940-6029 (Electronic))
153. Wilham JM, Orrú CD, Bessen RA, et al. Rapid end-point quantitation of prion seeding activity with sensitivity comparable to bioassays. *PLoS pathogens*. 2010/12/02/ 2010;6(12):e1001217. doi:10.1371/journal.ppat.1001217
154. Jackson GS, Hill AF, Joseph C, et al. Multiple folding pathways for heterologously expressed human prion protein. *Biochimica et Biophysica Acta (BBA) - Protein Structure and Molecular Enzymology*. 1999/04// 1999;1431(1):1-13. doi:10.1016/S0167-4838(99)00038-2
155. Dougherty R. *Animal virus titration techniques*. In: Harris RJC (ed) Techniques in experimental virology. Academic Press, Inc., City; 1964:pp 183–186.
156. Rissin DM, Kan Cw Fau - Campbell TG, Campbell Tg Fau - Howes SC, et al. Single-molecule enzyme-linked immunosorbent assay detects serum proteins at subfemtomolar concentrations. 2010;(1546-1696 (Electronic))
157. Glodzik-Sobanska L, Pirraglia E, Brys M, et al. The effects of normal aging and ApoE genotype on the levels of CSF biomarkers for Alzheimer's disease. *Neurobiology of aging*. 2009;30(5):672-681. doi:10.1016/j.neurobiolaging.2007.08.019
158. Chiu MJ, Fan LY, Chen TF, Chen YF, Chieh JJ, Horng HE. Plasma Tau Levels in Cognitively Normal Middle-Aged and Older Adults. 2017;(1663-4365 (Print))
159. Vågberg M, Norgren N, Dring A, et al. Levels and Age Dependency of Neurofilament Light and Glial Fibrillary Acidic Protein in Healthy Individuals and Their Relation to the Brain Parenchymal Fraction. 2015;(1932-6203 (Electronic))
160. Khalil M, Pirpamer L, Hofer E, et al. Serum neurofilament light levels in normal aging and their association with morphologic brain changes. *Nat Commun*. 2020/02/10 2020;11(1):812. doi:10.1038/s41467-020-14612-6
161. Orru CD, Groveman BR, Hughson AG, et al. RT-QuIC Assays for Prion Disease Detection and Diagnostics. *Methods Mol Biol*. 2017;1658:185-203. doi:10.1007/978-1-4939-7244-9_14
162. Nihat A, Mok TH, Odd H, et al. Development of novel clinical examination scales for the measurement of disease severity in Creutzfeldt-Jakob disease. *J*

Neurol Neurosurg Psychiatry. Apr 2022;93(4):404-412. doi:10.1136/jnnp-2021-327722
163. Ferrillo F, Plazzi G, Nobili L, et al. Absence of sleep EEG markers in fatal familial insomnia healthy carriers: a spectral analysis study. *Clin Neurophysiol*. Oct 2001;112(10):1888-92. doi:10.1016/s1388-2457(01)00600-9
164. Mosko T, Galuskova S, Matej R, Bruzova M, Holada K. Detection of Prions in Brain Homogenates and CSF Samples Using a Second-Generation RT-QuIC Assay: A Useful Tool for Retrospective Analysis of Archived Samples. *Pathogens*. Jun 13 2021;10(6)doi:10.3390/pathogens10060750
165. Cramm M, Schmitz M, Karch A, et al. Stability and Reproducibility Underscore Utility of RT-QuIC for Diagnosis of Creutzfeldt-Jakob Disease. *Molecular Neurobiology*. 2016/04// 2016;53(3):1896-1904. doi:10.1007/s12035-015-9133-2
166. van der Ende EL, Bron EE, Poos JA-O, et al. A data-driven disease progression model of fluid biomarkers in genetic frontotemporal dementia. 2022;(1460-2156 (Electronic))
167. Vaquer-Alicea J, Diamond MI, Joachimiak LA. Tau strains shape disease. *Acta Neuropathol*. Jul 2021;142(1):57-71. doi:10.1007/s00401-021-02301-7
168. Martinez-Valbuena I, Visanji NP, Kim A, et al. Alpha-synuclein seeding shows a wide heterogeneity in multiple system atrophy. *Transl Neurodegener*. Feb 7 2022;11(1):7. doi:10.1186/s40035-022-00283-4
169. Holec SAM, Lee J, Oehler A, et al. Multiple system atrophy prions transmit neurological disease to mice expressing wild-type human alpha-synuclein. *Acta Neuropathol*. Oct 2022;144(4):677-690. doi:10.1007/s00401-022-02476-7
170. Groveman BR, Orru CD, Hughson AG, et al. Rapid and ultra-sensitive quantitation of disease-associated alpha-synuclein seeds in brain and cerebrospinal fluid by alphaSyn RT-QuIC. *Acta Neuropathol Commun*. Feb 9 2018;6(1):7. doi:10.1186/s40478-018-0508-2
171. Kordower JH, Chu Y, Hauser RA, Freeman TB, Olanow CW. Lewy body-like pathology in long-term embryonic nigral transplants in Parkinson's disease. *Nature Medicine*. 2008/05// 2008;14(5):504-506. doi:10.1038/nm1747
172. Rossi M, Candelise N, Baiardi S, et al. Ultrasensitive RT-QuIC assay with high sensitivity and specificity for Lewy body-associated synucleinopathies. *Acta Neuropathol*. Jul 2020;140(1):49-62. doi:10.1007/s00401-020-02160-8
173. Stefani A, Iranzo A, Holzknecht E, et al. Alpha-synuclein seeds in olfactory mucosa of patients with isolated REM sleep behaviour disorder. *Brain*. May 7 2021;144(4):1118-1126. doi:10.1093/brain/awab005
174. Iranzo A, Fairfoul G, Ayudhaya ACN, et al. Detection of alpha-synuclein in CSF by RT-QuIC in patients with isolated rapid-eye-movement sleep behaviour disorder: a longitudinal observational study. *Lancet Neurol*. Mar 2021;20(3):203-212. doi:10.1016/S1474-4422(20)30449-X
175. Saijo E, Ghetti B, Zanusso G, et al. Ultrasensitive and selective detection of 3-repeat tau seeding activity in Pick disease brain and cerebrospinal fluid. *Acta Neuropathol*. May 2017;133(5):751-765. doi:10.1007/s00401-017-1692-z
176. Saijo E, Metrick MA, Koga S, et al. 4-Repeat tau seeds and templating subtypes as brain and CSF biomarkers of frontotemporal lobar degeneration. *Acta Neuropathologica*. 2020/01// 2020;139(1):63-77. doi:10.1007/s00401-019-02080-2
177. Metrick MA, 2nd, Ferreira NDC, Saijo E, et al. A single ultrasensitive assay for detection and discrimination of tau aggregates of Alzheimer and Pick diseases. *Acta Neuropathol Commun*. Feb 22 2020;8(1):22. doi:10.1186/s40478-020-0887-z

178. Bone I, Belton L, Walker AS, Darbyshire J. Intraventricular pentosan polysulphate in human prion diseases: an observational study in the UK. *Eur J Neurol*. May 2008;15(5):458-64. doi:10.1111/j.1468-1331.2008.02108.x
179. Otto M, Cepek L, Ratzka P, et al. Efficacy of flupirtine on cognitive function in patients with CJD: A double-blind study. *Neurology*. Mar 9 2004;62(5):714-8. doi:10.1212/01.wnl.0000113764.35026.ef
180. Collinge J, Gorham M, Hudson F, et al. Safety and efficacy of quinacrine in human prion disease (PRION-1 study): a patient-preference trial. *Lancet Neurol*. Apr 2009;8(4):334-44. doi:10.1016/S1474-4422(09)70049-3
181. Geschwind MD, Kuo AL, Wong KS, et al. Quinacrine treatment trial for sporadic Creutzfeldt-Jakob disease. *Neurology*. Dec 3 2013;81(23):2015-23. doi:10.1212/WNL.0b013e3182a9f3b4
182. Haik S, Marcon G, Mallet A, et al. Doxycycline in Creutzfeldt-Jakob disease: a phase 2, randomised, double-blind, placebo-controlled trial. *Lancet Neurol*. Feb 2014;13(2):150-8. doi:10.1016/S1474-4422(13)70307-7
183. Varges D, Manthey H, Heinemann U, et al. Doxycycline in early CJD: a double-blinded randomised phase II and observational study. *J Neurol Neurosurg Psychiatry*. Feb 2017;88(2):119-125. doi:10.1136/jnnp-2016-313541
184. Mead S, Khalili-Shirazi A, Potter C, et al. Prion protein monoclonal antibody (PRN100) therapy for Creutzfeldt-Jakob disease: evaluation of a first-in-human treatment programme. *Lancet Neurol*. Apr 2022;21(4):342-354. doi:10.1016/S1474-4422(22)00082-5
185. Smith PG, Bradley R. Bovine spongiform encephalopathy (BSE) and its epidemiology. *Br Med Bull*. 2003;66:185-98. doi:10.1093/bmb/66.1.185
186. Collinge J, Sidle KC, Meads J, Ironside J, Hill AF. Molecular analysis of prion strain variation and the aetiology of 'new variant' CJD. *Nature*. Oct 24 1996;383(6602):685-90. doi:10.1038/383685a0
187. Alpers MP. Review. The epidemiology of kuru: monitoring the epidemic from its peak to its end. *Philos Trans R Soc Lond B Biol Sci*. Nov 27 2008;363(1510):3707-13. doi:10.1098/rstb.2008.0071
188. Mead S, Stumpf MP, Whitfield J, et al. Balancing selection at the prion protein gene consistent with prehistoric kurulike epidemics. *Science*. Apr 25 2003;300(5619):640-3. doi:10.1126/science.1083320
189. Watson N, Brandel JP, Green A, et al. The importance of ongoing international surveillance for Creutzfeldt-Jakob disease. *Nat Rev Neurol*. Jun 2021;17(6):362-379. doi:10.1038/s41582-021-00488-7
190. Peden AH, Head MW, Ritchie DL, Bell JE, Ironside JW. Preclinical vCJD after blood transfusion in a PRNP codon 129 heterozygous patient. *Lancet*. Aug 7-13 2004;364(9433):527-9. doi:10.1016/S0140-6736(04)16811-6
191. Asante EA, Linehan JM, Desbruslais M, et al. BSE prions propagate as either variant CJD-like or sporadic CJD-like prion strains in transgenic mice expressing human prion protein. *EMBO J*. Dec 2 2002;21(23):6358-66. doi:10.1093/emboj/cdf653
192. Asante EA, Linehan JM, Gowland I, et al. Dissociation of pathological and molecular phenotype of variant Creutzfeldt-Jakob disease in transgenic human prion protein 129 heterozygous mice. *Proc Natl Acad Sci U S A*. Jul 11 2006;103(28):10759-64. doi:10.1073/pnas.0604292103
193. Gill ON, Spencer Y, Richard-Loendt A, et al. Prevalent abnormal prion protein in human appendixes after bovine spongiform encephalopathy epizootic: large scale survey. *BMJ*. Oct 15 2013;347:f5675. doi:10.1136/bmj.f5675

194. Collinge J, Whitfield J, McKintosh E, et al. Kuru in the 21st century--an acquired human prion disease with very long incubation periods. *Lancet*. 2006/06/24/ 2006;367(9528):2068-2074. doi:10.1016/S0140-6736(06)68930-7
195. Heath CA, Cooper SA, Murray K, et al. Validation of diagnostic criteria for variant Creutzfeldt-Jakob disease. *Ann Neurol*. Jun 2010;67(6):761-70. doi:10.1002/ana.21987
196. Lukic A, Mead S, Rudge P, Collinge J. Comment on validation of diagnostic criteria for variant Creutzfeldt-Jakob disease. *Ann Neurol*. Jan 2011;69(1):212; author reply 212-3. doi:10.1002/ana.22273
197. el Tawil S, Mackay G, Davidson L, Summers D, Knight R, Will R. Variant Creutzfeldt-Jakob disease in older patients. *J Neurol Neurosurg Psychiatry*. Nov 2015;86(11):1279-80. doi:10.1136/jnnp-2014-309397
198. Bougard D, Brandel JP, Belondrade M, et al. Detection of prions in the plasma of presymptomatic and symptomatic patients with variant Creutzfeldt-Jakob disease. *Science Translational Medicine*. 2016/12/21/ 2016;8(370):370ra182-370ra182. doi:10.1126/scitranslmed.aag1257
199. Bougard D, Bélondrade M, Mayran C, et al. Diagnosis of Methionine/Valine Variant Creutzfeldt-Jakob Disease by Protein Misfolding Cyclic Amplification. *Emerg Infect Dis*. 2018/07// 2018;24(7):1364-1366. doi:10.3201/eid2407.172105
200. Beck JA, Poulter M, Campbell TA, et al. PRNP allelic series from 19 years of prion protein gene sequencing at the MRC Prion Unit. *Hum Mutat*. 2010/07// 2010;31(7):E1551-1563. doi:10.1002/humu.21281
201. Lek M, Karczewski KJ, Minikel EV, et al. Analysis of protein-coding genetic variation in 60,706 humans. *Nature*. 2016/08/17/ 2016;536(7616):285-291. doi:10.1038/nature19057
202. Mok TH, Koriath C, Jaunmuktane Z, et al. Evaluating the Causality of Novel Sequence Variants in the Prion Protein Gene by Example. *Neurobiology of Aging*. 2018/05// 2018;doi:10.1016/j.neurobiolaging.2018.05.011
203. Cali I, Cracco L, Saracino D, et al. Case Report: Histopathology and Prion Protein Molecular Properties in Inherited Prion Disease With a De Novo Seven-Octapeptide Repeat Insertion. *Front Cell Neurosci*. 2020;14:150. doi:10.3389/fncel.2020.00150
204. Cali I, Miller CJ, Parisi JE, Geschwind MD, Gambetti P, Schonberger LB. Distinct pathological phenotypes of Creutzfeldt-Jakob disease in recipients of prion-contaminated growth hormone. *Acta Neuropathol Commun*. Jun 25 2015;3:37. doi:10.1186/s40478-015-0214-2
205. Cali I, Castellani R, Yuan J, et al. Classification of sporadic Creutzfeldt-Jakob disease revisited. *Brain*. Sep 2006;129(Pt 9):2266-77. doi:10.1093/brain/awl224
206. Abstracts of the 19th European Stroke Conference. Barcelona, Spain. May 25-28, 2010. *Cerebrovasc Dis*. 2010;29 Suppl 2:1-361. doi:10.1159/000315008
207. Antonyuk SV, Trevitt CR, Strange RW, et al. Crystal structure of human prion protein bound to a therapeutic antibody. *Proc Natl Acad Sci USA*. 2009/02/24/ 2009;106(8):2554-2558. doi:10.1073/pnas.0809170106
208. Biljan I, Ilc G, Giachin G, Legname G, Plavec J. NMR structural studies of human cellular prion proteins. *Curr Top Med Chem*. 2013 2013;13(19):2407-2418.
209. Adzhubei I, Jordan DM, Sunyaev SR. Predicting functional effect of human missense mutations using PolyPhen-2. *Curr Protoc Hum Genet*. 2013/01// 2013;Chapter 7:Unit7.20. doi:10.1002/0471142905.hg0720s76

210. Kumar P, Henikoff S, Ng PC. Predicting the effects of coding non-synonymous variants on protein function using the SIFT algorithm. *Nat Protoc*. 2009 2009;4(7):1073-1081. doi:10.1038/nprot.2009.86
211. Kircher M, Witten DM, Jain P, O'Roak BJ, Cooper GM, Shendure J. A general framework for estimating the relative pathogenicity of human genetic variants. *Nat Genet*. 2014/03// 2014;46(3):310-315. doi:10.1038/ng.2892
212. Karczewski KJ, Francioli LC, Tiao G, et al. The mutational constraint spectrum quantified from variation in 141,456 humans. *Nature*. May 2020;581(7809):434-443. doi:10.1038/s41586-020-2308-7
213. Brennecke N, Cali I, Mok TH, et al. Characterization of Prion Disease Associated with a Two-Octapeptide Repeat Insertion. *Viruses*. Sep 8 2021;13(9)doi:10.3390/v13091794
214. Goldfarb LG, Brown P, Little BW, et al. A new (two-repeat) octapeptide coding insert mutation in Creutzfeldt-Jakob disease. *Neurology*. Nov 1993;43(11):2392-4. doi:10.1212/wnl.43.11.2392
215. van Harten B, van Gool WA, Van Langen IM, Deekman JM, Meijerink PH, Weinstein HC. A new mutation in the prion protein gene: a patient with dementia and white matter changes. *Neurology*. Oct 10 2000;55(7):1055-7. doi:10.1212/wnl.55.7.1055
216. Liemann S, Glockshuber R. Influence of amino acid substitutions related to inherited human prion diseases on the thermodynamic stability of the cellular prion protein. *Biochemistry*. 1999/03/16/ 1999;38(11):3258-3267. doi:10.1021/bi982714g
217. Hart T, Hosszu LLP, Trevitt CR, et al. Folding kinetics of the human prion protein probed by temperature jump. *Proc Natl Acad Sci USA*. 2009/04/07/ 2009;106(14):5651-5656. doi:10.1073/pnas.0811457106
218. Wells MA, Jackson GS, Jones S, et al. A reassessment of copper(II) binding in the full-length prion protein. *Biochem J*. Nov 1 2006;399(3):435-44. doi:10.1042/BJ20060458
219. Sitbon M, d'Auriol L, Ellerbrok H, et al. Substitution of leucine for isoleucine in a sequence highly conserved among retroviral envelope surface glycoproteins attenuates the lytic effect of the Friend murine leukemia virus. *Proc Natl Acad Sci U S A*. Jul 1 1991;88(13):5932-6. doi:10.1073/pnas.88.13.5932
220. Alber T, Sun DP, Wilson K, Wozniak JA, Cook SP, Matthews BW. Contributions of hydrogen bonds of Thr 157 to the thermodynamic stability of phage T4 lysozyme. *Nature*. Nov 5-11 1987;330(6143):41-6. doi:10.1038/330041a0
221. Richards S, Aziz N, Bale S, et al. Standards and guidelines for the interpretation of sequence variants: a joint consensus recommendation of the American College of Medical Genetics and Genomics and the Association for Molecular Pathology. *Genet Med*. 2015/05// 2015;17(5):405-424. doi:10.1038/gim.2015.30
222. Asante EA, Gowland I, Grimshaw A, et al. Absence of spontaneous disease and comparative prion susceptibility of transgenic mice expressing mutant human prion proteins. *J Gen Virol*. 2009/03// 2009;90(Pt 3):546-558. doi:10.1099/vir.0.007930-0
223. Wadsworth JDF, Asante EA, Collinge J. Review: contribution of transgenic models to understanding human prion disease. *Neuropathol Appl Neurobiol*. 2010/12// 2010;36(7):576-597. doi:10.1111/j.1365-2990.2010.01129.x
224. Vital C, Gray F, Vital A, et al. Prion encephalopathy with insertion of octapeptide repeats: the number of repeats determines the type of cerebellar

deposits. *Neuropathol Appl Neurobiol*. Apr 1998;24(2):125-30. doi:10.1046/j.1365-2990.1998.00098.x
225. Mead S, Webb TE, Campbell TA, et al. Inherited prion disease with 5-OPRI: phenotype modification by repeat length and codon 129. *Neurology*. Aug 21 2007;69(8):730-8. doi:10.1212/01.wnl.0000267642.41594.9d
226. Gambetti P, Parchi P, Petersen RB, Chen SG, Lugaresi E. Fatal familial insomnia and familial Creutzfeldt-Jakob disease: clinical, pathological and molecular features. *Brain Pathol*. Jan 1995;5(1):43-51. doi:10.1111/j.1750-3639.1995.tb00576.x
227. Ladogana A, Puopolo M, Poleggi A, et al. High incidence of genetic human transmissible spongiform encephalopathies in Italy. *Neurology*. May 10 2005;64(9):1592-7. doi:10.1212/01.WNL.0000160118.26865.11

APPENDICES

Table of individual demographics

Table 11 Individual demographics of IPD-AR, IPD, CJD and Controls

IPD-AR								
Patient no.	***PRNP* mutation**	**Status**	**Sex**	**Codon 129**	**Age group at 1st sample**	**No. of plasma samples**	**No. of CSF samples**	**No. of years to predicted onset of latest sample**
1	5-OPRI	Carrier	F	MV	<40	6	0	-8.1
2	6-OPRI	Carrier	F	ND	<40	5	0	-12.2
3	6-OPRI	Carrier	F	MM	<40	4	1	-11.1
4	A117V	Carrier	F	MV	<40	7	4	-7.0
5	D178N-CJD	Untested at risk	M	ND	<40	1	1	-22.2
6	D178N-CJD	Untested at risk	M	ND	<40	1	1	-25.1
7	D178N-FFI	Carrier	F	MV	<40	6	0	-10.2
8	D178N-FFI	Carrier	M	MM	40-60	5	4	-14.2
9	D178N-FFI	Carrier	M	MM	<40	1	1	-14.3
10	D178N-FFI	Untested at risk	F	MV	40-60	1	1	-10.4
11	E200K	Carrier	M	MM	40-60	8	2	-6.5
12	E200K	Carrier	M	MV	40-60	2	1	-12.8
13	E200K	Carrier	F	MM	<40	4	1	-27.6
14	E200K	Untested at risk	F	ND	<40	3	0	-23.1
15	E200K	Carrier	M	MM	>60	7	0	-1.8
16	E200K	Carrier	M	MM	40-60	7	3	-6.8
17	E200K	Untested at risk	M	ND	40-60	2	1	-14.6
18	E200K	Carrier	F	MM	>60	5	1	-5.9

19	E200K	Carrier	M	MV	<40	1	1	-26.3
20	E200K	Carrier	M	MM	<40	4	2	-21.9
21	E200K	Carrier	F	MM	>60	2	1	-3.6
22	E200K	Carrier	F	MV	40-60	2	2	-5.1
23	E200K	Carrier	F	MM	40-60	2	2	-5.1
24	E200K	Carrier	F	MM	40-60	1	1	-8.3
25	E200K	Carrier	F	MV	40-60	1	1	-12.7
26	E200K	Untested at risk	F	ND	40-60	1	1	-7.6
27	E200K	Untested at risk	M	ND	<40	1	0	-39.7
28	E200K	Carrier	M	MM	>60	2	2	-3.4
29	E200K	Untested at risk	M	ND	<40	1	0	-12.7
30	E200K	Carrier	M	MV	<40	1	0	-21.4
31	P102L	Carrier	M	MV	<40	6	3	-10.6
32	P102L	Carrier	F	MM	<40	6	2	-15.2
33	P102L	Untested at risk	F	ND	<40	8	1	-12.0
34	P102L	Untested at risk	F	ND	40-60	4	2	-5.4
35	P102L	Carrier	F	MV	<40	2	0	-20.4
36	P102L	Carrier	F	?	<40	4	2	-10.3
37	P102L	Untested at risk	F	ND	40-60	5	1	-3.3
38	P102L	Untested at risk	M	ND	<40	6	1	-7.7
39	P102L	Carrier	F	MV	<40	2	0	-20.0
40	P102L	Untested at risk	F	ND	40-60	2	0	-10.8
41	P102L	Untested at risk	F	ND	40-60	1	0	-17.5
42	P102L	Untested at risk	M	ND	<40	6	4	-19.3
43	P102L	Carrier	F	MM	40-60	1	0	-4.5
44	P102L	Carrier	F	MV	40-60	3	1	-7.0
45	P102L	Carrier	F	MM	40-60	1	0	-10.7

46	P102L	Untested at risk	M	ND	<40	3	0	-14.4
47	P102L	Untested at risk	F	MM	40-60	1	1	-11.7
48	P102L	Untested at risk	M	ND	<40	1	1	-13.8
49	P102L	Carrier	F	MM	<40	1	0	-23.2
50	P102L	Untested at risk	M	ND	<40	1	1	-16.4
51	P102L	Carrier	M	MM	40-60	2	2	-4.8
52	P102L	Carrier	F	MV	<40	1	1	-20.9
53	P102L	Untested at risk	F	ND	40-60	8	5	-4.4
CONVERTERS								
Patient no.	***PRNP* mutation**	**Status**	**Sex**	**Codon 129**	**Age group at 1st sample**	**No. of plasma samples**	**No. of CSF samples**	**Range of years relative to onset**	**Last known status**
1	5-OPRI	Carrier	F	MM	<40	6	0	-2.3 to 7.2	Alive
2	6-OPRI	Carrier	F	MM	<40	3	0	-8.3 to 2.0	Alive
3	6-OPRI	Carrier	F	MM	<40	8	3	-5.3 to 4.3	Alive
4	D178N-FFI	Carrier	M	MM	40-60	9	1	-9.7 to 0.3	Died
5	D178N-FFI	Carrier	M	MV	<40	6	0	-6.5 to 0.4	Died
6	E200K	Carrier	F	MM	40-60	2	2	-0.2 to 0.4	Died
7	P102L	Carrier	F	MV	40-60	4	0	-5.9 to 0.4	Died
8	P102L	Carrier	M	MV	40-60	5	0	-7.7 to 1.7	Died
9	P102L	Carrier	F	MM	40-60	7	0	-5.3 to 1.0	Died
10	P102L	Carrier	M	MM	40-60	6	1	-2.8 to 1.5	Died
11	P102L	Carrier	M	MM	40-60	2	1	-9.9 to 0.3	Alive
12	P102L	Carrier	F	MV	40-60	13	1	-3.4 to 7.4	Died
13	P102L	Carrier	F	MM	40-60	9	2	-4.7 to 3.9	Died
14	P102L	Carrier	F	MV	40-60	6	1	-2.1 to 2.5	Died
15	P102L	Carrier	F	MM	>60	1	0	-1.4	Died
16	P102L	Carrier	F	MM	40-60	1	0	-0.5	Died
iCJD-AR								

Patient no.	Diagnosis	Sex	Codon 129	Age group at 1st sample	No. of plasma samples	No. of CSF samples	Range of years to predicted onset	Last known status
1	Invasive craniopharyngioma	F	MM	40-60	1	1	-1.9	Died
2	Complex partial epilepsy; otherwise asymptomatic	M	ND	40-60	0	1	-4.8	Alive
3	Asymptomatic	M	ND	40-60	2	2	-4.0 to -2.5	Alive
4	Alzheimer's Disease and Russell-Silver Syndrome	M	ND	40-60	0	1	-2.9	Alive

SYMPTOMATIC IPD AT 1st ASSESSMENT

Patient no.	*PRNP* mutation	Status	Sex	Codon 129	Age group at 1st sample	No. of plasma samples analysed	No. of CSF samples analysed	Range of years relative to onset	Last known status
1	6-OPRI	Carrier	M	MM	<40	3	1	1.1 to 4.0	Died
2	6-OPRI	Carrier	F	MM	<40	2	1	1.5 to 2.7	Alive
3	D178N	Carrier	M	MV	>60	3	1	0.6 to 1.1	Died
4	E200K	Carrier	F	MM	>60	2	1	0.1 to 0.4	Died
5	E200K	Carrier	F	MM	>60	1	1	0.2	Died
6	P102L	Carrier	F	MV	<40	1	1	1.6 to 2.9	Alive
7	P102L	Carrier	F	MM	40-60	1	1	2.20	Died
8	P102L	Carrier	F	MV	<40	1	1	0.4 to 0.5	Died
9	P105S	Carrier	M	MV	40-60	1	1	0.8	Died
10	P157X	Carrier	M	MV	40-60	2	0	2.5 to 2.8	Alive
11	Q212P	Carrier	M to F	MM	40-60	1	1	2.6	Died
12	Y163X	Carrier	M	MV	<40	3	1	2.1 to 6.5	Died
13	P102L	Carrier	F	MV	40-60	0	1	1.3	Alive

CJD CSF (RT-QuIC & SIMOA)

Patient no.	Diagnosis	Sex	Codon 129	Age group at 1st sample	No. of CSF samples analysed		No. of years from onset	Last known status
					RT-QuIC	SIMOA		
1	iCJD (h-GH)	M	MV	40-60	1	1	0.5	Died
2	iCJD (h-GH)	F	MV	40-60	1	1	0.9	Died
3	sCJD	F	MV	>60	1	1	1.2	Died

4	sCJD	M	MV	>60	1	1	0.4	Died
5	sCJD	M	MM	>60	1	1	1.0	Died
6	sCJD	F	MM	40-60	1	1	0.8	Died
7	sCJD	F	MV	>60	1	1	0.5	Died
8	sCJD	F	MV	40-60	1	1	1.1	Died
9	sCJD	M	MV	40-60	1	1	0.9	Died
10	sCJD	F	MM	>60	1	1	0.9	Died
11	sCJD	M	MM	>60	1	1	0.1	Died
12	sCJD	F	MV	40-60	1	1	0.1	Died
13	sCJD	F	MV	40-60	1	1	0.6	Died
14*	sCJD	F	MV	40-60	1	0	1.1	Died
15	sCJD	F	MM	>60	1	1	1.0	Died
16	sCJD	M	MM	40-60	1	1	0.9	Died
17	sCJD	M	MM	>60	1	1	0.2	Died
18*	sCJD	F	ND	>60	0	1	0.5	Died
CJD PLASMA FOR SIMOA								
Patient no.	**Diagnosis**	**Sex**	**Codon 129**	**Age group at 1st sample**	**No. of plasma samples**		**Range of years from onset**	**Last known status**
1	sCJD	M	VV	<40	3		0.9 to 1.0	Died
2	sCJD	M	MM	>60	2		0.8 to 1.0	Died
3	sCJD	M	MV	>60	2		0.3 to 0.4	Died
4	sCJD	M	MM	40-60	2		0.4 to 0.5	Died
5	sCJD	F	MM	>60	2		0.3 to 0.5	Died
6	sCJD	F	VV	>60	2		0.4 to 0.5	Died
7	sCJD	F	MV	>60	2		0.8 to 0.9	Died
8	c-hGH iCJD	M	MV	40-60	1		0.7	Died
9	c-hGH iCJD	F	MM	40-60	1		0.7	Died
10	c-hGH iCJD	M	MV	40-60	2		0.8 to 0.9	Died

11	c-hGH iCJD	M	MM	40-60	2	0.4 to 0.3	Died
12	sCJD	M	MV	>60	3	1.4 to 1.9	Died
13	sCJD	F	MV	40-60	1	2.6	Died
14	sCJD	M	MV	40-60	2	0.9 to 1.0	Died
15	sCJD	F	MV	40-60	2	2.1 to 2.2	Died
16	vCJD	F	MM	40-60	2	2.2 to 3.3	Died
17	vCJD	M	MM	<40	5	0.8 to 1.3	Died
18	vCJD	M	MV	<40	4	0.8 to 1.3	Died
CONTROL (non-prion) CSF FOR RT-QuIC							
Patient no.	**Diagnosis**	**Sex**	**Codon 129**	**Age at sample**	**No. of CSF samples**		
1	Normal	M	MV	62	1		
2	Alzheimer's disease	F	ND	87	1		
3	Alzheimer's disease	M	ND	68	1		
4	Non-Alzheimer’s neurodegeneration	M	ND	68	1		
5	Non-Alzheimer’s neurodegeneration	M	ND	62	1		
6	Alzheimer's disease	F	ND	77	1		
7	Non-Alzheimer’s neurodegeneration	F	ND	75	1		
8	Non-Alzheimer’s neurodegeneration	M	ND	65	1		
9	Non-Alzheimer’s neurodegeneration	F	ND	37	1		
10	Non-Alzheimer’s neurodegeneration	M	ND	69	1		
11	Non-Alzheimer’s neurodegeneration	M	ND	69	1		
12	Non-Alzheimer’s neurodegeneration	M	ND	78	1		
13	Alzheimer's disease	F	ND	82	1		
14	Alzheimer's disease	F	ND	83	1		
15	Non-Alzheimer’s neurodegeneration	M	ND	79	1		
16	Non-Alzheimer’s neurodegeneration	F	ND	51	1		
17	Non-Alzheimer’s neurodegeneration	M	ND	66	1		

18	Non-Alzheimer’s neurodegeneration	M	ND	57	1	
19	Non-Alzheimer’s neurodegeneration	F	ND	75	1	
20	Non-Alzheimer’s neurodegeneration	F	ND	81	1	
21	Alzheimer's disease	M	ND	83	1	
22	Alzheimer's disease	M	ND	76	1	
23	Alzheimer's disease	M	ND	81	1	
24	Non-Alzheimer’s neurodegeneration	F	ND	54	1	
25	Alzheimer's disease	F	ND	65	1	
26	Non-Alzheimer’s neurodegeneration	F	ND	79	1	
27	Alzheimer's disease	F	ND	80	1	
28	Alzheimer's disease	F	ND	77	1	
29	Alzheimer's disease	M	ND	78	1	
30	Non-Alzheimer’s neurodegeneration	F	ND	58	1	
31	Alzheimer's disease	F	ND	80	1	
32	Non-Alzheimer’s neurodegeneration	M	ND	61	1	
33	Non-Alzheimer’s neurodegeneration	M	ND	59	1	
34	Alzheimer's disease	M	ND	77	1	
35	Alzheimer's disease	M	ND	65	1	
36	Alzheimer's disease	F	ND	81	1	
37	Alzheimer's disease	F	ND	68	1	
38	Alzheimer's disease	F	ND	76	1	
39	Alzheimer's disease	M	ND	78	1	
40	Alzheimer's disease	M	ND	78	1	
41	Non-neurodegenerative disease	M	ND	35	1	
42	Non-neurodegenerative disease	F	ND	39	1	
43	Non-neurodegenerative disease	F	ND	Unknown	1	
44	Non-neurodegenerative disease	M	ND	Unknown	1	

45	Non-neurodegenerative disease	M	ND	63	1	
46	Non-neurodegenerative disease	M	ND	69	1	
47	Non-neurodegenerative disease	M	ND	35	1	
48	Non-neurodegenerative disease	M	ND	53	1	
49	Non-neurodegenerative disease	M	ND	62	1	
50	Non-neurodegenerative disease	M	ND	23	1	
51	Non-neurodegenerative disease	M	ND	60	1	
52	Non-neurodegenerative disease	F	ND	72	1	
53	Non-neurodegenerative disease	F	ND	55	1	
54	Non-neurodegenerative disease	M	ND	48	1	
55	Non-neurodegenerative disease	F	ND	73	1	
56	Non-neurodegenerative disease	F	ND	51	1	
57	Non-neurodegenerative disease	F	ND	53	1	
58	Non-neurodegenerative disease	F	ND	64	1	
59	Non-neurodegenerative disease	F	ND	36	1	
CONTROL (healthy) CSF FOR SIMOA N4PB						
Patient no.	**Cohort**	**Sex**	**Codon 129**	**Age at sample**	**No. of CSF samples**	
1	NPMC	M	MV	62	1	
2	Insight-46	F	ND	74	1	
3	Insight-46	M	ND	74	1	
4	Insight-46	M	ND	72	1	
5	Insight-46	F	ND	72	1	
6	Insight-46	F	ND	73	1	
7	Insight-46	M	ND	72	1	
8	Insight-46	F	ND	74	1	
9	Insight-46	M	ND	73	1	
10	Insight-46	F	ND	72	1	

11	Insight-46	M	ND	72	1	
12	YOAD	F	ND	54	1	
13	YOAD	F	ND	67	1	
14	YOAD	F	ND	66	1	
15	YOAD	F	ND	61	1	
16	YOAD	F	ND	59	1	
17	CONFLUID	M	ND	78	1	
18	CONFLUID	M	ND	74	1	
19	CONFLUID	M	ND	62	1	
20	CONFLUID	M	ND	65	1	
21	CONFLUID	F	ND	76	1	
22	CONFLUID	M	ND	63	1	
23	CONFLUID	F	ND	62	1	
24	CONFLUID	M	ND	82	1	
CONTROL (healthy) PLASMA FOR SIMOA N4PB						
Patient no.	**Cohort**	**Sex**	**Codon 129**	**Age at sample/ earliest sample**	**No. of plasma samples**	
1	NPMC	F	ND	38.2	2	
2	NPMC	M	ND	38.5	2	
3	NPMC	F	ND	51.1	2	
4	NPMC	M	ND	62.9	1	
5	NPMC	M	ND	58.8	1	
6	NPMC	F	ND	23.3	1	
7	NPMC	F	ND	50.8	1	
8	NPMC	M	ND	48.7	1	
9	NPMC	M	ND	66	1	
10	NPMC	F	ND	62.9	1	
11	NPMC	M	ND	46.1	2	

12	NPMC	M	ND	40.5	1	
13	NPMC	F	ND	55.4	1	
14	NPMC	F	ND	24.7	1	
15	NPMC	M	ND	47.5	5	
16	NPMC	M	ND	48	1	
17	NPMC	M	ND	45.1	2	
18	NPMC	F	ND	27.4	1	
19	NPMC	M	ND	45.2	2	
20	NPMC	F	ND	62.6	1	
21	NPMC	F	ND	38.2	2	
22	NPMC	M	ND	44.5	1	
23	NPMC	M	ND	68	2	
24	NPMC	M	ND	37.1	1	
25	NPMC	F	ND	60.6	2	
26	NPMC	M	ND	63.2	1	
27	NPMC	M	ND	35	2	
28	NPMC	F	ND	46.7	1	
29	NPMC	F	ND	42.4	1	
30	NPMC	M	ND	58.1	1	
31	NPMC	F	ND	53.3	1	
32	NPMC	F	ND	75.9	1	
33	NPMC	M	ND	48.6	1	
34	NPMC	M	ND	54.4	1	
35	NPMC	M	ND	70.9	1	
36	NPMC	F	ND	32.8	2	
37	NPMC	F	ND	54	1	
38	NPMC	M	ND	64.4	1	

39	NPMC	M	ND	52.4	1	
40	NPMC	M	ND	30.2	1	
41	NPMC	M	ND	28.5	1	
42	NPMC	F	ND	64.3	1	
43	NPMC	F	ND	74.4	1	
44	NPMC	M	ND	43	2	
45	NPMC	F	ND	40.4	1	
46	NPMC	F	ND	38	1	
47	NPMC	F	ND	47.6	2	
48	NPMC	F	ND	50.4	1	
49	NPMC	F	ND	65.1	2	
50	NPMC	M	ND	61.8	2	
51	NPMC	M	ND	57.2	1	
52	NPMC	F	ND	74.2	1	
53	NPMC	M	ND	33.6	1	
54	NPMC	F	ND	65.5	1	
55	NPMC	M	ND	39.7	1	
56	NPMC	M	ND	73.7	1	
57	NPMC	M	ND	57.7	1	
58	NPMC	M	ND	31.6	1	
59	NPMC	F	ND	46.9	1	
60	NPMC	M	ND	53.7	2	
61	NPMC	M	ND	50	1	
62	NPMC	M	ND	73.9	1	
63	NPMC	F	ND	59.9	1	
64	NPMC	M	ND	53.3	1	
65	NPMC	F	ND	67.5	1	

66	NPMC	F	ND	73.4	I	
67	NPMC	M	ND	64.4	I	
68	NPMC	F	ND	40.7	I	
69	NPMC	M	ND	51.5	I	
70	GENFI***	F	ND	69.9	I	
71	GENFI***	F	ND	69.2	I	
72	GENFI***	F	ND	69.9	I	
73	GENFI***	F	ND	65.6	I	
74	GENFI***	M	ND	39.8	I	
75	GENFI	F	ND	42	I	
76	GENFI	F	ND	65	I	
77	GENFI	F	ND	55	I	
78	GENFI	F	ND	33	I	
79	GENFI	F	ND	38	I	
80	GENFI	F	ND	49	I	
81	GENFI	F	ND	37	I	
82	GENFI	F	ND	54	I	
83	GENFI	F	ND	64	I	
84	GENFI	M	ND	23	I	
85	GENFI	M	ND	32	I	
86	GENFI	F	ND	59	I	
87	GENFI	M	ND	33	I	
88	GENFI	F	ND	40	I	
89	GENFI	M	ND	56	I	
90	GENFI	M	ND	26	I	
91	GENFI	F	ND	68	I	
92	GENFI	M	ND	37	I	

93	GENFI	M	ND	21	1	
94	GENFI	M	ND	22	1	
95	GENFI	M	ND	36	1	
96	GENFI	F	ND	58	1	
97	GENFI	M	ND	53	1	
98	GENFI	F	ND	39	1	
99	GENFI	F	ND	53	1	
100	GENFI	F	ND	19	1	
101	GENFI	M	ND	39	1	
102	GENFI	M	ND	39	1	
103	GENFI	F	ND	55	1	
104	GENFI	F	ND	44	1	
105	GENFI	F	ND	60	1	
106	GENFI	M	ND	45	1	
107	GENFI	F	ND	50	1	
108	GENFI	F	ND	44	1	
109	GENFI	M	ND	59	1	
110	GENFI	F	ND	36	1	
111	GENFI	F	ND	64	1	
112	GENFI	F	ND	41	1	

*CSF sample tested only by RT-QuIC; not tested by Simoa N4PB
**CSF sample tested only by Simoa N4PB; not tested by RT-QuIC
***GENFI healthy control plasma samples used to measure coefficients of variance